

# Chemotaxis of *Escherichia coli* to compounds present in human gut



## DISSERTATION

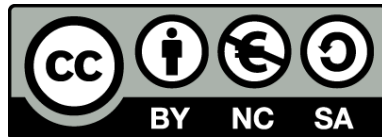
zur  
Erlangung des Doktorgrades  
der Naturwissenschaften  
(Dr. rer. nat.)

Dem Fachbereich Biologie  
der Philipps-Universität Marburg  
vorgelegt von

**Joana Lopes**  
aus Lissabon, Portugal

Marburg, Mai 2018

Originaldokument gespeichert auf dem Publikationsserver der  
Philipps-Universität Marburg  
<http://archiv.ub.uni-marburg.de>



Dieses Werk bzw. Inhalt steht unter einer  
Creative Commons  
Namensnennung  
Keine kommerzielle Nutzung  
Weitergabe unter gleichen Bedingungen  
3.0 Deutschland Lizenz.

Die vollständige Lizenz finden Sie unter:  
<http://creativecommons.org/licenses/by-nc-sa/3.0/de/>

Die Untersuchungen zur vorliegenden Arbeit wurden von Mai 2014 bis Mai 2018 am Max-Planck-Institut für terrestrische Mikrobiologie in Marburg unter der Leitung von Prof. Dr. Victor Sourjik durchgeführt.

Vom Fachbereich Biologie der Philipps Universität Marburg

als Dissertation angenommen am 07.05.2018

Erstgutachter: Prof. Dr. Victor Sourjik

Zweitgutachter: Prof. Dr. Martin Thanbichler

Weitere Mitglieder der Prüfungskommission:

Prof. Dr. Torsten Waldminghaus

Tag der mündlichen Prüfung: 20.06.2018



Zum Zeitpunkt der Einreichung dieser Dissertation wird die folgende Originalpublikation  
vorbereitet, um die erzielten Ergebnisse zu veröffentlichen:

**Lopes, J. & Sourjik, V. (2018)** "Chemotaxis of *Escherichia coli* to major hormones and  
polyamines present in human gut". ISME Journal (accepted)



## ACKNOWLEDGEMENTS

**"Science and everyday life cannot and should not be separated."**

Rosalind Franklin

## Contents

ABBREVIATIONS.....	9
ZUSAMMENFASSUNG.....	11
SUMMARY .....	13
INTRODUCTION .....	15
1. Bacterial chemotaxis .....	15
1.1. Receptors.....	16
1.1.1. Bacterial Hybrids Receptors .....	18
1.2. Motor.....	18
1.3. Chemotaxis signaling pathway in <i>Escherichia coli</i> .....	19
1.4. Stimulus spectrum of <i>Escherichia coli</i> chemotaxis.....	22
2. Microbial endocrinology.....	24
2.1. Brain disorders related to gut modulation.....	26
2.2. Commensal <i>Escherichia coli</i> in the mammalian large intestine .....	26
2.3. Hormones .....	27
2.3.1. Catecholamines .....	28
2.3.2. Thyroid hormones .....	31
2.3.3. Sex hormones .....	32
2.3.4. Insulin .....	34
2.4. Polyamines.....	35
3. Iron uptake systems in <i>Escherichia coli</i> .....	37
AIMS .....	40
MATERIAL AND METHODS .....	41
1. Chemicals and consumables.....	41
2. Media and buffer solutions .....	43
2.1. Media.....	43
2.2. Buffer .....	44
2.3. Antibiotic and inducers solutions.....	46
3. Bacterial strains .....	47
4. Plasmids and oligonucleotides .....	48
5. Molecular cloning.....	51

5.1.	Polymerase Chain Reaction (PCR).....	51
5.2.	Competent cells .....	53
5.2.1.	Chemical competent cells with calcium chloride.....	53
5.2.2.	One-step preparation of competent cells.....	53
5.3.	Transformation .....	53
5.4.	Restriction .....	54
5.5.	Ligation.....	54
5.6.	Gene deletion strains derived from Keio collection .....	55
5.7.	Plasmid cloning by PCR .....	55
6.	RNA Isolation and Deep Sequencing.....	56
6.1.	RNA sequencing data .....	56
6.2.	Reverse transcription polymerase chain reaction quantitative real time: qRT-PCR .....	57
7.	Reaction kits.....	58
8.	Microscopy.....	59
8.1.	Stimulus-dependent ratiometric FRET (flow-FRET) .....	59
8.1.1.	Preparation of cells .....	60
8.1.2.	Data acquisition and analysis.....	61
8.1.3.	Preparation of stimulus solutions .....	62
8.2.	Microfluidics assay .....	62
8.2.1.	Chamber fabrication .....	62
8.2.2.	Data acquisition .....	63
8.3.	Chemotactic drift assay.....	64
8.3.1.	Chamber fabrication .....	64
8.3.2.	Data acquisition .....	65
9.	Growth experiments .....	67
9.1.	Growth analysis.....	67
9.2.	Colony Forming Unit (CFU) assay.....	68
	RESULTS .....	69
1.	Chemotaxis to gut compounds .....	69
1.1.	Chemotactic response of wild-type <i>E. coli</i> .....	69
1.1.1.	FRET assay .....	69
1.1.2.	Microfluidic assays.....	76

1.2.	Mechanism of hormone sensing .....	79
1.2.1.	Responses to hormones mediated by an interplay between Tar and Tsr.....	79
1.2.2.	Response to hormones are mainly mediated by the signaling domain .....	83
1.3.	Mechanism of the spermidine response .....	91
1.3.1.	Trg receptor mediates response to spermidine .....	92
1.3.2.	Response to spermidine requires periplasmic BP PotD .....	93
2.	Physiological importance.....	95
2.1.	Effects of the gut compounds on <i>E. coli</i> growth.....	95
2.2.	Effects of the gut compounds on pathogenic bacteria .....	98
2.3.	Hormones influence gene expression .....	98
2.4.	Dopamine growth effect .....	101
	DISCUSSION .....	105
1.	Chemotactic responses correlate with the compound availability in the gut .....	106
2.	Hormone sensing mechanism - interplay between Tar and Tsr.....	108
2.1.	Repellent response to hormones .....	109
2.2.	Biphasic response to hormones .....	110
3.	Repellent response to spermidine mediated by Trg/PotD.....	112
4.	Correlation between chemotactic response and growth effects.....	113
4.1.	NE might behave as a signaling compound.....	114
4.2.	Melatonin modulates the microbiome .....	115
4.3.	Dopamine growth effect .....	116
5.	Concluding remarks.....	118
	REFERENCES .....	120
	APPENDIX .....	136



### ABBREVIATIONS

rpm – Rotation per minute

min – minutes

h - hours

L- liter

mL- milliliter

DNA - deoxyribonucleic acid

dNTP - deoxyribonucleotide triphosphate

EDTA - ethylene diamine -tetra-acetic acid

OD - optical density

PCR - polymerase chain reaction

ddH<sub>2</sub>O - sterile ultra-pure water



### ZUSAMMENFASSUNG

Vor kurzem wurde gezeigt, dass Mikroorganismen des Magen-Darm-Trakts mit diesem kommunizieren und daher einen Einfluss auf den Stoffwechsel, das Immunsystem sowie auf das Verhalten des Wirtstiers nehmen. Eine steigende Anzahl an Anhaltspunkten zeigen, dass dieser Austausch auch in entgegengesetzter Richtung stattfinden kann und zwar durch das Wahrnehmen von Hormonen und anderer vom Wirt ausgeschiedenen chemischen Verbindungen durch die Mikroorganismen. Wir haben uns in dieser Arbeit mit einem der Schlüsselemente der Wirts-Mikroben-Kommunikation befasst, in dem wir das Chemotaxis System untersucht haben, das externe Stimuli wahrnehmen kann. So haben wir die chemotaktische Antwort des symbiotischen Modelbakteriums *Escherichia coli* auf mehrere chemische Verbindungen, die sich im Magen-Darm-Trakt anreichern, untersucht: Katecholamine 3,4-Dihydroxyphenylalanin, Dopamin, Norepinephrin und 3,4-Dihydroxymandelsäure; die Schilddrüsenhormone Serotonin und Melatonin; die Sexualhormone  $\beta$ -Estradiol und Testosteron; Insulin; und die Polyamine Putrescin und Spermidin. Für Melatonin, Testosteron und Spermidin konnte gezeigt werden, dass sie chemotaktisch abweisend sind, wobei die stärkste abweisende Reaktion für Sperimidine beobachtet wurde und Epinephrin zeigte eine anziehende Wirkung. Für Dopamin, Norepinephrin, 3,4-Dihydroxymandelsäure und Insulin konnte eine zweiphasige Antwort beobachtet werden.

Um den zugrundeliegenden Wahrnehmungsmechanismus für diese chemischen Verbindungen zu ermitteln haben wir die chemotaktischen Antworten von Stämmen untersucht, die Hybridrezeptoren mit der Kombination der Domänen der zwei am häufigsten vorkommenden Rezeptoren in *E. coli*, Tar und Tsr, exprimieren. Wir haben auch die Reaktion von mutierten Tar Rezeptoren untersucht, die eine umgekehrte chemotaktische Antwort aufweisen, was es uns erlaubt hat, die Rezeptorregionen zu identifizieren, welche auf die einzelnen chemischen Verbindungen reagieren.

Während Hormone indirekt wahrgenommen werden, was hauptsächlich auf die Perturbation der Signaldomäne von Tar und Tsr zurückzuführen ist, schließt die Reaktion auf Spermidin den wenig vorhandenen Chemorezeptor Trg ein sowie das periplasmatische Bindeprotein PotD des Spermidinaufnahmesystems. Um schließlich die physiologische

Bedeutung für das Wahrnehmen dieser chemischen Verbindungen für *E. coli* zu bestimmen, haben wir deren Auswirkungen auf das Wachstum untersucht. Der chemotaktische Effekt der untersuchten Verbindungen korreliert mit dem Einfluss auf das Wachstum und der Stabilität der Stoffe im Magen-Darm-Trakt, was auf die Spezifität des beobachteten Verhaltens hindeutet. Wir nehmen an, dass die abweisende Reaktion auf die chemischen Verbindungen, die eine Reaktion hervorrufen, es den Bakterien bei hohen Konzentrationen erlaubt, schadhafte Mengen von Hormonen und Polyaminen im Darm zu vermeiden.

**SUMMARY**

Microorganisms of the gastrointestinal (GI) tract were recently shown to communicate and consequently influence the metabolism, immunity, and behavior of animal hosts. Increasing evidence suggest that communication can also occur in the opposite direction, with hormones and other host-secreted compounds being sensed by microorganisms. Here, we addressed one key aspect of the host-microbe communication by studying a very-well known system that senses external stimulus, the chemotaxis system. We analyzed the chemotactic response of a model commensal bacterium, *Escherichia coli*, to several compounds that accumulate in the GI tract, namely the catecholamines 3,4-dihydroxyphenylalanine, dopamine, norepinephrine, epinephrine and 3,4-dihydroxymandelic acid; the thyroid hormones serotonin and melatonin; the sex hormones  $\beta$ -estradiol and testosterone; insulin; and the polyamines putrescine and spermidine. Melatonin, testosterone and spermidine were shown to be chemorepellents, with the strongest repellent response observed for spermidine, and epinephrine showed an attractant response. Biphasic responses were observed to dopamine, norepinephrine, 3,4-dihydroxymandelic acid and insulin.

To determine the underlying sensing mechanism of these compounds, we investigated the chemotactic responses of strains expressing hybrid receptors that combine domains of each of the two most abundant receptors in *E. coli*, Tar and Tsr. We also studied the responses of mutated Tar receptors that show inverted chemotactic responses, which enable us to identify regions of receptors that sense individual compounds. While the hormones are sensed indirectly, mainly perturbing the signaling domain of Tar and Tsr, the response to spermidine involves the low-abundant chemoreceptor Trg and the periplasmic binding protein PotD, of the spermidine uptake system.

Finally, to determine the physiological importance of these compounds to *E. coli*, we studied their effects on bacterial growth. The chemotactic effects of the tested compounds apparently correlate with their influence on growth and with their stability in the GI tract, pointing to the specificity of the observed behavior. We hypothesize that the repellent responses observed at high concentrations of chemoeffective compounds might enable bacteria to avoid harmful levels of hormones and polyamines in the gut.



---

## INTRODUCTION

### 1. Bacterial chemotaxis

Bacteria have evolved systems that enables them to sense and move according to the different chemicals present in the environment. Motility provides an evolutionary advantage, as it enables bacteria to find suitable niches for survival and growth (1). Several types of motility have been reported in bacteria, including swimming, twitching and gliding (2). The most common way bacteria move is by swimming through their flagella, long helical filaments emerging from the cell surface. Each flagellum is anchored to the cell membrane driven by a motor and uses a transmembrane proton or sodium potential as energy source (3, 4).

The enterobacterium *Escherichia coli* is propelled by three to eight flagella that are randomly distributed around the cell body. *E. coli* moves in a sequence of runs and tumbles referred to as random walk. When all the flagella rotate counterclockwise (CCW), a large bundle that uniformly rotates is formed propelling the cells in a forward direction, leading to a smooth swimming – called run. When at least one of the flagella changes its rotational direction from CCW to clockwise (CW), the bundle is disrupted, reorienting the direction of the cell which leads the cell to tumble (5-7). In the absence of any chemical gradient, bacteria motion is unbiased with runs lasting around 1-2 seconds and the tumbles around 0.1 seconds (5), resulting in an efficient random walk that allows cells to explore their environment. However, in the presence of a chemical gradient (i.e. attractant or repellent chemicals, temperature), bacteria moves in a bias random walk with longer runs and reduced frequency of tumbling, allowing the cells to move up or down a gradient. This biased net movement of cells in a presence of a chemical gradient is termed chemotaxis (6, 8, 9). The bacterial chemotaxis strategy relies on temporal comparisons for sensing changes of chemoeffector concentrations in the environment (10), rather than a spatial measure of the gradient along the cell body, as is the case for eukaryotic cells (5, 11).

To detect and respond to their environment, chemotactic bacteria rely on three main molecular components:

- Receptors: multiple clustered arrays of membrane spanning methyl accepting proteins (MCPs), mainly located at the polar ends of the cell
- Motor: rotary molecular motors that drive helical flagella
- Signaling: internal intracellular biochemical signaling cascade that connects the receptors to flagellar motors, and allows the cells to adapt to varying levels of external stimuli

*E. coli* chemotaxis is extremely sensitive and robust. The chemotactic receptors can detect minute changes in the level of stimulation (12), close to the physical limit set by the noise of ligand binding (13). Receptors can also integrate multiple stimuli, enabling navigation of bacteria in mixed chemical gradients (14, 15). Moreover, intracellular signaling is highly robust against perturbations, such as variations in ambient ligand concentrations or in protein levels (16, 17), which allows cells to maintain efficient chemotaxis in varying environments.

### 1.1. Receptors

Receptors, or homodimers, form mixed clusters of trimers of dimers, where receptor trimers of dimers form the basic signaling units (18). *E. coli* has four ligand-binding chemotaxis receptors Tsr, Tar, Trg, and Tap. These are organized in three domains: a transmembrane sensory domain, a signal conversion domain, and a signaling domain that interacts with the kinase, CheA (Figure 1B). A fifth receptor, Aer, has a different topology with no periplasmic domain but an additional Per-Arnt-Sim domain (PAS) at its N-terminus. PAS domain typically employs a flavin adenine dinucleotide to sense redox changes along the membrane (19, 20). The transmembrane sensory domain is composed of an extracellular sensory domain and two transmembrane helices (TM1 and TM2). When a ligand binds to the pocket inside the sensory domain, it triggers conformational changes in the TM regions. This conformational signal is further transduced to the cytoplasmic part of the receptor by the signal conversion domain, consisting of a Histidine kinase adenyl cyclase methyl-accepting chemotaxis protein-phosphatase (HAMP) domain. The signaling domain contains

a methylation helix (MH) bundle, a flexible bundle, and a protein contact region that interacts with the kinase to regulate its activity (Figure 1B).

*E. coli* receptors can be classified based on their binding substrates. The first class comprises the major, or high abundant, receptors Tar and Tsr, which bind to amino acids directly by the periplasmic domains. The second class comprises the minor, or low abundant, receptors Trg and Tap, which recognize sugars and dipeptides respectively via their periplasmic substrate-binding proteins (BPs) of ATP-binding cassette (ABC) transporters. Early chemotaxis studies already indicated that the differences between the two classes of receptors in the magnitude and range of responses derived from the two types of ligands (14, 21, 22), but the origin of those differences remained largely unclear. Apart from the different substrates, recognize by these receptors, major and minor receptors were believed also to differ in their copy numbers. The total number of minor receptors was previously estimated to be <1 000 copies *per* cell compared with ~10 000 for major receptors (23), and this difference was frequently assumed to explain the apparently weaker responses mediated by minor receptors. Minor receptors also have truncated C-terminus and lack the binding site for the adaptation enzymes, making them dependent on the proximity of neighboring major receptors for efficient adaptation (24). However, a more recent study found that the difference in copy number is smaller than previously calculated, constituting more than a quarter of the total receptor pool (25). It was proposed that a distinction must be made between directly and indirectly binding ligands, where indirect ligand binding has greater flexibility in the modulation of response sensitivity (25). Chemotactic response to mixtures of effectors showed that simultaneous stimulation by ligands of different receptors is additive, and that adaptation to ligands of one receptor does not interfere with signaling by other receptors (25). The signaling units formed by the mixed clusters can also amplify the signal by cooperativity (8, 26), leading to a higher sensitivity at low ligand concentrations and providing gain at higher ligand concentrations (27).

### **1.1.1. Bacterial Hybrids Receptors**

Bacterial hybrid sensors are a powerful tool for characterizing specificity of novel ligands and for bacterial biosensors applications. The range of detectable ligands of a chemotaxis system can be expanded through the construction of hybrid receptors. Extracellular sensory domains from “donor” chemotaxis receptors can be conjugated with chemotaxis receptors or histidine kinases found in other species to form hybrid receptors. There are several examples of functional hybrid receptors from the same species, such as Tsr-Tar (28), Trg-Tsr (29), and Tap-Tar (30) in *E. coli* and McpB-McpC in *Bacillus subtilis* (31), as well as hybrids between PctA, PctB, and PctC from *Pseudomonas aeruginosa* (32, 33) and hybrid receptors from different species such as McpG from *Pseudomonas putida* and *E. coli* Tar (33). While there has been some success in engineering functional hybrids receptors, designing functional receptor hybrids remains a challenging task (34). One of the issues is the high sensitivity of chemotaxis receptors to small conformational perturbations, that can interfere with the signal transduction through the receptor (35).

### **1.2. Motor**

The bacterial flagellar motor is a rotary machine that drives the helical flagellum. The purified flagellum consist of a long helical filament, a short hook, and a basal structure of four rings mounted on a rod (36-38), comprising of approximately 50 genes (39). The filament assembles from the end that is distal to the bacterium and forms a semi-rigid helix, the wavelength and handedness of which alters with changes in the direction of motor rotation. In the stator of the motor, protons move through the independent force-generating units composed by the Mot complexes anchored to the peptidoglycan layer. These protons interact with the ring of ~32 FliG proteins that are associated with the cytoplasmic component of the rotor, and this drives rotation. The exact mechanism by which the electrochemical gradient is coupled to mechanical rotation is unclear, but it probably involves electrostatic interactions between the stator and the rotor proteins (40). Phosphorylated CheY binds FliM proteins that are associated with the FliG rotor to generate a switch in the motor rotation direction (41).

### 1.3. Chemotaxis signaling pathway in *Escherichia coli*

In *E. coli*, chemotaxis is regulated by the histidine kinase, CheA. CheA is anchored to the membrane receptors through an adaptor protein, CheW, which is associated and interacts with the large array of receptors, at their cytoplasmic end. Conformational changes of the receptors, triggered e.g. by the binding of chemoeffectors to the receptors and by changes in the level of receptor methylation modulate the autophosphorylation activity of CheA (42, 43), in a cooperative manner. Attractant ligand binding decreases CheA activity while repellent binding enhances autophosphorylation. CheW is required for this regulation, although its exact function remains unclear. In the presence of a repellent, following the activation of CheA, the phosphoryl group is transferred to its cognate response regulator CheY, thereby activating it. Phosphorylated CheY (CheY-P) diffuses and binds to the flagellar motors to enhance the probability of a CW rotation, causing the cell to tumble. Sub-second dephosphorylation of CheY-P, which is ensured by the phosphatase CheZ (44), allows the CheY-P concentration in the cell to accurately follow and reflect the average autophosphorylation activity of the cell's kinases. However, in the presence of an attractant, increased receptor stimulation results in CheA inactivation and suppression of tumbles, thus promoting continued swimming in this direction (44)(Figure 1A).

As the cells swims in a gradient, receptors are also subjected to adaptation for it to reset and be receptive to changing conditions. Receptor adaptation is controlled by CheR and CheB, and catalyze methylation and demethylation respectively of four specific glutamate residues on the receptors (16, 45, 46). Methylation tunes the ability of the receptors to activate CheA, increased methylation activates CheA and decreases receptor sensitivity to attractants, resulting in sensory adaptation. Thus, enabling the cell to detect further changes in concentration, as it swims in chemical gradients. This resets the pathway activity upon an initial stimulation to the steady state, counteracting the effects of ligand binding - termed precise adaptation (11, 26, 47). Under most conditions, the signaling apparatus mediating bacterial chemotaxis exhibits perfect adaptation to chemoattractants, so that, the steady-state behavior of the system is independent of the concentration of a

homogeneous distribution of the attractant. However, to higher concentrations of attractants the chemotaxis pathway shows increasingly imprecise adaptation, with a clear correlation between the time of adaptation to a step-like stimulus and the extent of imprecision. The imprecision results from a gradual saturation of receptor methylation sites at high levels of stimulation, which prevents full recovery of the pathway activity by disrupting the conditions required for precise adaptation (48). Because the process of receptor modification is slower than the initial response due to the enzymatic properties of CheR and CheB and their low copy numbers, receptor methylation provides a short-term memory of past conditions (47, 49, 50). In addition, CheB possesses an inhibitory domain, which is subject to negative feedback from CheA-dependent phosphorylation.

In summary, the response process of the chemotaxis signaling pathway in *E. coli* occurs in the following way:

1. The receptors sense canonically changes in the environment through binding of an extracellular ligand attractant to the sensory domain.
2. Increase in attractant leads to the inactivation of CheA, leading to a reduction in the phosphorylation levels of intracellular proteins.
3. The change or decrease in phosphorylated CheY levels change the motor rotational direction bias, thus leading to a rotational switch of the flagella from CW to CCW.
4. The receptors adapt to sensory input in step 1 via methylation, by the CheR and CheB proteins that constitute the adaptation system.
5. The final phase returns the system to its initial pre-stimulus state leaving it free to detect further changes in the extracellular ligand concentration.

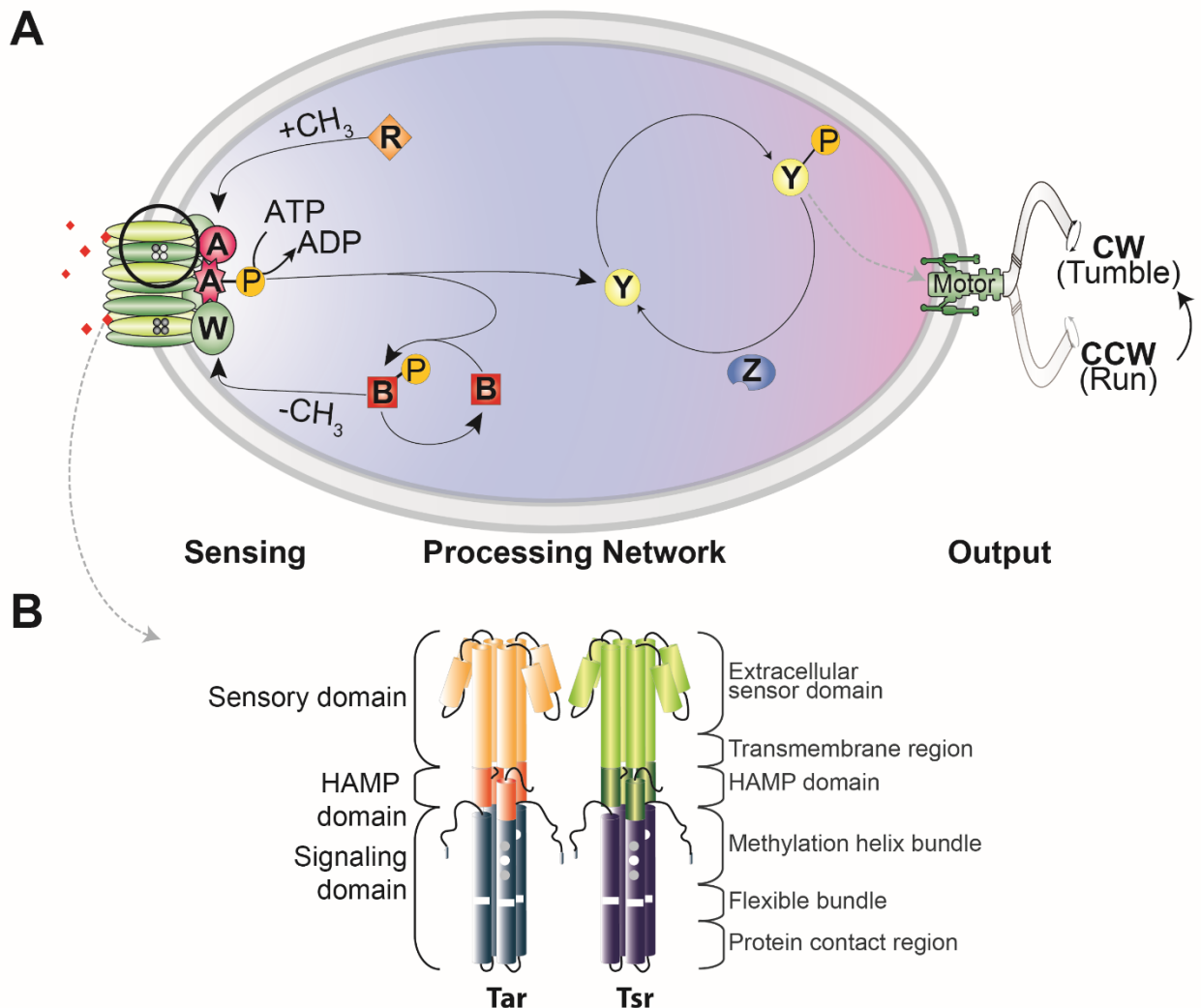


**Figure 1: (A) Chemotaxis signaling pathway in *E. coli*.** Receptors form a sensory complex with the kinase CheA and the adaptor protein CheW. Binding of attractant or repellent to the sensory complex regulates the kinase CheA autophosphorylation activity. Phosphoryl groups from CheA can be transferred to the response regulators CheY, that controls flagellar rotation, and CheB, that controls sensory adaptation. CheY-P interacts with the motor switch complex, causing flagellar rotation to change from counterclockwise (CCW) to clockwise (CW), and the cell tumbles. CheY-P is rapidly dephosphorylated by the phosphatase CheZ, leading to a fast termination of the response. CheB-P acts on receptors by removing methyl-groups added by the methyltransferase CheR. **(B) Schematic drawing of the Tar and Tsr receptors.** Ligands bind to the periplasmic receptor domain. In the cytoplasm, a HAMP region, a methylation region, a flexible bundle region and a trimer contact region are indicated. Methylation sites are indicated by filled or empty circles. Figure adapted from (35).

#### 1.4. Stimulus spectrum of *Escherichia coli* chemotaxis

Due to the exposure to a constantly changing environment, bacteria have evolved the ability to detect various stimuli. *E. coli* mainly recognizes nutrients and toxins that affect cell growth and survival. Examples of nutrients include L-amino acids, sugars and dipeptides. The most effective amino acid attractants are aspartate and serine, which elicit chemotactic pathway responses in *E. coli* at concentrations as low as 10-100 nM. Less effective attractants are threonine, asparagine, cysteine, glutamate, glycine, alanine and methionine (21, 51). *E. coli* is also attracted to sugars, such as D-glucose, maltose and N-acetyl-D-glucosamine, which elicit chemotactic responses at concentrations of around 10  $\mu$ M (14). Dipeptides can also be sensed by *E. coli*, such as Gly-L-Leu and L-Leu-L-Pro, with a threshold similar to sugars (52). In addition to an attractant response, *E. coli* also shows a repellent response to toxins, such as cobalt ( $\text{Co}^{2+}$ ), nickel ( $\text{Ni}^{2+}$ ) and some aromatic compounds (53). The taxis of *E. coli* cells in gradient of these chemicals is unidirectional, with cells always seeking the highest concentration of the attractants and lowest concentration of repellents. On the contrary, the taxis in gradients of many environmental factors, such as temperature (54), pH (28), osmolarity (55), and oxygen (19), is bidirectional. In this case, the cells swim either up or down the gradient depending on the ambient condition, and accumulate at an intermediate condition, rather than at the highest or lowest level. This intermediate is often thought to correspond to a physiological optimum for the cell. For example, *E. coli* is repelled to both very low and very high osmotic pressure, which enables it to accumulate at the more physiologically optimal intermediate osmolarity conditions (55-57). While unidirectional taxis of *E. coli* is comparatively well understood, mechanisms of bidirectional taxis in bacteria remain to be fully established. The bidirectional taxis behavior is likely to rely on counteracting repellent and attract responses of two receptors, where their strength are modulated by the ambient conditions. Examples of bidirectional taxis are the pH taxis, where Tar and Tsr oppose each other (53, 58-60), and temperature taxis, where highly methylated and low methylated receptors oppose each other (61-64). A recent study identified that low methylated receptors are thermophilic (heat seeking) and high methylated receptors cryophilic (cold seeking). In the absence of chemical attractants *E. coli* is thermophilic at all temperatures, on the other hand when high levels of chemical

attractants are present for both Tar and Tsr *E. coli* is cryophilic, and it accumulates at intermediate temperatures when only one of the receptors is adapted to high levels of its chemical ligands (61).

Most of the attractants reported so far are nutrients that can be metabolized by *E. coli*, but metabolism-independent attractants were also found (21). *E. coli* also was shown to perform chemotaxis to self-secreted signals that can mediate collective behaviors, such as the autoinducer-2 dependent autoaggregation and biofilm formation (65, 66). Additionally, several previous studies have suggested that the animal pathogens *Helicobacter pylori*, *Campylobacter jejuni* and *Salmonella enterica* exhibit chemotaxis toward several compounds derived from the human gastric epithelium (67-71) and that such chemotaxis plays an important role in bacterial invasion as well as survival in the intestine (72-74). Moreover, both commensal *E. coli* K-12 and enterohemorrhagic *E. coli* (EHEC) were proposed to sense human hormones, namely norepinephrine (NE) as a chemoattractant (75-77). This response was suggested to require conversion of NE to 3,4-dihydroxymandelic acid (DHMA) by the monoamine oxidase TynA and the aromatic aldehyde dehydrogenase FeaB of *E. coli*, with DHMA then serving as the chemoattractant recognized by Tsr in a nanomolar concentration range (75, 77, 78). These results indicate that hormone taxis might be common among enteric bacteria and not limited to pathogens, but the scope of this behavior remains unclear.

## 2. Microbial endocrinology

The gastrointestinal (GI) tract is a highly innervated organ that possesses its own nervous system, the enteric nervous system (ENS). The ENS is in constant communication with the central nervous system (CNS), through various nerves such as the vagus nerve, which directly connects portions of the gut to the brain (Figure 2) (79). Due to this connection, the GI accumulates high concentration of hormones that are released into the duct system or lumen by the endocrine cells and neurons. These hormones have an important role in the immune response and in the containment of the commensal flora and elimination of pathogenic infections (80, 81).

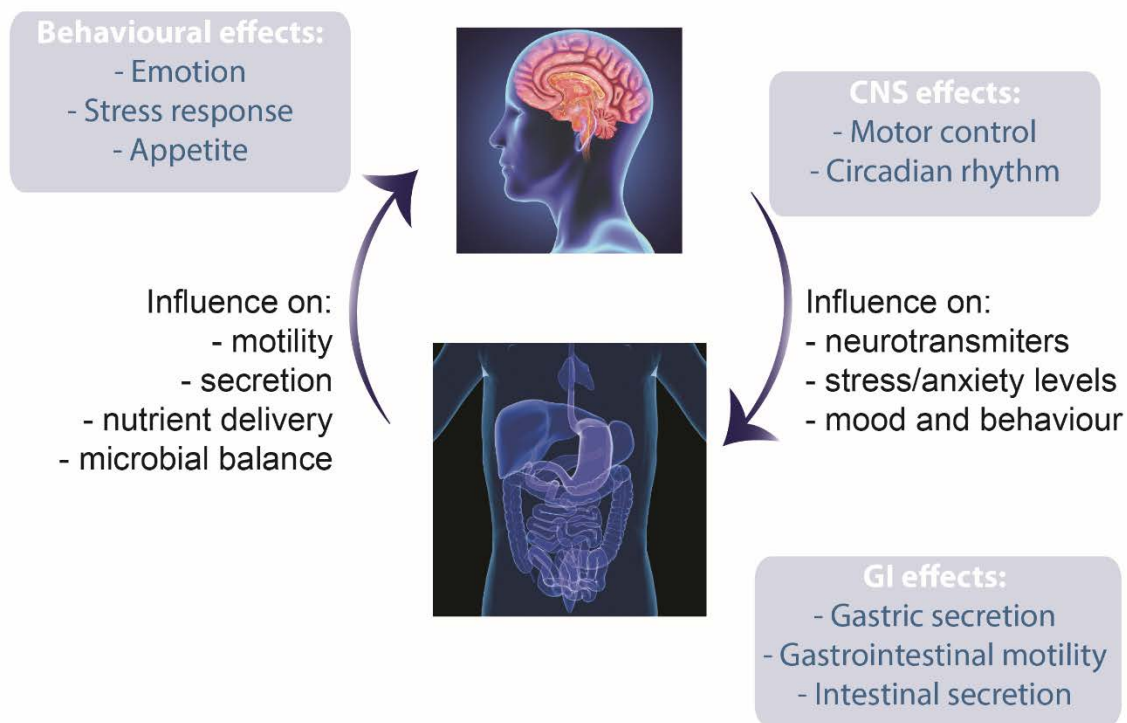


**Figure 2: Brain-microbiome communication.** Abbreviations: CNS – Central Nervous System, GI – gastrointestinal.

The GI tract also hosts the most diverse microbial community of the human body. It is estimated that the gut microbiome comprises several thousand species of bacteria, archaea, eukarya, and viruses (82). In this highly complex ecosystem, the different species of microbes compete and cooperate with one another and with the host cells in order to

survive. Host-microbe interactions take place primarily along the mucosal surfaces. The gastrointestinal mucosa is the largest surface area within the body (approximately 40 m<sup>2</sup>), where only one layer of epithelia cells separates the contents of the lumen from the internal milieu. Environmental factors such as diet and antibiotics can affect the diversity of the microbiome. The gut microbiota plays important roles in host metabolism and immunity, by breaking down dietary components, educating the immune system and degrading toxins (83, 84). The gut microbiota may even influence human emotional states and diseases, such as stress related irritable bowel syndrome (IBS; (85)), and autism ((86, 87), discussed later in section 2.1). These surprising findings show that the microbiota can modulate host behavior, raising the question of how these effects work functionally. In fact, the gut microbiome is now considered by some as a virtual organ in its own right (88), due to its interaction with the host through immune, neuroendocrine and neural pathways (89) and produce an array of bioactive molecules that directly interact with the endocrine, nervous and immune systems of their host (90-92). These pathways are components of the brain–gut–microbiota axis.

Lyte and Ernst were the firsts to define a new field of research after observing that stress-induced neuroendocrine hormones can influence bacterial growth (93). This field is named microbial endocrinology and assumes that through their long coexistence with animals and plants, microorganisms have evolved systems for sensing host-associated signals such as hormones. Detecting such signals enables the microbes to recognize suitable locations in the host and initiate expression of genes needed for host colonization (94-96). This interplay is bidirectional, since the microbiota has been shown to be both affected and to affect host hormones. It can also be direct, when the microbiota produce hormones (97-101), or indirect, when microbes may modulate the function of the adrenal cortex (which controls the anxiety and stress responses), or modulate inflammation and immune responses (85, 96, 102). So far, two major groups of hormones have been identified as possible players in the bacterial effects on host behavior: the neurohormones, including serotonin and the catecholamines dopamine, epinephrine and norepinephrine and stress hormones, including cortisol, corticosterone, adrenocorticosterone and corticotropin.

## 2.1. Brain disorders related to gut modulation

Several studies found an association between gut–brain interactions and functional bowel disorders, chronic abdominal pain syndromes and even eating disorders. One of the most studied examples is the irritable bowel syndrome (IBS) that has been correlate with the microbiota composition (85). Additionally, a high comorbidity, i.e. the presence of one or more additional diseases or disorders co-occurring, was found between stress-related mental symptoms, as anxiety, and IBS (103), where over 50% of patients with IBS have comorbid depression or anxiety. In IBS patients, not only the quantity of commensal bacteria in the intestine is reduced, but also the diversity of the microbiota is altered (104-107). In addition, preliminary studies have shown differences in the composition of the gut microbiota in patients with depression compared with healthy individuals (103, 108-110). Modulation of the gut–brain axis is increasingly being proposed as an appropriate target for the development of novel treatments for a wide variety of disorders that range from depression and anxiety to IBS, obesity and neurodevelopmental disorders (111, 112).

## 2.2. Commensal *Escherichia coli* in the mammalian large intestine

A wide variety of bacteria colonize the large intestines of humans and animals. The bacterial populations involved are relatively stable, consisting of hundreds of species that interact to achieve a relatively constant numerical balance (113). In human adults, the obligate anaerobes make up more than 99.9% of the cultivable bacteria (114). Prominent genera include *Bacteroides*, *Bifidobacterium*, *Clostridium*, *Eubacterium*, *Fusobacterium*, *Lactobacillus*, *Peptococcus*, *Peptostreptococcus*, and *Veillonella* (115). *Escherichia coli* is the predominant facultative anaerobe in the gastrointestinal tracts of mammals (116). How *E. coli* colonizes the mammalian large intestine is not well understood, however increasing evidence suggests that the commensal *E. coli* niche in the GI tract is the mucus layer of the large intestine (117). Fluorescence *in situ* hybridization of mouse intestinal showed that *E. coli* BJ4, a rat commensal isolate, is dispersed in the mucus layer but is not associated with the epithelium (118). The same appears to be true for the human commensal strain, *E. coli* MG1655 (119). *In vitro*, rapid growth in intestinal mucus, but not in luminal contents,

advocates that *E. coli* and *Salmonella enterica* serovar *Typhimurium* grow on nutrients acquired from mucus (120, 121). Thus, the ability of *E. coli* to grow and survive in mucus appears to be critical for intestinal colonization. If so, commensal strains of *E. coli* have to bind to gut receptors to avoid rapid washout (122).

### 2.3. Hormones

In the mucus layer, *E. coli* is exposed to numerous host signals, such as hormones. In the next chapters we will discuss some gut signals to which *E. coli* might be exposed.

Hormones are chemical molecules produced by the endocrine glands and then transported by the circulatory system to target distant organs to regulate physiology and behavior. The endocrine system regulates our heart rate, metabolism, appetite, mood, sexual function, reproduction, growth, development and sleep cycles (123). Hormones have diverse chemical structures, mainly of three classes: eicosanoids, steroids, and amino acid/protein derivatives. Hormones affect distant cells by binding to specific receptor proteins in the target cell, resulting in a change in cell function. When a hormone binds to its receptor, it activates a signal transduction pathway that typically activates gene transcription and increases expression of target proteins.

Hormone secretion occurs in response to specific biochemical signals from a wide range of regulatory systems. Upon secretion, certain hormones, including protein hormones and catecholamines, are readily transported through the circulatory system, since they are water-soluble. Other hormones, including steroid and thyroid hormones, are lipid-soluble, so in order to spread, these hormones must bond to carrier plasma glycoproteins (e.g., thyroxine-binding globulin) to form ligand-protein complexes. Some hormones are completely active when released into the bloodstream (as is the case for insulin and growth hormones), while others are prohormones that must be activated in specific cells through a series of activation steps that are usually highly regulated. The endocrine system secretes hormones directly into the bloodstream typically into fenestrated capillaries, whereas the exocrine system secretes its hormones indirectly using ducts.

Neurohormones are secreted from neuroendocrine cells in response to a neuronal input. Although they are secreted into the blood for a systemic effect, they can also act as neurotransmitters. Neurotransmitters are endogenous chemicals enabling the transmission of signals across the chemical synapses, such as a neuromuscular junction, from one neuron to another target neuron, muscle cell, or gland cell (124). Neurotransmitters are released from synaptic vesicles in synapses into the synaptic cleft, where they are received by neurotransmitter receptors on the target cells. Many neurotransmitters are synthesized from simple and abundant precursors such as amino acids, which are readily available from the diet and only require a small number of biosynthetic steps for conversion (125).

In this section, we will discuss in more detail the class of hormones studied throughout this work: catecholamines, thyroid hormones, sex hormones and the peptide hormone insulin.

### ***2.3.1. Catecholamines***

Structurally, the catecholamine family is a group of widely acting effector compounds derived from tyrosine and other dietary amino acid sources. They chemically comprise a benzene ring with two adjacent hydroxyl groups and an opposing amine side chain (126). The synthesis pathway for catecholamines begins with dietary L-tyrosine, which is ingested within the food or synthesized in the liver. L-tyrosine is taken up from blood and concentrated within the brain and other catecholamine-synthesizing tissues by a transporter for neutral amino acids. L-tyrosine is converted to 3,4-dihydroxyphenylalanine (L-DOPA). L-DOPA is enzymatically converted into dopamine, norepinephrine (NE) and finally epinephrine (or adrenaline) (Figure 3). Besides playing endocrinological roles such as controlling cognitive abilities, mood and gut motility, dopamine, NE and epinephrine also directly function as neurotransmitters and are used in both the CNS and peripheral nervous systems. Receptors for NE and dopamine, called noradrenergic and dopaminergic receptors, containing nerve terminals are widely distributed within the mammalian body, including the GI tract where they are components of the ENS (79, 125, 126). Dopamine is synthesized in non-sympathetic enteric neurons located within the intestinal wall (79, 125-127) and it is responsible for maintaining a sufficiently high level of locomotive activity and helping the

performance of complex voluntary movements while suppressing involuntary ones and maintaining an active wakeful state. This hormone has been found in large amounts within the GI, with high levels occurring in organs, such as the stomach, and in extracellular fluids, such as gastric juice (127, 128). The hormones epinephrine and norepinephrine are released from the adrenal medulla throughout the body, including the intestinal tract, being part of the fight-or-flight response. Within the gut NE is released from storage within sympathetic nerve fibers within the pre-vertebral ganglia innervating the gut mucosa, and it has been shown that up to half of the NE made within the mammalian body is synthesized and utilized within the ENS (126). However, neurons containing phenylethanolamine *N*-methyltransferase, the enzyme required for the synthesis of epinephrine from NE, are not expressed in the intestinal mucosa (79), making it unlikely that adrenaline would normally be present at any significant level. Norepinephrine activates the brain, increases locomotive activity, decreases the anxiety level, and promotes human/animal aggressive behavior. In addition to neuron cells, immune cells appear to be capable of synthesizing, releasing and degrading catecholamines. There is an abundance of immunocytes throughout the intestinal lamina propria, and these cells, may represent an alternate non-neural source of dopamine and NE in the intestine wall (128). NE can be reduced to 3,4-dihydroxyphenylglycolaldehyde, by monoamine oxidase, that can be oxidized in a less favored reaction into DHMA and its real concentration in the gut is unknown.

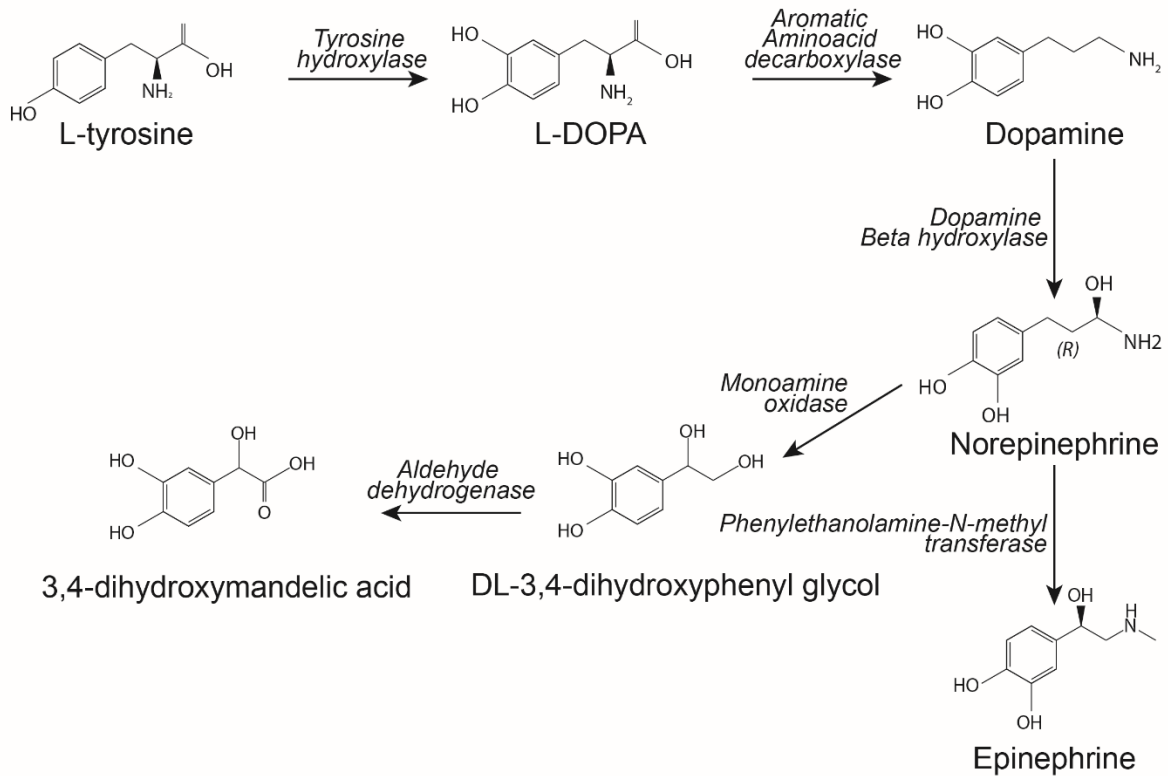


**Figure 3:** Scheme of the catecholamine biosynthetic pathway in humans.

Owing to the abundance of catecholamines hormones in the GI tract, most microbial endocrinology studies have focused on the interaction of gut bacteria with the catecholamines epinephrine, norepinephrine (NE) and dopamine. The first studies focused on the link between stress and the risk of developing an infection and found a correlation between the release of stress hormones with a reduction in the immune function (96, 110, 129). In bacteria, catecholamines were also reported to alter growth, motility, biofilm formation and/or virulence (94-96, 130). In more detail, *Helicobacter pylori* has been shown to change L-DOPA levels in the gut correlating with an increase in the risk of developing Parkinson disease (131). It has also been suggested that NE increases the growth and virulence of enteric bacteria (93, 132), through signaling via adrenergic receptors located either on intestinal epithelial cells or in the bacteria (133). In enterohemorrhagic *E. coli* (EHEC), adrenaline and NE signaling affects bacterial virulence and motility (134).

In terms of determining the *in vivo* levels of catecholamines, there are some considerable technical challenges. For the gut, variations in food catecholamine content, rapid enzymatic

turnover of gut catecholamines, and the adsorbent nature of fecal matter have all posed technical barriers to a definitive statement on active catecholamine levels (135, 136).

### 2.3.2. *Thyroid hormones*

Thyroid hormones are commonly derived from tyrosine and tryptophan amino acids. They are produced by the thyroid gland and are primarily responsible for the regulation of the metabolism. The L-tryptophan pathway is in charge of the synthesis of two important hormones: serotonin and melatonin (Figure 4).

Serotonin (5-hydroxytryptamine (5-HT)) is one of the main neurotransmitters in the brain. It is found in the central nervous system of mammals, although over 90% of the mammalian host's serotonin is found in the intestine (137). Intestinal serotonin secretion is affected by diet, and regulates intestinal movement, mood, appetite, sleep and cognitive functions. Serotonin has been implicated in GI pathologies such as IBS and Crohn's disease (138). The first direct effect of the microbiome on serotonin was demonstrated in germ-free (GF) mice, which had lower plasma serotonin levels than conventional mice (139).

Melatonin (5-methoxy-N-acetyltryptamine) is found in animals, plants, fungi and photosynthetic bacteria (140). In mammals, it senses the photoperiod and is involved in the entrainment (synchronization) of the circadian rhythms of physiological functions including sleep timing, blood pressure regulation, seasonal reproduction and many others, its secretion is regulated by NE. Especially during the daytime, the GI tract releases significant concentrations of melatonin, which influences the regeneration and function of epithelium, enhancing the immune system of the gut, and reducing the tone of gastrointestinal muscles. The release of gastrointestinal melatonin seems to be related to the periodicity of food intake (141-143). Recent papers also postulated that melatonin may also alter the microbiome composition (144), by for example increasing the proliferation of *Enterobacter aerogenes* (145).

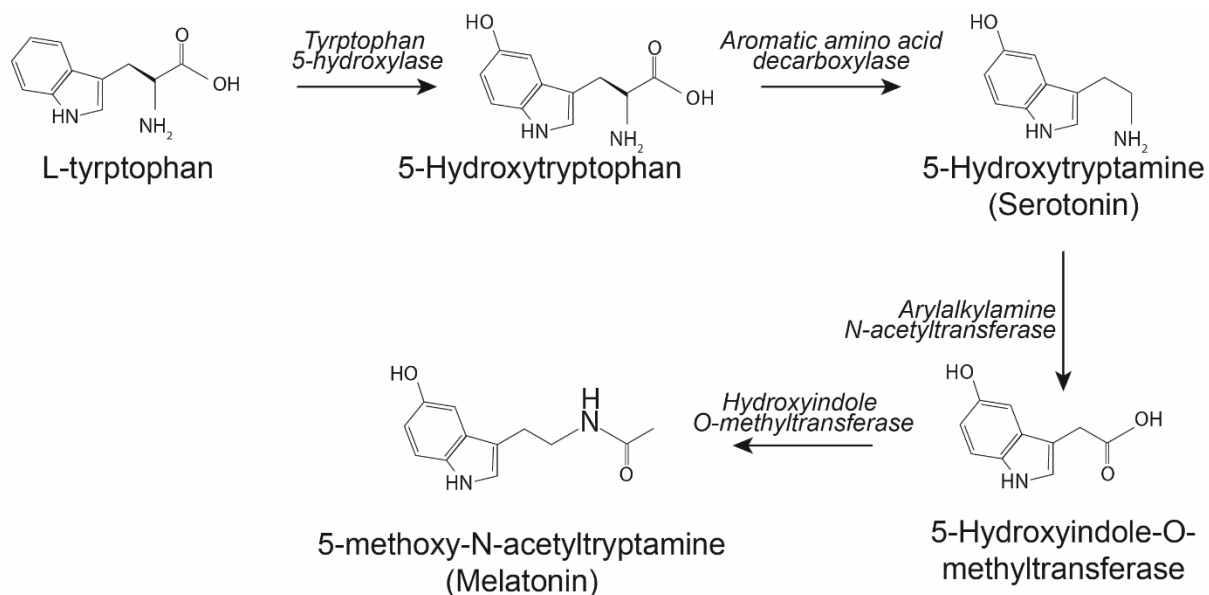


**Figure 4:** Scheme of the biosynthetic pathway of melatonin in the pineal gland of humans.

### 2.3.3. Sex hormones

Sex hormones, or steroid hormones, include estrogens, androgens, and progestogens naturally produced in the gonads by adrenal glands or by the conversion from other steroids. They influence the development of genital organs (estrogen and androgen), maintenance of pregnancy (progestogens), ovulation (estrogens), spermatogenesis (androgens), and sexual differentiation of the brain (estrogen and androgen). The actions of these hormones are mediated through the estrogen receptor, androgen receptor, and progesterone receptor (146). The two main classes of sex steroids are androgens and estrogens, of which the most important human derivatives are testosterone and estradiol, respectively. The third class, progestogens, includes progesterone the most important and only naturally occurring human progestogen (Figure 5).

Examples of bacteria affected by sex hormones have been reported since the 1980s. For instance, *Prevotella intermedius* takes up estradiol and progesterone, which enhance its growth (147). *Clostridium scindens* was reported to convert glucocorticoids to androgens (148). Sex hormones were also involved in the development of obesity and metabolic disorders, however the interrelationship between the balance of sex hormones and metabolism is complex, and the underlying mechanisms are still unclear (149).

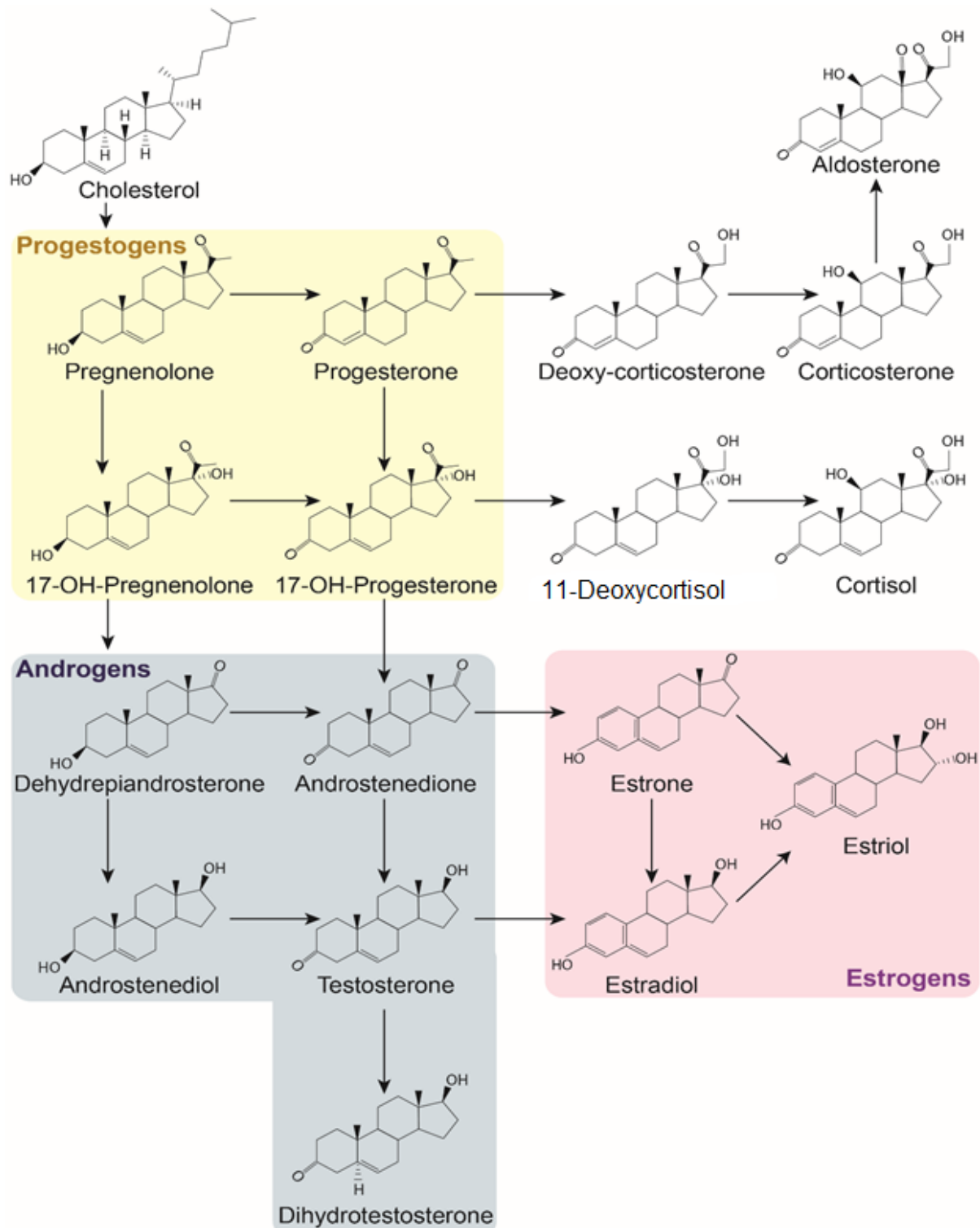


**Figure 5:** Scheme of the biosynthetic pathway of sex hormones classes: progesterones, estrogens and androgens of humans.



## 2.4. Polyamines

Polyamines are signaling compounds that do not fulfil the true definition of hormones, but have similar functions. They are widely distributed from prokaryotic (153) to eukaryotic cells (154) and are found at especially high concentration in proliferating cells, such as cancer cells (155). Polyamines are aliphatic amines with two or more amino groups in their chemical structure. The main polyamines are putrescine, spermidine and spermine and they are synthesized from the amino acid ornithine (Figure 7). The first step in the pathway is the production of ornithine from arginine by the mitochondrial enzyme arginase. Three main sources for polyamines exist in organisms: food intake, cellular synthesis and microbial synthesis in the gut, where ingested food is the major one (156). Shortly after a meal, polyamine concentrations in the duodenal and jejunal lumen reach almost millimolar levels, but 120 min after the meal luminal polyamine content returns to fasting level in the order of tens to hundreds of micromolar concentrations (140). Polyamines play an important role in cell proliferation and differentiation (153), because they stabilize nucleic acid structure (157) and promote protein synthesis (158).

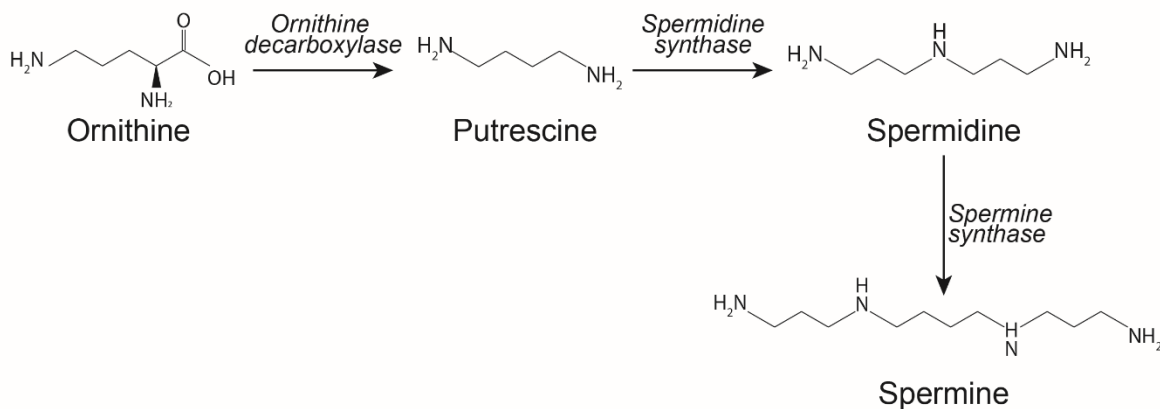


**Figure 7: Polyamine synthesis pathway in humans.**

Polyamines were described to protect bacteria against toxic effects of oxygen, superoxide, and hydrogen peroxide (159). Polyamines have been also implicated in the control of biofilm formation in several human pathogens (160). The bacterial polyamine uptake,

synthesis and degradation are coordinated to stringently regulate intracellular polyamine levels. In *E. coli*, polyamine uptake is energy dependent, and the putrescine transport system is different from the spermidine and spermine transport systems (161). Both are ABC (ATP binding cassettes) transporters consisting of a substrate binding protein in the periplasm, two channel-forming transmembrane proteins, and a membrane-associated ATPase that is involved in energy supply. The putrescine uptake system is composed by PotF, PotG, PotH and PotI proteins and the spermidine uptake system by PotA, PotB, PotC and PotD proteins. The uptake system consists of a periplasmic protein (PotD and PotF), a membrane associated protein with a nucleotide-binding site (PotA and PotG), and two membrane proteins (PotB/PotC and PotH/PotI) with six membrane-spanning segments linked by hydrophilic segments of variable length (Figure 8) (162, 163).

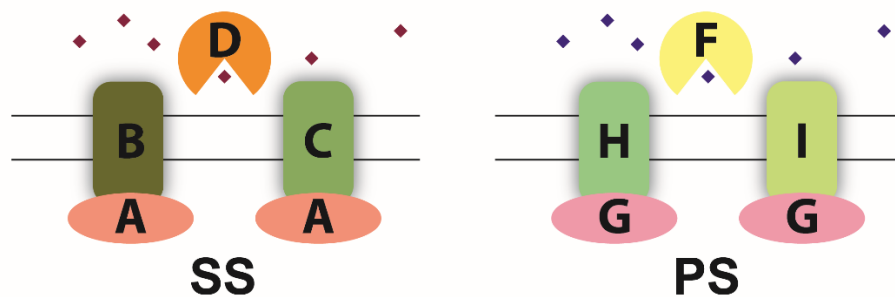


**Figure 8: Schematics of preferential transport systems for spermidine (SS) and putrescine (PS).** Spermidine is represented by red diamonds, putrescine is represented by blue diamonds that bind to the periplasmic proteins (PotD and PotF), which pass the signal to the membrane associated proteins (PotB/PotC and PotH/PotI) attached to the ATPase proteins (PotA and PotG).

### 3. Iron uptake systems in *Escherichia coli*

Several studies demonstrated that gram-negative and gram-positive bacteria exhibit increased growth following supplementation of culture medium with dopamine and other catecholamines (132, 164). These effects do not appear to be mediated by a mammalian-type adrenergic receptor, as the growth enhancement could not be blocked by standard pharmacological blocker (93). Since catechol rings are known siderophores in bacteria, it has been proposed that these effects are due to siderophore activity of the catecholamines, that enhance growth by improving iron uptake in growth-limiting media (165).

Bacteria use a variety of iron sources, the most common is  $\text{Fe}^{3+}$ . Since  $\text{Fe}^{3+}$  is insoluble in water, solubilization is required before for its uptake into the cell. Siderophores are low-molecular-weight compounds that bind  $\text{Fe}^{3+}$  tightly and specifically (166). Siderophores are synthesized by microorganisms and secreted into the surroundings. The  $\text{Fe}^{3+}$ -siderophores complexes are actively transported into the cells. Once in the cytoplasm, iron is released usually by reduction to  $\text{Fe}^{2+}$  and the siderophores degraded, modified and secreted for the next cycle of  $\text{Fe}^{3+}$  transport. Iron is transported into *Escherichia coli* by a number of chelating compounds, as citrate, ferrichrome, enterobactin, aerobactin, yersiniabactin, and heme through ABC transport systems. Transport across the outer membrane requires energy generated by the proton motive force of the cytoplasmic membrane and transmitted to the outer membrane via the TonB-ExbB-ExbD proteins (167). Binding of substrates induces structural changes in the transport proteins, but it does not open the channel. It is thought that the channel is opened by energy input from the cytoplasmic membrane. Although a basic understanding of how the transport proteins could function were obtained from crystal structures studies of three outer membrane proteins of *E. coli* and from many genetic and biochemical experiments, numerous fundamental questions still remain open. Transcription of the transport protein genes is regulated by the Fur protein, which when loaded with ferrous iron functions as a repressor. Fur also positively regulates genes of iron-containing proteins by repressing synthesis of an anti-sense RNA. Regulation of ferric citrate transport genes via a transmembrane device has become the paradigm of the regulation of a variety of systems, including the hypersensitivity response of plants to

bacterial infections (168, 169). Eight outer membrane proteins - FepA, Fiu, Cir, FhuA, FhuF, FhuE, IutA and FecA - transporting ferric siderophores have been determined (Figure 9).

The FecA protein transports ferric citrate across the outer membrane and regulates the transcription of the ferric citrate transport (170). FhuA is a multifunctional protein that transports ferrichrome (171). The FepA protein transports ferric-enterobactin across the outer membrane and serves as receptor for colicins B and D. The IutA protein transports ferric-aerobactin. Aerobactin is a siderophore synthesized by certain naturally isolated strains of *E. coli* (172). Further transport of ferric-aerobactin across the cytoplasmic membrane is mediated by the FhuBCD transport system of ferrichrome and other ferric-hydroxamate siderophores (173). The FhuE protein functions as the receptor for ferric coprogen and ferric-rhodotorulic acid (174). FhuF mediates the transport to ferrioximine B (175). Lastly, Cir and Fiu proteins were described to transport dihydroxybenzoyl serine (176, 177).

*E. coli* also grows under anoxic conditions, which predominate in the gut. In a reducing environment, iron is present as  $Fe^{2+}$ , which has a much higher solubility than  $Fe^{3+}$ . A transport system for  $Fe^{2+}$  has been characterized genetically (178). Three genes, *feoABC*, are required for  $Fe^{2+}$  uptake, where FeoB seems to be the transport protein. The function of the *feoA* gene and *feoC* gene are not known.  $Fe^{2+}$  can also be taken up by the  $Mg^{2+}$  transport system and may accumulate to toxic concentrations (95). A  $Mn^{2+}$  transport system encoded by the *mntH* gene also transports  $Fe^{2+}$  with low affinity. *mntH* is repressed by  $Fe^{2+}$ -Fur and  $Mn^{2+}$ -MntR, a specific repressor of *mntH* transcription (179).

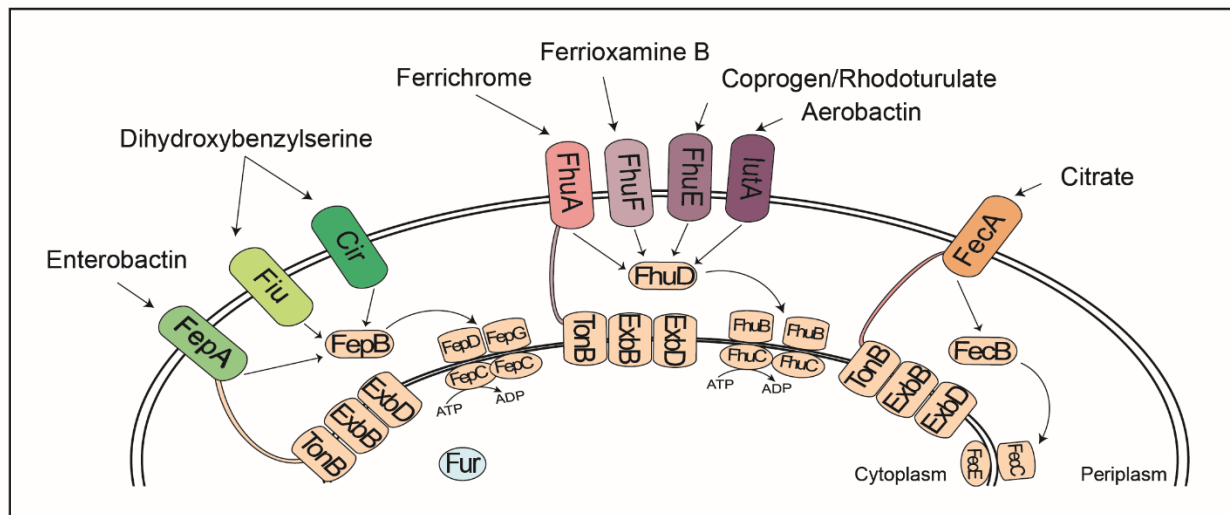


**Figure 9: Scheme of the iron transport proteins in *E. coli*.** The eight outer membrane proteins are highlighted in different colors – FepA, Fiu, Cir, FhuA, FhuF, FhuE, IutA and FecA, as well as the transport regulator Fur.

## AIMS

In the last decade, the perspective about microbial endocrinology has drastically changed with the discovery of a broader range of hormones that can affect bacteria physiologically along with the reports of bacteria that produce mammalian-like hormones. The evolution of the bacteria in the human gut suggests that it could sense and respond to the hormones in the GI tract. Since bacteria have a well-known system that sense external stimuli, the chemotaxis system, the main goal of this work was to evaluate if *E. coli* can respond chemotactically to different concentrations of compounds present in the GI tract, namely catecholamines, thyroid hormones, sex hormones, insulin and polyamines. To investigate the mechanism of these responses, we also aimed to determine their respective effects on strains expressing individual receptors, as well as various Tar constructs and hybrid receptors. Finally, we tested the effects of these compounds on bacterial growth in order to unravel the physiological importance of these hormones to bacteria.

## MATERIAL AND METHODS

### 1. Chemicals and consumables

Main chemicals and consumables used in this work are listed in Table 1.

**Table 1: List of chemicals**

Chemicals	Company
Agar bacteriology	Applichem
Agarose ultra-pure	Difco
Albumin Fraktion V	Roth
Ammonium Sulfate ((NH <sub>4</sub> ) <sub>2</sub> SO <sub>4</sub> )	Sigma
Ammonium Nitrate (NH <sub>4</sub> NO <sub>3</sub> )	Roth
Ampicillin	Applichem
Arabinose	Roth
Bacto yeast extract	BD Biosciences
Bacto tryptone	BD Biosciences
Chloramphenicol	Applichem
D-glucose	Applichem
Dimethyl sulfoxide (DMSO)	Sigma-Aldrich
DL-3,4-Dihydroxymandelic acid (DHMA)	Sigma-Aldrich
Dopamine hydrochloride	Sigma-Aldrich
D-ribose-5-phosphate	Roth
EDTA	Merck
(-)-Epinephrine	Sigma-Aldrich
β-Estradiol	Sigma-Aldrich
Glacial acetic acid	Roth
Glycerol 99.5%	Gerbu
Isopropyl-β-D-thiogalactoside (IPTG)	Roth
Insulin	Applichem
Kanamycin sulphate	Sigma-Aldrich
Lactic acid	Sigma-Aldrich
L-Arabinose	Applichem
L-Aspartate	Sigma-Aldrich
L-Dopa-(phenyl-d3) (L-3,4-dihydroxyphenylalanine)	Sigma-Aldrich
L-Leucine	Roth
L-Serine	Acros Organics
L-Threonine	Sigma-Aldrich

---

L-Tyrosine	Applichem
Magnesium sulfate (MgSO <sub>4</sub> )	Sigma-Aldrich
Melatonin powder	Sigma-Aldrich
Methionine	Roth
α-methyl-DL-aspartate (MeAsp)	Sigma-Aldrich
(-)-Norepinephrine	Sigma-Aldrich
O-xylene	Sigma-Aldrich
Poly-L-Lysine	Sigma-Aldrich
Potassium phosphate monobasic (KH <sub>2</sub> PO <sub>4</sub> )	Sigma-Aldrich
Potassium phosphate dibasic (K <sub>2</sub> HPO <sub>4</sub> )	Sigma-Aldrich
Leu-Pro hydrochloride	Sigma-Aldrich
Polyethylene glycol (PEG)	ThermoFisher
Proteinase K	ThermoFisher
Putrescine dihydrochloride	Sigma-Aldrich
Serotonin hydrochloride	Sigma-Aldrich
Sodium citrate dihydrate (C <sub>6</sub> H <sub>5</sub> Na <sub>3</sub> O <sub>7</sub> )	Sigma-Aldrich
Sodium chloride (NaCl)	Roth
Sodium salicylate	Sigma-Aldrich
Spermidine (≥99% purity)	Sigma-Aldrich
Testosterone	Sigma-Aldrich
Thiamine hydrochloride	Sigma-Aldrich
Tris base	Roth
Tryptone	Roth
Yeast Extract	Applichem

---

## 2. Media and buffer solutions

### 2.1. Media

#### **LB**

10 g	Tryptone
5 g	Yeast extract
5 g	NaCl

Adjusted to pH 7 and ddH<sub>2</sub>O was added up to a total volume of 1 L. For preparing LB agar plates, 15 g of agar were added to 1 L of LB liquid medium.

#### **TB**

10 g	Tryptone
5 g	NaCl

Adjusted pH to 7 and ddH<sub>2</sub>O was added up to a total volume of 1 L.

#### **Minimal A**

5 x minimal A salts:

26.25 g	K <sub>2</sub> HPO <sub>4</sub>
11.25 g	KH <sub>2</sub> PO <sub>4</sub>
2.5 g	(NH <sub>4</sub> ) <sub>2</sub> SO <sub>4</sub>
1.25 g	C <sub>6</sub> H <sub>9</sub> Na <sub>3</sub> O <sub>9</sub>

ddH<sub>2</sub>O was added up to a volume of 500 mL.

5 mg/mL AA-mix: L-Threonine, L-Histidine, L-Methionine, L-Leucine in ddH<sub>2</sub>O

To prepare 100 mL 1 x media:

20 mL	5 x minimal A salts
1 mL	20% glycerol
100 µL	1 M MgSO <sub>4</sub>
800 µL	5 mg/mL AA-mix
200 µL	50 mg/mL thiamine

50 mL 0.5 % agar

27.7 mL ddH<sub>2</sub>O

### **SAPI Medium**

1.25 mL 1 M NH<sub>4</sub>NO<sub>3</sub>

370 µL 1 M KH<sub>2</sub>PO<sub>4</sub>

670 µL 1 M KCl

378 µL 1M glucose

60 mL Adult bovine serum (30%)

137,3mL ddH<sub>2</sub>O

### **Glycerol-salts Medium**

2 g Glycerol

1 g (NH<sub>4</sub>)<sub>2</sub>SO<sub>4</sub>

9 g KH<sub>2</sub>PO<sub>4</sub>

0.4 g MgSO<sub>4</sub>

Adjusted pH to 6.3 and ddH<sub>2</sub>O was added up to a total volume of 1 L.

## **2.2. Buffer**

### **Phosphate buffer**

1.742 g K<sub>2</sub>HPO<sub>4</sub>

1.361 g KH<sub>2</sub>PO<sub>4</sub>

0.901 g lactic acid

Adjusted with NaOH to pH 7 and ddH<sub>2</sub>O was added up to a total volume of 1 L.

### **Tethering buffer**

5 mL 1 M K<sub>2</sub>HPO<sub>4</sub>

5 mL 1 M KH<sub>2</sub>PO<sub>4</sub>

0.2 mL 0.5 M EDTA

0.1 mL 10 mM Methionine

1 mL 90% lactic acid

Adjusted to pH 7 and ddH<sub>2</sub>O was added up to a total volume of 1L.

### **Motility buffer**

10 mL 1 M KPO<sub>4</sub>

0.2 mL 0.5 M EDTA

3.91 g NaCl

Adjusted to pH 7 and ddH<sub>2</sub>O was added up to a total volume of 1L.

### **TSS (Transfer Storage Solution)**

200 mL LB

20 g PEG 4000

10 mL DMSO

2.46 g MgCl<sub>2</sub>

Adjusted to pH 6.5.

### **TAE buffer (Tris-Acetate-EDTA - 50 x)**

242 g Tris base

57.1g Glacial acetic acid

100 mL 0.5 M EDTA, pH 8

ddH<sub>2</sub>O was added up to a total volume of 1 L.

### 2.3. Antibiotic and inducers solutions

Ampicillin (Amp): 100 mg/mL in ddH<sub>2</sub>O

Chloramphenicol (Cam): 34 mg/mL in ethanol

Kanamycin (Kan): 50 mg/mL in ddH<sub>2</sub>O

Tetracycline (Tet): 5 mg/mL in ethanol

0.1 M IPTG in ddH<sub>2</sub>O

10 % L-Arabinose in ddH<sub>2</sub>O

100 mM Sodium salicylate in ddH<sub>2</sub>O

### 3. Bacterial strains

All strains used in this work are shown in Table 2.

**Table 2: List of strains**

Strains	Relevant genotype	Source
MG1655	<i>E. coli</i> RP437 F <sup>-</sup> ( $\lambda$ ) <i>rph-1</i>	(180)
RP437	<i>E. coli</i> wild type for chemotaxis	(181)
VS104	<i>E. coli</i> RP437 $\Delta$ ( <i>cheY cheZ</i> )	(26)
VS149	<i>E. coli</i> RP437 $\Delta$ ( <i>cheR cheB cheY cheZ</i> )	(26)
VS181	<i>E. coli</i> RP437 $\Delta$ ( <i>cheY cheZ</i> ) $\Delta$ <i>tsr</i> $\Delta$ <i>tap</i> $\Delta$ <i>tar</i> $\Delta$ <i>trg</i> $\Delta$ <i>aer</i>	(26)
VH1	<i>E. coli</i> RP437 $\Delta$ ( <i>cheR cheB cheY cheZ</i> ) $\Delta$ <i>tsr</i> $\Delta$ <i>tap</i> $\Delta$ <i>tar</i> $\Delta$ <i>trg</i> $\Delta$ <i>aer</i>	(182)
UU1250	<i>E. coli</i> RP437 $\Delta$ ( <i>tar tsr trg tap aer</i> )	(183)
$\Delta$ <i>trg</i>	<i>E. coli</i> RP437 $\Delta$ ( <i>cheR-cheZ</i> ) <i>trg::Tn10</i>	(15)
$\Delta$ <i>tap</i>	<i>E. coli</i> RP437 $\Delta$ ( <i>cheY cheZ</i> ) <i>tap</i>	(8)
$\Delta$ <i>potA</i>	<i>E. coli</i> BW25113 $\Delta$ <i>potA::Km<sup>R</sup></i> , <i>Km<sup>R</sup></i> removed	This work
$\Delta$ <i>potD</i>	<i>E. coli</i> BW25113 $\Delta$ <i>potD::Km<sup>R</sup></i> , <i>Km<sup>R</sup></i> removed	This work
$\Delta$ <i>flgM::\Delta</i> <i>potD</i>	$\Delta$ <i>potD</i> ; $\Delta$ <i>tsr tar tap trg aer</i> ; $\Delta$ <i>flgM</i>	This work
$\Delta$ <i>flgM::\Delta</i> <i>potA</i>	$\Delta$ <i>potA</i> ; $\Delta$ <i>tsr tar tap trg aer</i> ; $\Delta$ <i>flgM</i>	This work
$\Delta$ <i>fhuA</i>	<i>E. coli</i> BW25113, JW0146	(184)
$\Delta$ <i>fecA</i>	<i>E. coli</i> BW25113, JW4251	(184)
$\Delta$ <i>fepA</i>	<i>E. coli</i> BW25113, JW5086	(184)
$\Delta$ <i>fiu</i>	<i>E. coli</i> BW25113, JW0790	(184)
$\Delta$ <i>cirA</i>	<i>E. coli</i> BW25113, JW2142	(184)
$\Delta$ <i>fhuF</i>	<i>E. coli</i> BW25113, JW4331	(184)
$\Delta$ <i>fhuE</i>	<i>E. coli</i> BW25113, JW1088	(184)
$\Delta$ <i>fur</i>	<i>E. coli</i> BW25113, JW0669	(184)
<i>S. typhimurium</i>	<i>Salmonella enterica subsp. enterica serovar typhimurium</i> (ATCC® 14028™)	(185)
EcoR64	<i>E. coli</i> (Migula) Castellani and Chalmers (ATCC® 35383™)	(186)

#### 4. Plasmids and oligonucleotides

All plasmids used in this work are shown in Table 3 and all primers are listed in Table 4 and Table 5.

**Table 3: List of plasmids**

Plasmids	Relevant genotype	Induction	Source
pBAD33	Expression plasmid, Cm <sup>R</sup>	Arabinose	(187)
pKG 166	Expression vector, p15A ori, Cm <sup>R</sup>	Sodium salicylate	(188)
pKG 110	Expression vector, p15A ori, nahG promoter, Cm <sup>R</sup>	Sodium salicylate	Gift from Sandy Parkinson
pVS88	CheY-EYFP / CheZ-EYFP expression plasmid, pTrc99a derivative	IPTG	(8)
pVS1092	Tar expression plasmid, pKG110 derivative	Sodium salicylate	Gift from David Kentner
pPA114	Tsr expression plasmid, pKG110 derivative	Sodium salicylate	(183)
pcp20	FLP <sup>+</sup>		(189)
pJL2	PotD expression plasmid, pKG116 derivative	Sodium salicylate	This study
Tar-Pinhead	$\Delta tsr tar tap trg aer$ ; $\Delta tar$ (44-183)=Tar <sup>o</sup> ; cheZ-ecfp / cheY-eyfp	Sodium salicylate	(190)
Tsr-Pinhead	$\Delta tsr$ [L53-V182]; pRR53 derivative	IPTG	Gift from Sandy Parkinson
Tsar	Hybrid Tsr-Tar expression plasmid; pKG116 derivative	Sodium salicylate	(190)
Tasr	Hybrid Tar-Tsr expression plasmid; pKG116 derivative	Sodium salicylate	(190)
Tar <sup>TM</sup>	Tar TM2 added II before 200V	Sodium salicylate	Shuangyu Bi, not published
Tar <sup>HAMP</sup>	Tar[1-266]-GVPQM-[272-553]	Sodium salicylate	Shuangyu Bi, not published

Table 4: List of primers

Primers	Nucleotide Sequence (5'-3')	Restriction site	Target	Source
ERI121	CAGTCATAGCCGAATAGCCT	–	Km <sup>R</sup> cassette knockouts	(191)
ERI122	CGGTGCCCTGAATGAACTGC	–		
JL01	TGTATTTCTACAACGGACCGAG	–	<i>potD</i> rev	This work
JL02	GATGATCGTCAAAGCGGTGGT	–	<i>potD</i> fw	
JL03	CAAACAACACAAGCCAAC	–	<i>potA</i> rev	This work
JL04	GCTCAAGTAGTTTATCCAT	–	<i>potA</i> fw	
JL05	GATGATGAAGGGCAAAACAA	–	<i>potF</i> rev	This work
JL06	CAGTTATAAATGTGGAGTGT	–	<i>potF</i> fw	
JL07	<u>GAATTC</u> TTAACGTCCTGCTTTTCAGCT	<i>EcoRI</i>	<i>potD</i> rev	This work
JL08	<u>CATATG</u> ATGAAAAAATGGTCACGCCAC	<i>NdeI</i>	<i>potD</i> fw	
JL09	CAGGGGGTGGTGAAAAATCA	–	Tsr-Pinhead rev	This work
JL10	TCGCTGATGTAAGTACAAGC	–	Tsr-Pinhead fw	

Table 5: List of primers for real-time qPCR

Primers	Nucleotide Sequence (5'-3')	Target	Source
JL11	GCATTTTCCATTTCCGGTGGT	<i>ypdI</i> rev	This work
JL12	GTGGCGCATCTTCTCAT	<i>ypdI</i> fw	
JL13	GCTACTGCACCGGCAAATA	<i>ykhH</i> rev	This work
JL14	GCGTATACCGCGAGGAC	<i>ykhH</i> fw	
JL15	CTCCCTCGGCCAGCATC	<i>acrS</i> rev	This work
JL16	CAATCCGCTGAAGGCAC	<i>acrS</i> fw	
JL17	GCCGATACTTTTCGAGTCAA	<i>yegJ</i> rev	This work
JL18	GTTTGTAACAATACCAGGGTCAAT	<i>yegJ</i> fw	
JL19	GTCACAGGTTGGCTTCTCATC	<i>yffS</i> rev	This work
JL20	CAAAGCGCATTTCATCAGCG	<i>yffS</i> fw	
JL21	GGTTAATGCCATTGAGCAA	<i>bdm</i> rev	This work
JL22	CACTGAGGATGTCGTTATC	<i>bdm</i> fw	
JL23	GACCTGATCATTGCCGACA	<i>fecB</i> rev	This work
JL24	GTGCCTGCATCTCTCGCT	<i>fecB</i> fw	
JL25	GCTTTCACCTGGCTCCCGTT	<i>fecA</i> rev	This work
JL26	CTCGATACCAAAGTCCTGCGG	<i>fecA</i> fw	
JL27	GCCTGCCGTGGAAATATTATGA	<i>tdcD</i> rev	This work
JL28	CACTCTGACCGTTGCGAA	<i>tdcD</i> fw	
JL29	TTTGATATCTCTCGCCCGGC	<i>tdcE</i> rev	This work
JL30	GATCAGTTCTGTGCCTGCT	<i>tdcE</i> fw	
JL31	GCAATTCGGCTGGACTAAT	<i>ynak</i> rev	This work

<b>JL32</b>	CAGAATCCATTTTGAGCATTTTC	<i>ynak</i> fw	
<b>JL33</b>	AACAACGAATCCCTGGTGTG	<i>ydaF</i> rev	This work
<b>JL34</b>	CTGTGTGCTTCTCCAACCAT	<i>ynak</i> fw	
<b>JL35</b>	ACTCTGTCATTTGGCGTGTT	<i>ybiJ</i> rev	This work
<b>JL36</b>	TTTCTCAGCCAGTTTCGCTT	<i>ybiJ</i> fw	
<b>JL37</b>	CTATGCCTCCCTGCGTGT	<i>yhaK</i> rev	This work
<b>JL38</b>	CTGAACATGATTGCCTTCGCT	<i>yhaK</i> fw	
<b>JL39</b>	AACCAACCGATGATGATCCG	<i>fhuF</i> rev	This work
<b>JL40</b>	TTCCGGCGACACATCTAATG	<i>fhuF</i> fw	
<b>JL41</b>	CAATCATGGAAAAGGCTTAC	<i>ydfB</i> rev	This work
<b>JL42</b>	GAACTGGAAAGCGCCT	<i>ydfB</i> fw	
<b>JL43</b>	ATCATCGTCAGAGAGCTGCG	<i>qseC</i> rev	This work
<b>JL44</b>	GAACGACGCTTTACCTCCGA	<i>qseC</i> fw	

## 5. Molecular cloning

### 5.1. Polymerase Chain Reaction (PCR)

The PCR reactions were performed in the thermocyclers TPersonal (Biometra) and peqSTAR (PEQLAB). The resulting fragments were analyzed in a 1% TAE-agarose gel and purified with the GeneJET DNA Purification Kit or the GeneJET Gel Extraction Kit.

#### Single Colony PCR

25 $\mu\text{L}$	DreamTaq Green PCR Master Mix (2x)
1 $\mu\text{L}$	forward primer (10 pmol/ $\mu\text{L}$ )
1 $\mu\text{L}$	reverse primer (10 pmol/ $\mu\text{L}$ )
	colony picked from plate
up to 50 $\mu\text{L}$	ddH <sub>2</sub> O

#### **Thermocycler settings**

95 °C	3 min	
95 °C	30 sec	} 30 cycles
55 °C	30 sec	
72 °C	variable (1 min/ 1 kb)	
72 °C	5 min	

#### PCR with Q5 polymerase

10 $\mu\text{L}$	Q5 reaction buffer
2.5 $\mu\text{L}$	forward primer (10 pmol/ $\mu\text{L}$ )
2.5 $\mu\text{L}$	reverse primer (10 pmol/ $\mu\text{L}$ )
1 $\mu\text{L}$	dNTPs (10 mM)
0.5 $\mu\text{L}$	Q5 high fidelity DNA polymerase
1 $\mu\text{L}$	template DNA

up to 50  $\mu\text{L}$  ddH<sub>2</sub>O

### Thermocycler settings

98 °C	30 sec	
98 °C	10 sec	} 30 cycles
Variable temperature	30 sec	
72 °C	variable (1 min/ 1 kb)	
72 °C	2 min	

### PCR with PrimeSTAR GXL polymerase

10  $\mu\text{L}$  5 x PrimeSTAR GXL Buffer  
1  $\mu\text{L}$  forward primer (10 pmol/  $\mu\text{L}$ )  
1  $\mu\text{L}$  reverse primer (10 pmol/  $\mu\text{L}$ )  
1  $\mu\text{L}$  dNTPs (10 mM)  
0.5  $\mu\text{L}$  PrimeSTAR GXL DNA Polymerase  
1  $\mu\text{L}$  template DNA  
up to 50  $\mu\text{L}$  ddH<sub>2</sub>O

### Thermocycler settings

98 °C	30 sec	
98 °C	10 sec	} 30 cycles
Variable temperature	30 sec	
72 °C	variable (1 min/ 1 kb)	
72 °C	2 min	

### 5.2. Competent cells

For producing competent cells, two different procedures were used: chemical method and one-step preparation.

#### 5.2.1. Chemical competent cells with calcium chloride

For the chemical method, 1 mL cells of an LB overnight culture were diluted into 100 mL fresh LB media and grown at 37 °C to an  $OD_{600} = 0.6$ . After harvesting the cells by centrifugation for 5 min at 4000 rpm, the pellet was resuspended in 10 mL ice-cold 0.1 M CaCl and incubated on ice for 20 min. Cells were centrifuged for 5 min at 4000 rpm and the pellet was resuspended in 5 mL ice-cold 0.1 M CaCl<sub>2</sub>, followed by another 20 min on ice. Next, cells were centrifuged as previous and resuspended in 1 mL TB with 20% glycerol and aliquoted. The aliquots were treated with liquid nitrogen and frozen at -80 °C.

#### 5.2.2. One-step preparation of competent cells

Chung *et al.* (192) developed a one-step procedure for the preparation of competent *Escherichia coli* cells, which use a transformation and storage solution (TSS). This is a much faster method, especially useful when just small amounts of competent cells are needed. 100 µL of a LB overnight culture of the cells were diluted in 3 mL fresh LB medium and grown at 37 °C to an  $OD_{600} = 0.6$ . The cells were cultured 20 min on ice. 1 mL of culture was centrifuged at 8000 rpm for 1 min and resuspended in 100 µL of TSS. The cells were then ready for transformation with the desired plasmid.

### 5.3. Transformation

#### Heat shock

0.5 µL plasmid DNA or 5µL ligation were mixed gently with 100 µL chemical competent cells in a 1.5 mL reaction tube and kept on ice for 30 min. For heat shock, the sample was heated to 42°C for 45 s in a heating block. After the heat shock, the tube was immediately placed

on ice for 5 min. 900  $\mu\text{L}$  of LB medium were added and the cells were incubated at 37 °C. After 45 min, cells were harvested and plated on LB agar plates with selective antibiotics. Plates were incubated over night at 37 °C.

#### 5.4. Restriction

Enzymes used for restriction digests were *EcoRI* and *NdeI* from Fermentas (Massachusetts, United States).

Preparative restriction digest was performed using

10 $\mu\text{L}$	Template DNA
3 $\mu\text{L}$	10x Restriction buffer 1 $\mu\text{L}$
1 $\mu\text{L}$	restriction enzymes (if same activity in double digestion)
15 $\mu\text{L}$	ddH <sub>2</sub> O

Mixture was incubated for 2-3 h at 37 °C.

#### 5.5. Ligation

Ligations were performed at room temperature for 1 h or at 16 °C overnight.

##### Ligation system

Vector DNA	1 - 2 $\mu\text{L}$ (10 - 20 ng)	Variable, according to DNA concentration
Insert DNA	3 - 5 $\mu\text{L}$ (50 -100 ng)	Variable, according to DNA concentration
10 x Ligase buffer	2 $\mu\text{L}$	1 x
Ligase	1 $\mu\text{L}$	1 U
ddH <sub>2</sub> O	up to 20 $\mu\text{L}$	

Followed by heat inactivation at 65°C for 10 min.

### 5.6. Gene deletion strains derived from Keio collection

The kanamycin resistant single-gene deletion strains of the Keio collection were used as donor strains for P1 phage transduction (193), into the MG1655 background. The resulting strains were tested for correct insertion of the FRT-site flanked kanamycin cassette into the genome, using gene and kanamycin cassette specific primers, ERI121 and ERI122 (Table 4). The kanamycin cassette was removed from the deletion strains using the temperature sensitive pCP20 plasmid encoding a FLP recombinase (189) and tested for the loss of antibiotic resistance after several rounds of growth on LB plates at 42°C. The resulting strains carry an 82-85 nucleotide scar in place of the disrupted gene (194).

### 5.7. Plasmid cloning by PCR

To determine the effect of PotD, the plasmid pJL2 was constructed. The gene *potD* was amplified using the primers JL07 and JL08. The resulting fragment was digested with *EcoRI* and *NdeI* and ligated to pKG116. The pJL2 plasmid was used to complement  $\Delta potD$  strain. To verify the correctness of the sequence, the purified plasmid DNA was sent for sequencing to the Eurofins MWG Operon (Ebersberg) company. Sequences were analyzed using the program ContigExpress of the Vector NTI advance suite 11 software (Invitrogen).

## 6. RNA Isolation and Deep Sequencing

RNA was isolated with the EURX GeneMATRIX Universal RNA Purification kit. Overnight cultures were grown in 5 mL TB medium at 30 °C at 200 rpm, from which 100 µL were inoculated into 10 mL of TB medium, with and without the tested compounds. These day cultures were grown at 37°C to early exponential phase. The isolation was performed according to the supplier's manual and, after a treatment with the TURBO DNA-free kit, tested for degradation on a formaldehyde gel. The samples were depleted for rRNA and sequenced at the Max Planck-Genome center, Cologne.

### 6.1. RNA sequencing data

The data analysis of the RNA sequencing project was performed in the ArrayStar program using student's t-test for statistical analysis and the Benjamini Hochberg procedure for multiple testing correction. Genes with a linear expression level  $<1$  in either of the samples were excluded from the data sets to perform quantile normalization. Genes with a  $\log_2$  expression level  $< 1$  have a low number of unique mapped reads and were excluded from the analysis as well.

For the analysis of the MG1655 RNA sequencing project the mean expression value of the duplicates was calculated. To study variations in the expression levels of genes between different experiments we use the fold change between one experiment serving as a control, where no supplements were added, and the second experiment, where the desired compounds were added. Fold changes are often depicted in tables or scatter plots. Tables list the logarithm of the ratio of expression in presence and in absence of the compound. In the scatter plot each dot represents a gene, its abscise being the log of the gene expression in absence, and its ordinate in presence, of the compound, where a fold change of 0 represents no changes in the gene expression between the two experiments and appears on the identity line in the middle of the plot. A fold change more than 2 can be found outside the fold lines parallel to the identity line of the scatter plot. Genes upregulated in comparison with the control experiment have a positive value in tables and can be found in the upper half of the scatter plot. Consequently, genes on the lower half of

the plot are downregulated in comparison with the control experiment and have a negative value in tables (Appendix-Figure 2).

### 6.2. Reverse transcription polymerase chain reaction quantitative real time: qRT-PCR

All samples to be compared were processed in parallel and 3 replicas of the same sample were performed. PCR reaction was done with 96 well plates (MicroAmp) covered with optical adhesive covers (Applied Biosystems). The instrument used was ABI PRISM 7700 Sequence Detection System or ABI PRISM 7000 Sequence Detection System (Applied Biosystems). The reference gene used for the experiments was *rssA*, that has been shown to be the most stably expressed gene under osmotic and acid stress in *E. coli* (195). Reaction master mix was made according to KAPA SYNR FAST one-step qRT-PCR protocol. KAPA SYBR FAST One-Step qRT-PCR Kits contain M-MuLV Reverse Transcriptase, RNase Inhibitor and a novel DNA Polymerase engineered via molecular evolution. The kit is optimized for rapid one-step, one-tube RNA quantification. The qRT-PCR reactions were carried out in a total volume of 5  $\mu$ L containing:

0.025 $\mu$ L	RT PCR Dye (200x)
0.2 $\mu$ L	Nuclease-free water
2.5 $\mu$ L	KAPA SYBR FAST qPR Master Mix (2x)
0.1 $\mu$ L	Forward primer (10 $\mu$ M)
0.1 $\mu$ L	Reverse prime (10 $\mu$ M)
0.1 $\mu$ L	KAPA RT Mix (50x)
2 $\mu$ L	Template RNA (1 ng/ $\mu$ L)

Relative gene expression levels were calculated using the comparative Ct method.

## 7. Reaction kits

The kits were used according to the guidelines given by the manufacturers.

- GeneJET DNA Purification Kit, ThermoFisher Scientific, Dreieich
- GeneJET Gel Extraction Kit, ThermoFisher Scientific, Dreieich
- GeneJET Plasmid Miniprep Kit, ThermoFisher Scientific, Dreieich
- Q5 Site-Directed Mutagenesis Kit, New England BioLabs GmbH, Frankfurt a.M.
- EURX GeneMATRIX Universal RNA Purification Kit, Roboklon GmbH, Berlin
- TURBO DNA-free Kit, Ambion ThermoFisher Scientific, Dreieich
- KAPA SYBR FAST One-Step qRT-PCR Kit, KAPA Biosystems, Wilmington, Massachusetts

## 8. Microscopy

To investigate the chemotactic responses of *E. coli* to the studied gut compounds, three different microscopy techniques were performed: flow-FRET, a microfluidic assay and a chemotactic drift assay.

### 8.1. Stimulus-dependent ratiometric FRET (flow-FRET)

The intracellular response of the chemotaxis pathway of *E. coli* was monitored using a method based on the Förster (fluorescence) Resonance Energy Transfer (FRET), between two fluorescent proteins in close proximity, when the emission band on the first covers the absorption band of the second (26). The assay relies on the phosphorylation-dependent interaction between CheY fused to yellow fluorescent protein (CheY-YFP) and its phosphatase CheZ fused to cyan fluorescent protein (CheZ-CFP) (8, 26). The FRET pair CheY-YFP and CheZ-CFP was expressed from pVS88, a bi-cistronic construct (8). When CheY is phosphorylated FRET occurs because CheY-YFP and CheZ-CFP are in close proximity, leading to a decreased YFP emission and an increased CFP. A decreased level of phosphorylation leads to a reduced interaction, decreasing YFP emission and increasing CFP emission. To minimize effects of absolute fluorescence changes due e.g. to illumination fluctuations, the amount of FRET is quantified by the ratio YFP/CFP. Binding of attractant to receptors inhibits the kinase activity of CheA, leading to a decrease in FRET. This decrease in FRET is observed as a decrease in the YFP/CFP ratio due to the reduced numbers of CheY-P-CheZ complexes. Conversely, removal of attractant or binding of repellents to the receptors leads to an increase in the YFP/CFP ratio. Hence, the YFP/CFP ratio gives a direct readout of intracellular changes of kinase activity upon stimulation (Appendix-Figure 1). Microscopy setup for the FRET measurements is shown in Figure 10. Measurements were performed as described before on custom-modified Zeiss Axiovert 200 or Axio Imager Z1 microscopes (25, 26, 196).

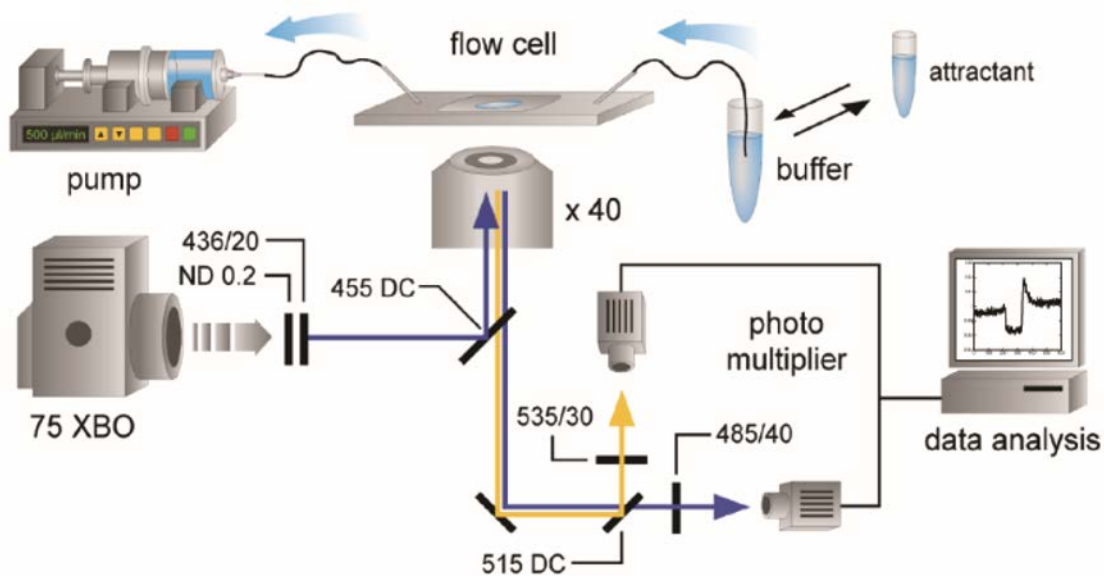


**Figure 10: Flow-FRET assay apparatus.** The microscopy setup is shown for a Zeiss Axiovert 200 microscope (Figure adapted from (196)).

### 8.1.1. Preparation of cells

Overnight cultures were grown in 10 mL (in flasks) TB supplemented with appropriate antibiotics at 30°C. 10 mL day culture were prepared with 250  $\mu$ L from overnights cultures and grown in a rotary shaker at 34 °C and 275 rpm, supplemented with appropriate antibiotics and inducers. Cells were harvested at  $OD_{600}$  0.6. by centrifugation (4000  $\times g$  for 5 min), washed with tethering buffer and stored at 4°C for 30 min to inhibit protein synthesis. Circular coverslips ( $\varnothing$  12mm) were prepared with 20  $\mu$ L of poly-L-lysine and let stand for 20 min. To prepare the samples for FRET measurements, 1.5 mL cell culture were centrifuged at 8000 rpm for 1 min and the cell pellet was resuspended in 20-40  $\mu$ L residual tethering buffer. The concentrated cells were attached to a poly-lysine-coated coverslip for 10 min and then placed into a flow-chamber that was maintained under a constant flow (0.3 mL/min) of tethering buffer using a syringe pump (Harvard Apparatus).

### 8.1.2. Data acquisition and analysis

The sample was excited at a CFP-specific wavelength of 436/20 nm by a 120W Hg-Lamp (EXFO X-Cite® 120) attenuated 500-fold with neutral density filters (upright microscope) or a 75W Xenon lamp (Hamamatsu, Bridgewater, NJ) attenuated 550-fold by neutral density filters (inverted microscope). A 455 nm dichroic mirror served to separate excitation from emission light and a second, 515 nm dichroic mirror was used to split up emission light in two spectral parts *per* second. Cells were focused with a 40x objective (Zeis Plan-Neofluar 40x/0.75) and a section of a dense and unitary monolayer comprising 500-600 cells was chosen for experimentation. Fluorescence of the cells was continuously recorded in the cyan and yellow channels using photon counters with a 1.0 s integration time and a PCI-6034E counting board connected to a computer with LabView7/Template software was used for data acquisition as counts of detected photons *per* second. Cells were allowed to adapt to the tethering buffer for at least 10 min. To stimulate the cells, solutions of different stimuli or buffer at different concentrations (see Figure 10) were rapidly exchanged with the buffer reservoir, and the change in YFP/CFP ratio was monitored for about 100 seconds for a dose response and 2-20 min for adaptation measurements.

The response was tested by stimulating cells expressing the FRET pair with serial dilutions of chemicals and measuring the subsequent change in the FRET ratio (i.e., the ratio of the YFP to CFP fluorescence emission). Stimulation with an attractant results in a rapid decrease in the FRET ratio, while stimulation with a repellent has an opposite effect. Because continuous stimulation elicits adaptive changes in receptor methylation that gradually offset the effects of either attractant or repellent, the FRET ratio typically transiently overshoots upon removal of the chemoeffector (Appendix-Figure 1) (8, 26).

FRET response was measured as the change in the ratio of YFP/CFP and normalized to the ratio change of buffer-adapted cells responding to saturating stimulation with chemical attractant, either  $\alpha$ -methyl-DL-aspartate (MeAsp) or L-serine or O-xylene.

Thus, FRET can be calculated from the changes in the ratio of YFP and CFP signals as followed:

$$FRET = \frac{\Delta R_{Max} - \Delta R}{\alpha + R_0 + \Delta R_{Max} - \Delta R}$$

where  $\Delta R$  is the change in the ratio due to energy transfer,  $\Delta R_{Max}$  is the maximal change in the ratio due to saturation amount of stimulus and  $R_0$  is the ratio in the absence of FRET. The constant  $\alpha$  is the ratio of the absolute changes of YFP over CFP fluorescence signals due to energy transfer, which is dependent on the respective sensitivities of CFP and YFP signal detection.

### **8.1.3. Preparation of stimulus solutions**

Chemical solutions were prepared in tethering buffer at a concentration of 100 mM or at the highest possible concentration if the solubility is poor. The pH of all solutions was adjusted to pH 7.0 and solutions were stored at 4 °C. For the solutions, which oxidized, fresh solutions were prepared each time on the day of the experiment.

## **8.2. Microfluidics assay**

The microfluidics assay was performed as previously described (197) *E. coli* UU1250 expressing GFP proteins were grown at 34 °C in TB supplemented with antibiotics and inducers until the  $OD_{600}$  reached 0.6. Cells were harvested by centrifugation at 3000 rpm for 3 min and washed twice with tethering buffer. The compounds were dissolved in tethering buffer and adjusted to pH 7.0.

### **8.2.1. Chamber fabrication**

For the chamber fabrication, we used a chip with 8 parallel units, as previously described (197). The distance between each unit is 9 mm, each unit has two wells at the ends serving as source and sink. The diameter of each well is 4 mm, and the volume is about 30  $\mu$ L. On the source side, there are 20 parallel channels (5  $\mu$ m wide and 300  $\mu$ m long) which are filled with agarose gel (named as agarose gel channel), and on the sink side there is a channel (200  $\mu$ m wide and 600  $\mu$ m long) which is free for cell swimming (observation channel). The

agarose gel channel is 5  $\mu\text{m}$  high while the observation channel is 20  $\mu\text{m}$  high, which is fabricated using a standard two-layer photolithography method (Figure 11). After the SU-8 master is prepared on the silicon wafer, Poly-di-methylsiloxane (PDMS), a bicomponent silicone elastomer (SYLGARD 184, 1:10 crosslinker to base ratio, Dow Corning, USA), was cast freshly mixed and let to polymerize on the master by overnight heating at 65  $^{\circ}\text{C}$ , peeled off, cut to shape and bonded on a glass slide after oxygen plasma treatment. After the agarose gel based semi-permeable channel is set up, 30  $\mu\text{L}$  chemotaxis buffer was added into the wells. As the surface is hydrophilic and PDMS can re-absorb gas within 1 h after the plasma treatment, the chemotaxis buffer solution will flow into the observation channel from the sink side well and press out the tracked air in the observation channel. The prepared device can be stored in a liquid environment before being used.

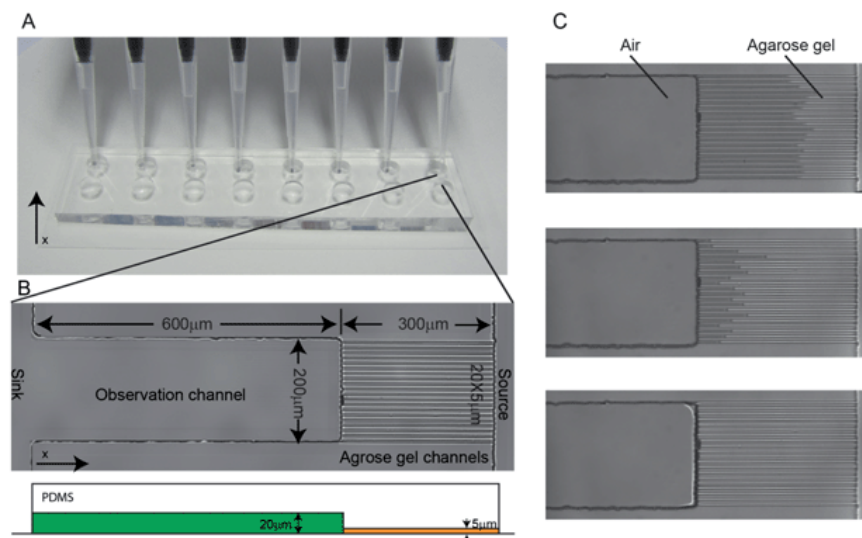


**Figure 11:** (A) A panoramic picture of the microfluidic chip. (B) The top view and the side view of the observation channel and agarose gel channel. (C) Agarose gel filling process. Figure from (197).

### 8.2.2. Data acquisition

*E. coli* cells were added at the sink side well of the device to a final  $\text{OD}_{600}$  of 1.2–2 and equilibrated for 40 min in the observation channel. Compound solutions were added at the source side well and allowed to diffuse into the observation channel for an indicated time to

establish a concentration gradient. Fluorescence microscopy on a Nikon Ti-E microscope system (Nikon Instruments Europe BV, Amsterdam, Netherlands) with a 20× objective lens was used to detect the fluorescence intensity of cells in the right side of the channel. Cellular response was characterized by the fluorescence intensity in the analysis region ( $300\ \mu\text{m} \times 200\ \mu\text{m}$ ) of the observation channel. Data were analyzed using ImageJ (Wayne Rasband, National Institutes of Health, USA).

### **8.3. Chemotactic drift assay**

The measurement of the chemotactic drift was performed as previously described (198). Cells harvested at mid-exponential growth phase were harvested by centrifugation (4000 rpm for 5 min), washed with motility buffer and stored at 4°C for 30 min to inhibit protein synthesis. Afterwards, the sample was placed in the chamber (see below). After 30 min, a linear gradient of chemoattractant is formed in the channel to which the cells respond.

#### ***8.3.1. Chamber fabrication***

The chemotaxis chambers were made by bonding glass slides and PDMS chips shaped on a SU8 master mold prepared by photolithography, similarly to the previous technique. They consisted of two reservoirs ( $0.5 \pm 0.1\ \text{cm}^2 \times 50 \pm 2\ \mu\text{m}$ ) linked via a small channel (length  $L = 2\ \text{mm}$ , width  $w = 1\ \text{mm}$ ) (Figure 12). The chambers were loaded by filling one chamber with suspended bacteria and the other suspended bacteria mixed with the target compound at the indicated concentration  $c_0$ . After filling the chamber, its openings were sealed with petroleum jelly.

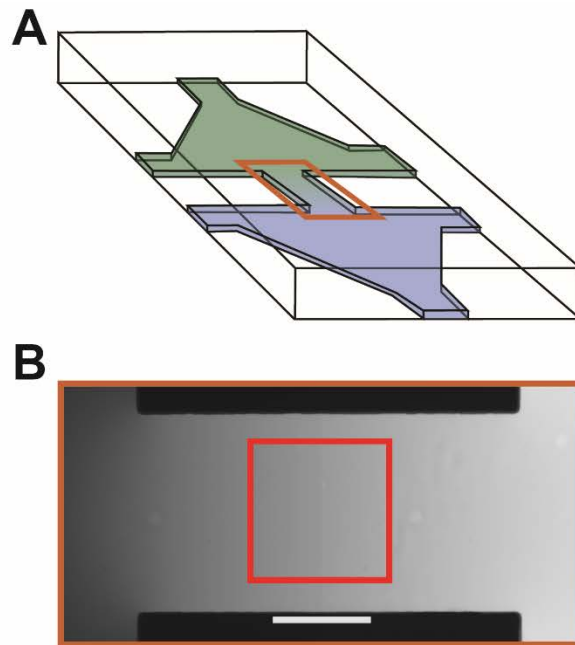


**Figure 12: Experimental set-up for measurement of chemotactic drift (A). Scheme of the experimental sample chamber made of two reservoirs, containing attractant concentrations  $c = c_0$  and  $c = 0$  (B).** The reservoirs are in contact through a narrow channel in the center highlighted by the orange rectangle. (B) Zoom on the channel in which a gradient of attractant forms, visualized here using the fluorescent dye fluorescein. The red square indicates the area of measurement. White scale bar is 500  $\mu\text{m}$ . Figure from (198).

### 8.3.2. Data acquisition

The sample was kept at room temperature ( $20 \pm 1^\circ\text{C}$ ) and the bacteria were observed with a Nikon microscope equipped with a 10 $\times$  objective (NA 0.3), under phase contrast illumination. The movement of the bacteria was recorded in the middle of the channel using a Mikrotron EoSens 4CXP camera running (Mikrotron GmbH, Unterschleissheim, Germany) at 100 Hz for 100 s, with a  $512 \times 512 \text{ px}^2$  ( $722 \times 722 \mu\text{m}^2$ ) field of view and piloted by a Matrox Radiant eV-CXP frame grabber (Matrox Electronic Systems Ltd., Dorval, Quebec, Canada) and the software StreamPix 7 (NorPix Inc., Montreal, Quebec, Canada). The focal plane was chosen halfway through the  $50 \pm 2 \mu\text{m}$  depth of the sample. Background images were computed by time averaging the movie and subtracted from each frame. The relative gradient  $\left(\frac{1}{c} \frac{\partial c}{\partial x}\right)$  is set by the fixed geometry (length) of the channel and constant for all experiments. A high throughput computer analysis of the films yielded the average

chemotactic velocity of the population  $v_{ch}$ , the population averaged swimming speed of the swimming cells  $v_0$  and the fraction of swimming cells,  $\alpha$ , which enables to estimate the chemotactic bias  $v_{ch}/\alpha v_0$ , where zero corresponds to non-responding cells and one to a population where all cells swim directly down the gradient.

## 9. Growth experiments

*E. coli* cells from an overnight culture (37°C and 200 rpm in TB) were diluted until OD<sub>600</sub> 0.05 in a total volume of 110 µL of TB medium was supplemented with the analyzed compounds in a 96-well plate (Greiner Bio-One, Frickenhausen, Germany) and OD<sub>600</sub> was measured in a plate reader (Tecan Infinite M1000, Tecan Deutschland GmbH, Crailsheim, Germany) for 14h at 37°C and 180 rpm. For the dopamine experiments, an additional baseline subtraction was required, obtained from a well containing TB supplemented with dopamine at the required concentration and no added cells.

### 9.1. Growth analysis

Growth was analyzed calculating the area under the curve divided by the duration for each individual experiment (14h), yielding a time averaged OD. For each experiment, the time averaged OD was normalized to the time-averaged OD of the control culture in TB (Figure 13). Statistical analysis was performed to assess the difference to the control with a one-tailed student t-test, p-values lower than 0.05 were considered statistically significant.

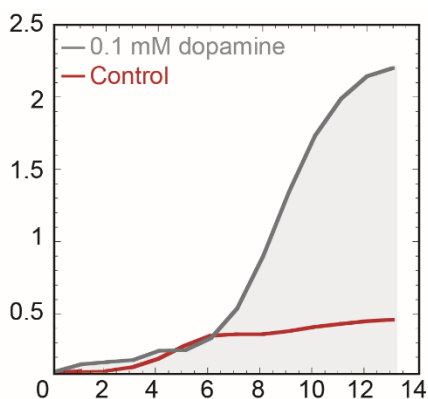


**Figure 13: Example of growth curve analysis.** The time-averaged OD was calculated as the area below the curve (grey area) divided by the duration of the experiment. For each experiment, the time averaged OD was normalized to the time-averaged OD of the control culture in TB (red dashed line).

## 9.2. Colony Forming Unit (CFU) assay

To test the effect in growth of dopamine, CFU assay was performed. *E. coli* cells from an overnight culture (37°C in TB) were diluted 1:100 in a total volume of 10 mL, mixed with dopamine at concentrations between 0-10 mM for 6 h. Cells were serial diluted until  $10^{-6}$  and  $10^{-7}$  and 100  $\mu$ L of the samples were plated on LB plates; each concentration was plated in triplicates. Plates were left at 37°C overnight. The number of colonies in each plate was counted and the CFU/mL (number of colonies/volume of inoculation x dilution) was calculated.

---

## RESULTS

### 1. Chemotaxis to gut compounds

#### 1.1. Chemotactic response of wild-type *E. coli*

To analyze the possible chemotactic response of *E. coli* to gut compounds, we performed three different assays. We first investigated the response intracellularly with the FRET assay. Second, we used a simple phenotypic swimming technique that measures the fluorescent intensity by the accumulation of bacteria in the end of the observation chamber. And third, a more sophisticated assay that measures the chemotactic drift by following the motion of thousands of individual bacterial cells was performed.

##### 1.1.1. FRET assay

As previously referred (see Material and Methods), the Förster (fluorescence) Resonance Energy Transfer (FRET) assay relies on the phosphorylation-dependent interaction between CheY fused to the yellow fluorescent protein (CheY-YFP) and its phosphatase CheZ fused to the cyan fluorescent protein (CheZ-CFP, Appendix-Figure 1) (8, 26), which allows to measure the intracellular pathway response to chemotactic stimuli.

##### 1.1.1.1. Catecholamines

The intracellular response of the *E. coli* chemotaxis pathway to the catecholamine group, the most widely studied compounds in molecular endocrinology, was first analyzed. In order to determine whether *E. coli* responds specifically to the compounds present in the gut, or rather to compounds with similar chemical structure, all players of the biosynthetic pathway for catecholamines were analyzed (Figure 3).

We did not observe a chemotactic response to L-tyrosine, consistent with previous work (190), and there was also no substantial response to L-3,4-dihydroxyphenylalanine (L-DOPA) (Appendix-Figure 3A). Notably, although L-tyrosine and L-DOPA can be detected in the GI

tract, these precursors are rapidly converted into dopamine in the gut lumen and therefore unlikely to form stable gradients (127, 199, 200).

In contrast, the two major neurotransmitters of the catecholamine pathway, dopamine and NE, elicited biphasic responses. Dopamine was sensed as a repellent when cells were stimulated with concentrations below 1 mM, since the FRET ratio increased upon addition of dopamine, and decreased upon its removal. In addition, at high concentration (10 mM dopamine), the response changed to attractant, similar to the MeAsp response (Figure 14A, B).

The response to NE was generally less pronounced, and it had an inverse pattern compared to the dopamine response. NE responded as a weak attractant at low concentrations, as previously reported (75, 76), but produced a repellent response above 1 mM (Figure 14C, D). The response to DHMA was similar, but stronger than the NE response, with a very weak attractant response until approximately 50  $\mu$ M that at higher concentrations changed to a strong repellent response (Figure 14E, F). An attractant response to DHMA had also been previously observed in the same study, and it was concluded that the NE response observed was actually due to its conversion to DHMA (75)

Lastly, we analyzed the response to epinephrine, the last compound in the catecholamine pathway. Though epinephrine elicited a repellent response (Appendix-Figure 4), interpretation of these data was complicated due to a strong autofluorescence of epinephrine that interfered with FRET measurements, and we instead used microfluidics to assess the chemotaxis response to epinephrine (see section 1.1.2).

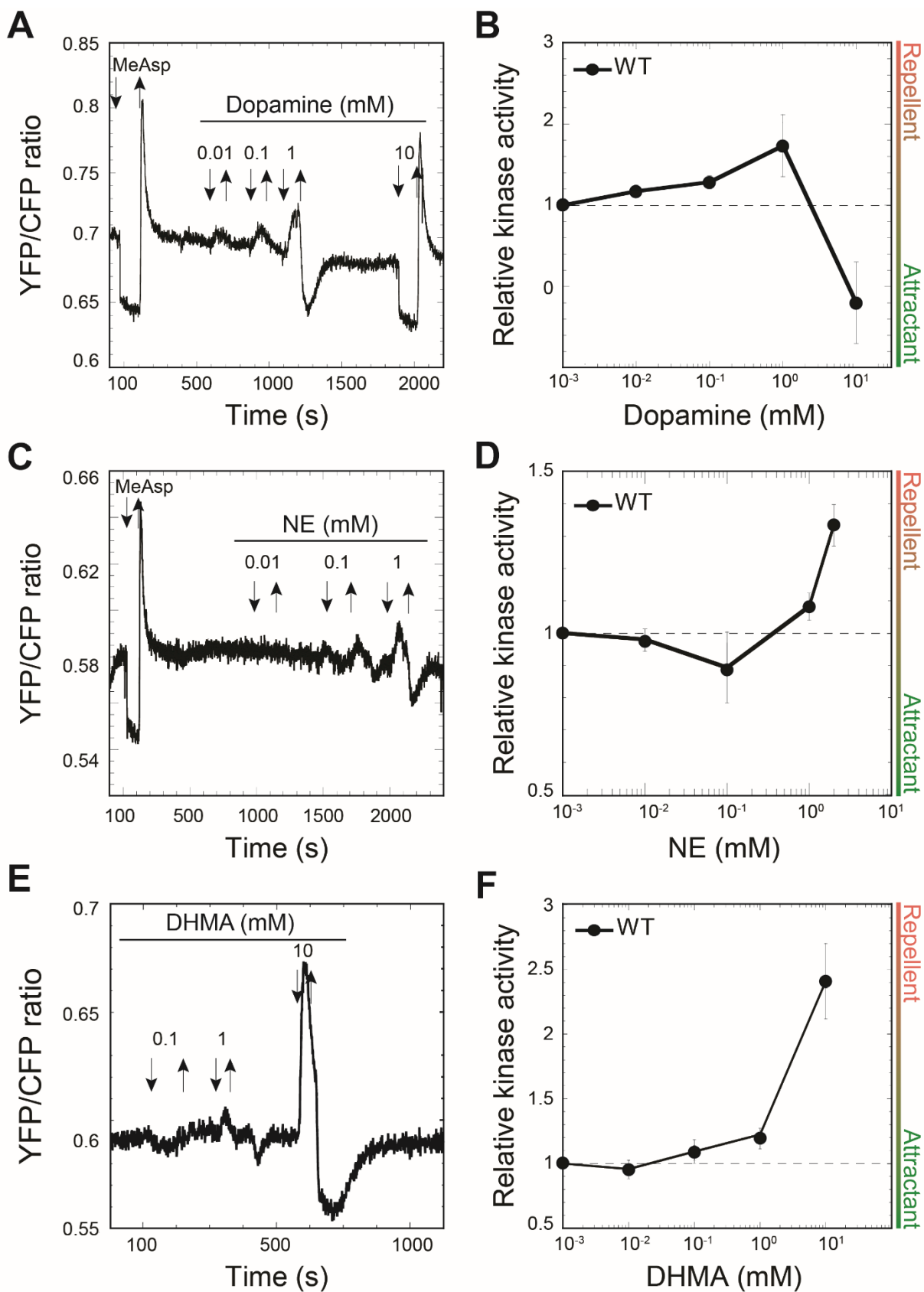


**Figure 14: Typical chemotactic pathway response for wild type to dopamine (A), norepinephrine (NE) (C) and 3,4-dihydroxymandelic acid (DHMA) (E).** The ratio of YFP/CFP fluorescence reflects the activity of the chemotaxis pathway. Buffer-adapted cells were stimulated with step-like addition and subsequent removal of compounds, indicated by downward and upward arrows, respectively. Saturating stimulation with 1 mM  $\alpha$ -methyl-DL-aspartate (MeAsp) was used as a positive control. **Dose responses of wild-type cells to dopamine (B), NE (D) and DHMA (F).** Each point represents the mean FRET-measured values of the kinase activity, normalized to the baseline in buffer, from at least three independent experiments, with error bars indicating the standard error of the mean. Values above one correspond to a repellent response, while values below one correspond to an attractant response, as indicated.

### 1.1.1.2. Thyroid hormones

We analyzed the responses of the two major thyroid hormones, serotonin and melatonin (Figure 4). *E. coli* was previously shown to not respond to the precursors of the thyroid hormones, L-tryptophan (190). While no significant chemotactic response was observed for serotonin (Appendix-Figure 3B), wild-type *E. coli* cells exhibited strong dose-dependent repellent response to melatonin, at concentrations above 0.1 mM (Figure 15A, B). The lack of response towards serotonin was surprising, since it is present in the enterochromaffin cells of the gastrointestinal mucosa and within neurons in the enteric nervous system (201) and therefore available in high concentration in the gut, where it plays a role in microbial endocrinology (202-204).

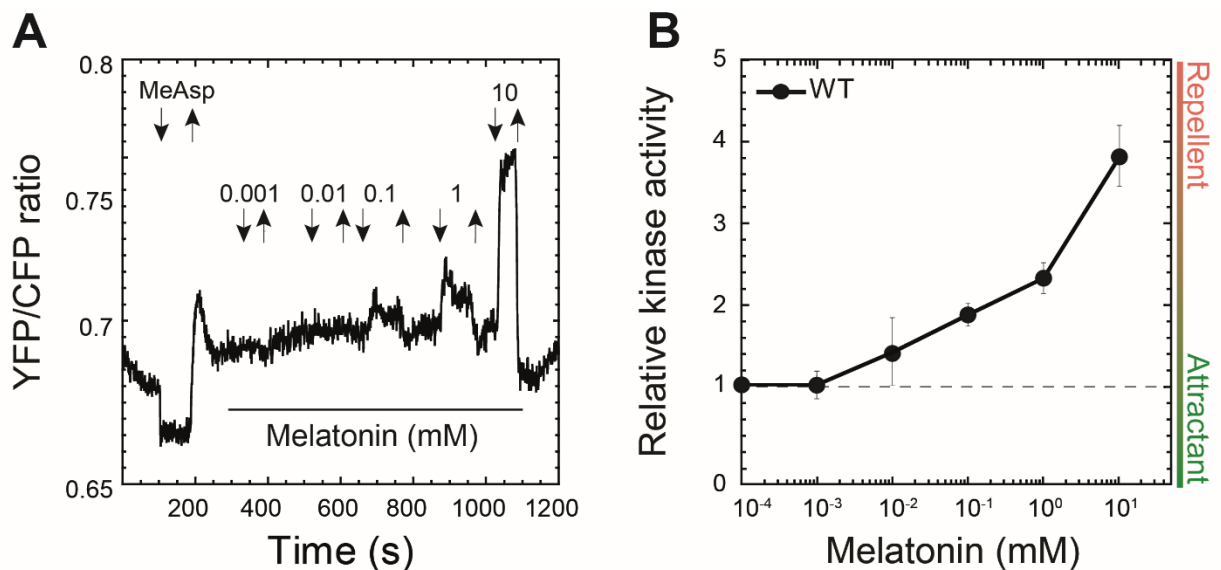


**Figure 15: Typical chemotactic pathway response (A) and dose response (B) of wild type to melatonin,** performed as in Figure 14.

### 1.1.1.3. Polyamines

Among the two tested polyamines, putrescine and spermidine, *E. coli* did not exhibit any significant response to putrescine (Appendix-Figure 3B), consistent with the fact that putrescine does not accumulate in the GI lumen since it is rapidly taken up or converted to spermidine and spermine in the small intestine (205). In contrast, we observed a strong repellent response to spermidine in the millimolar concentration range (Figure 16A, B). The exact concentration of spermidine in the gut lumen is still unclear, but it is believed that it can reach tens to hundreds of micromolar concentration (140).

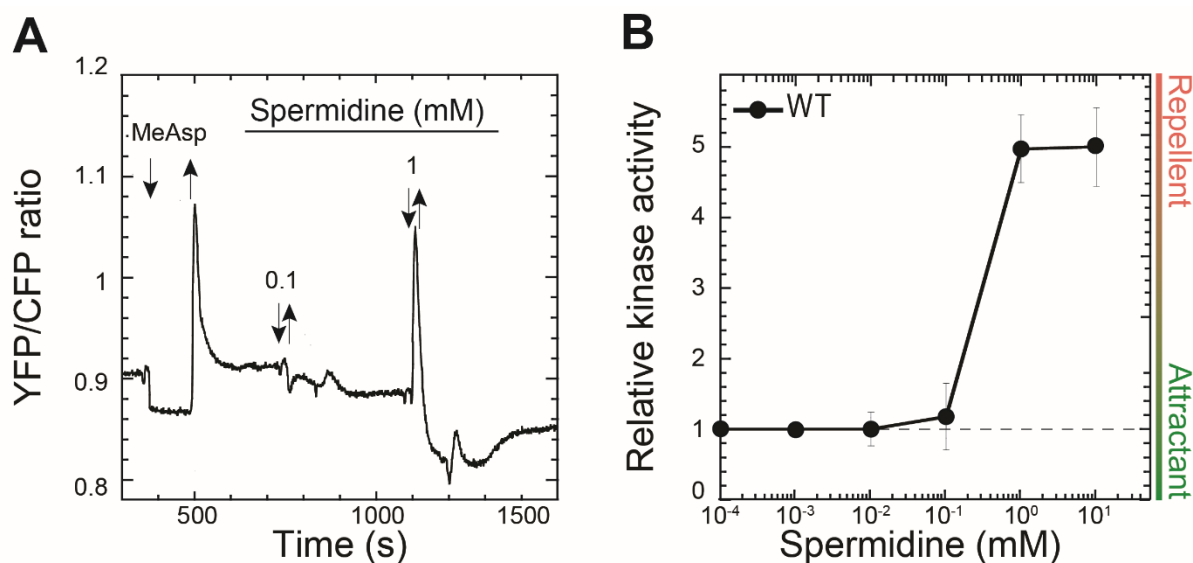


**Figure 16:** Typical chemotactic pathway response (A) and dose response (B) of wild type to spermidine, performed as in Figure 14.

### 1.1.1.4. Other hormones: $\beta$ -estradiol, testosterone and insulin

Additionally to the above described compounds, we analyzed other hormones that may be present in the human gut, the sex hormones  $\beta$ -estradiol and testosterone, and insulin. While we did not observe a response for  $\beta$ -estradiol, a strong repellent response was observed for testosterone (Figure 17). This response is likely to be related to membrane stress, since testosterone is a product of cholesterol that is known to interfere with the

membrane of *E. coli* (206). The real concentration of sex hormones in the GI tract is unknown, but several reports describing interactions between bacteria and sex hormones have reported (147, 148).

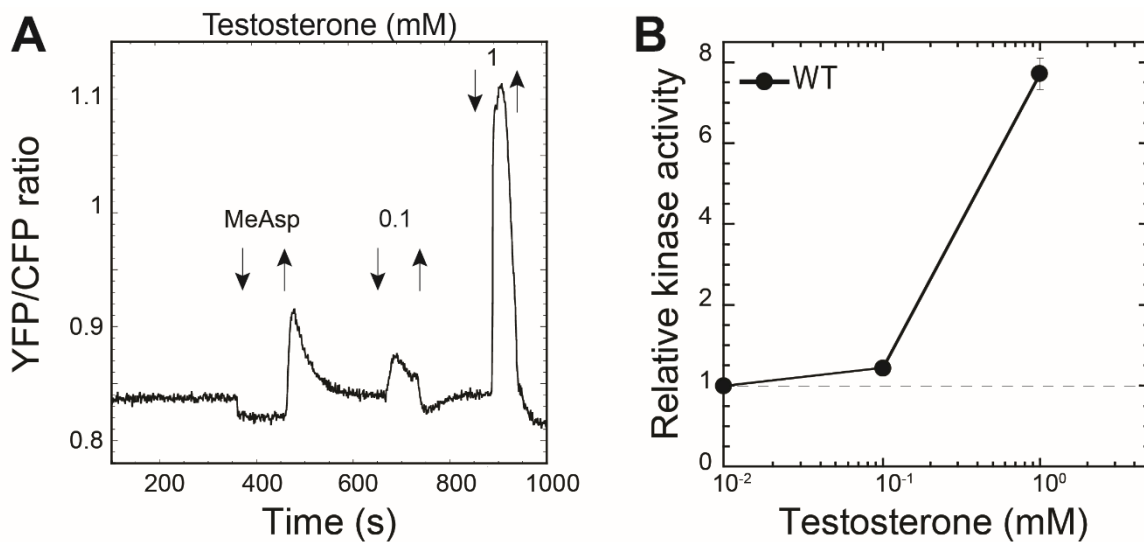


**Figure 17:** Typical chemotactic pathway response for wild type to testosterone (A), performed as in Figure 14.

Interestingly, we observed a biphasic response for insulin that changed from attractant to repellent, around 1mM, possibly due to the development of some toxic effect at high concentrations (Figure 18). Since insulin is much larger than other *E. coli* ligands (5.8 KDa, compared with e.g. dopamine  $\approx$  0.19 KDa or aspartate  $\approx$  0.13 KDa), it was surprisingly that we obtained a chemotactic response. Insulin is composed of two peptide chains referred to as the A-chain and B-chain. A- and B-chain are linked together by two disulfide bonds, and an additional disulfide is formed within the A-chain. In most species, the A-chain consists of 21 amino acids and the B-chain of 30 amino acids (Figure 6). Degradation of commercial insulin due to shaking and high temperatures, specially by deamination, has been previously described (207). To ensure that the observed response was not due to amino acid residues or residues in the insulin buffer, we partial digested and denatured insulin, to determine if the chemotactic response changed. Insulin was denatured at high temperatures (95°C) and digested with proteinase K. Although the response to insulin did not ceased with the denatured insulin, it shifted from repellent to attractant at 1 mM (Figure 18). The results to

digested insulin were inconclusive because proteinase K, which could not be entirely removed from the solution, interfered with the FRET signal (data not shown). Additionally, we analyzed the response to only the A-chain of insulin (Figure 18). The pathway responded to the A-chain of insulin only at 1 mM. The A-chain of insulin elicited a slightly weaker repellent response than the intact insulin at this concentration (Appendix-Figure 5). These results support the hypothesis that the repellent response observed at this range is specific to insulin and that the attractant response, obtained with denatured insulin, is due to the presence of single amino acids.

Taken together, *E. coli* senses insulin as an attractant that shifts its response to repellent at high concentrations. However, the attractant response at lower concentrations is likely due to degradation of amino acids. Nevertheless, this response needs to be further investigated and confirmed.

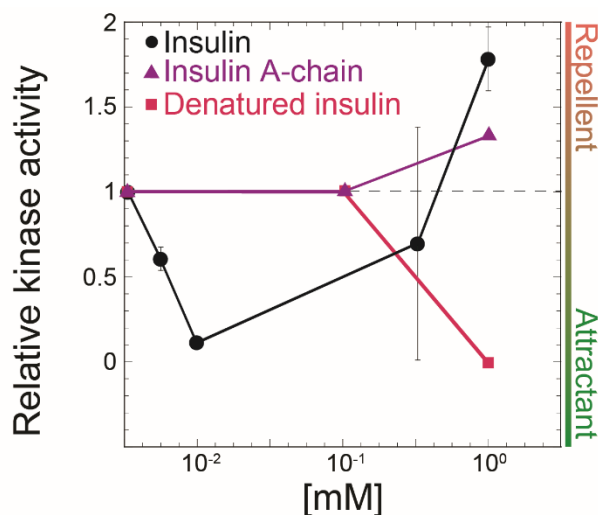


**Figure 18:** Dose responses of wild-type cells to filtered insulin (circles), insulin A-chain (triangle) and denatured insulin (square), performed as in Figure 14.

### 1.1.2. Microfluidic assays

To confirm the FRET results we analyzed the chemotactic behavior of *E. coli* to gut compounds with two different microfluidic assays.

In the first assay, the responses of wild-type cells to catecholamines were tested in microfluidic channels. The microfluidic device used has a gel-based membrane that prevents bacteria to get across, but permits the diffusion of small molecules, in a flow-free channel that generates a concentration gradient for bacterial chemotaxis (see Material and Methods).

Although the observed attractant chemotactic behavior were consistent with the FRET data, repellent responses were more difficult to detect. Since dopamine elicits biphasic responses at different concentrations, the wild-type cells were tested in gradients of 0, 1 and 10 mM of dopamine. As shown in Figure 19, the highest concentration produces a strong attractant response, as in FRET, opposite to the weak response observed at 1 mM. Correspondingly, the response to NE in the wild type was less obvious, when compared to the repellent response in FRET. The response to DHMA for the wild-type strain was in agreement with the obtained repellent response in FRET (Figure 19).

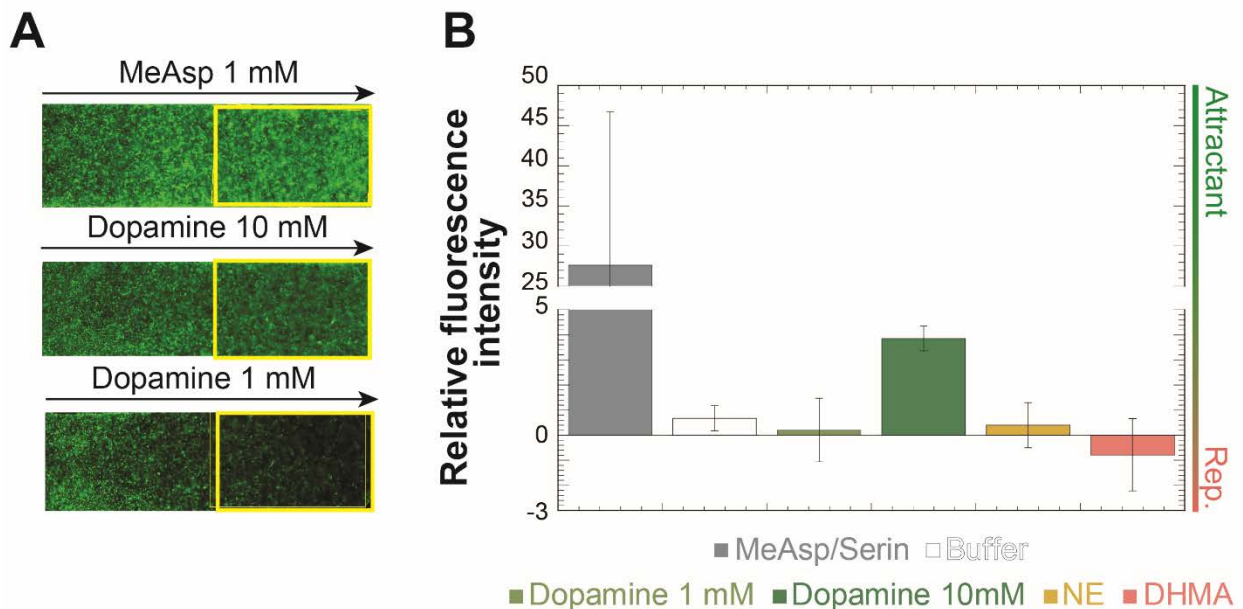


**Figure 19:** (A) Typical examples of the chemotactic response in microfluidic assay to 1 mM of MeAsp and to 1 and 10 mM of dopamine. The arrow on the image indicates the direction up the concentration gradient of each ligand, where the highest concentration of ligand is located on the right edge of the observation

chamber. The response is characterized by measurements of the fluorescence intensity in the end of the observation chamber, indicated by a yellow rectangle (300  $\mu\text{m}$   $\times$  200  $\mu\text{m}$ ). **(B) Relative fluorescence intensity values of the tested compounds to wild-type cells.** The values of the fluorescence intensities in the referred area 30 min after ligand addition were normalized to the fluorescence intensity at time 0. The highest concentration analyzed was 10 mM of dopamine, all the remaining compounds were analyzed at 1 mM of concentration. Values above 0 correspond to an attractant response, while values below 0 correspond to a repellent response, as indicated. For the positive control, the fluorescent intensity was measured in a gradient of 1 mM MeAsp and buffer was used as a negative control. Error bars indicate the standard error of the mean of at least three independent measurements.

To get further insights into the motion of a bacterial cell population we used a different technique, the chemotactic drift assay. This assay applies a recently described technique that allows measurements of the average motion of a bacterial population in linear chemical gradients, characteristic for chemotaxis (198, 208). The observed chemotactic behavior was consistent with the FRET responses for the wild-type strain (Figure 20). The wild-type strain showed repellent response to all tested hormones in the 0 to 1 mM gradient, similar to the dominant response observed in this concentration range by FRET. For epinephrine, we observed an attractant response, consistent with a previous report (76). In addition, melatonin showed a repellent response, consistent with the FRET data. Finally, the wild type showed a strong repellent response to spermidine. Although the observed chemotactic drift away or towards the gut compounds was overall weaker than the drift in gradients of MeAsp (198, 208), it was similar to chemotaxis observed towards metabolized strong attractants of Tar or Tsr, aspartate and serine, respectively. Furthermore, statistical analysis was performed to confirm the difference between the chemotactic drift responses and zero, which corresponds to non-responding cells. The wild-type cells showed statistically significant responses towards all tested compounds, what suggests that degradation of attractants generally weakens the response that can be measured using this microfluidic assay, which is not surprising given the relatively high density of bacteria within the channel in these experiments.

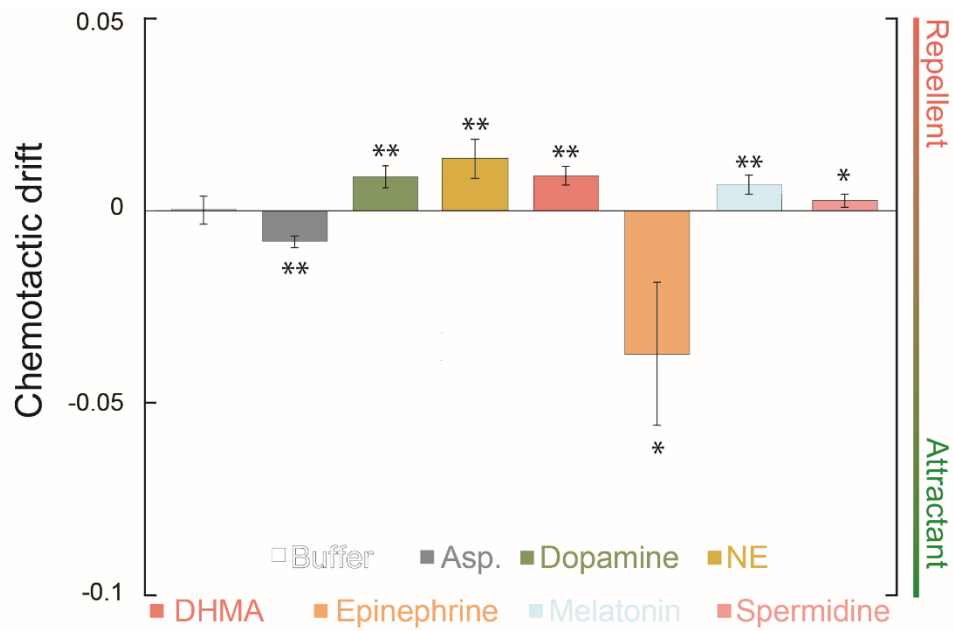


**Figure 20: Chemotactic response in gradients of gut compounds.** Chemotactic drift (see Material and Methods) was measured in gradients of dopamine, NE, DHMA, Epinephrine, Melatonin or Spermidine established in a microfluidic device. Zero chemotactic drift corresponds to non-responding cells and one to direct swimming up (negative values) or down (positive values) the gradient. For the negative control, drift of the wild-type cells was measured in buffer in absence of gradients. For the positive control, the drift was measured in a gradient of 0 to 1 mM aspartate (Asp.) for the wild type. As a reference (not shown), the chemotactic drift of the wild-type cells in a gradient of non-metabolized attractant MeAsp had an average value of -0.1 (198). Error bars indicate the standard error of the mean. One-tailed student t-test was performed to assess the significance of the response being different from 0 (\*\*:  $P \leq 0.05$ ; \*:  $P \leq 0.1$ ).

## 1.2. Mechanism of hormone sensing

In order to identify which receptor(s) sense each hormone at different concentrations, and how hormones are sensed in general (e.g. by the periplasmic, cytoplasmic or membrane perturbation), we performed FRET experiments in strains with different receptor backgrounds. Strains expressing only one chemoreceptor, just the cytoplasmic part of the receptors, hybrids that combine domains from different receptors, and mutants of Tar with changes in the transmembrane region and in the HAMP domain, were analyzed.

Briefly, the topology of the ligand-binding chemotaxis receptors is composed of a transmembrane sensory domain, a signal conversion domain, and a signaling domain that interacts with the kinase. The transmembrane sensory domain consists of an extracellular sensory domain and two transmembrane regions TM1 and TM2. When ligand binds to the pocket inside the sensory domain, it triggers conformational changes in the TM region. This conformational signal is further transduced to the cytoplasmic part of the receptor that converts the signal, consisting of a HAMP domain. The signaling domain contains a MH bundle, a flexible bundle, and a protein contact region that interacts with the kinase and regulates its activity. The conventional response to known ligands is mediated by the ligand binding to the periplasmic sensory domain (25).

### 1.2.1. Responses to hormones mediated by an interplay between Tar and Tsr

Known ligands of *E. coli*, such as amino acids, are recognized to be mediated by the two more abundant chemotaxis receptors Tar and Tsr (21, 51). In order to identify the role of these two major receptors in the overall chemotactic response to gut compounds, FRET measurements were also performed in strains expressing only one of the chemoreceptors, at levels similar to the net endogenous expression in the wild type (Appendix-Figure 6).

We observed that both Tar and Tsr could mediate responses to the four analyzed catecholamines, indicating that chemotaxis of wild-type *E. coli* results from an interplay between Tar- and Tsr-mediated responses. The Tsr-mediated response apparently makes a

larger contribution to the behavior of the wild-type cells, consistent with Tsr being the most abundant receptor under our growth conditions (15, 209).

Specifically, Tar mediated an attractant response to dopamine, whereas the Tsr-only strain showed the same biphasic trend as the wild type, switching from repellent to attractant (Figure 21A, Appendix-Figure 6A, B). For NE, Tar showed an attractant response (Appendix-Figure 6C), whereas Tsr sensed NE as a repellent over the entire concentration range (Figure 21B, Appendix-Figure 6D). For DHMA, both Tar and Tsr mediated repellent responses (Figure 21C, Appendix-Figure 6E, F). These results suggest that – in contrast to a previous report (75) – the NE sensing could not be solely explained by the conversion of NE into DHMA, since Tar responses to NE and DHMA were clearly different.

Additionally, in the case of melatonin, Tar and Tsr mediated a repellent response, similar to the response of the wild-type strain (Figure 21D, Appendix-Figure 6G, H). In Tsr-only cells, the relative kinase activity change was the strongest. Thus, *E. coli* sensing melatonin imply, as for the catecholamines, an interplay between the major chemoreceptors Tar and Tsr, which results in an intermediary response in the wild type cells.

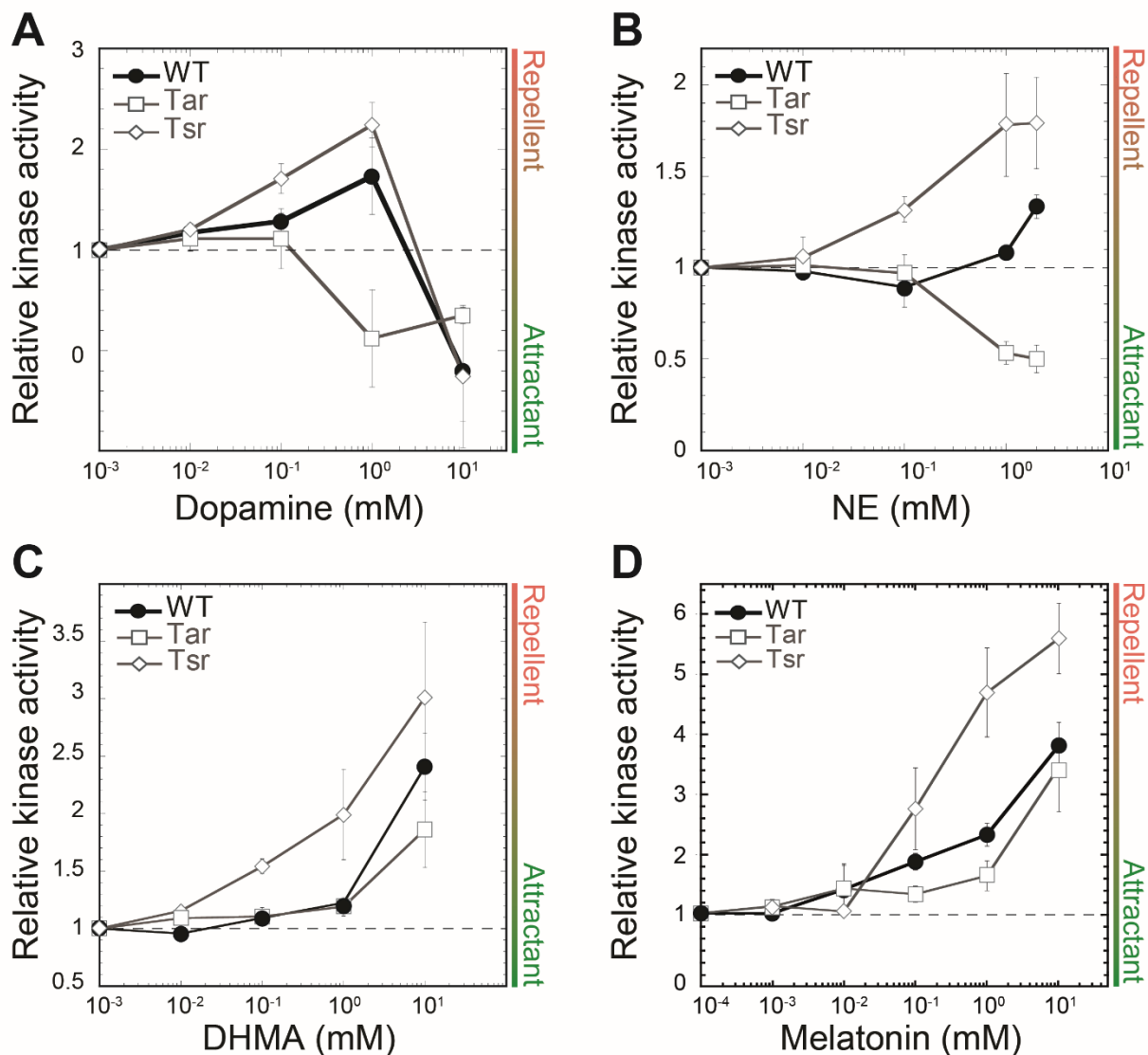


**Figure 21:** Dose responses of wild-type cells (circles), Tar-only cells (squares) or Tsr-only cells (diamonds) to dopamine (A), NE (B), DHMA (C) and melatonin (D), performed as in Figure 14. Error bars correspond to the standard error of the mean of three independent experiments.

The insulin response for Tsr and Tar-only cells strains showed always an attractant response towards insulin. As detected for the remaining hormones, the response of the Tsr-only cells was more sensitive than the remaining strains (Figure 22, Appendix-Figure 7A, B). In opposition to the previous hormones, the wild type response to insulin cannot be accounted by a combination of Tar- and Tsr-mediated responses. However, it remains

unknown whether these responses are indirect or mediated by one of the low-abundance receptors, Tap or Trg, and more experiments are required.

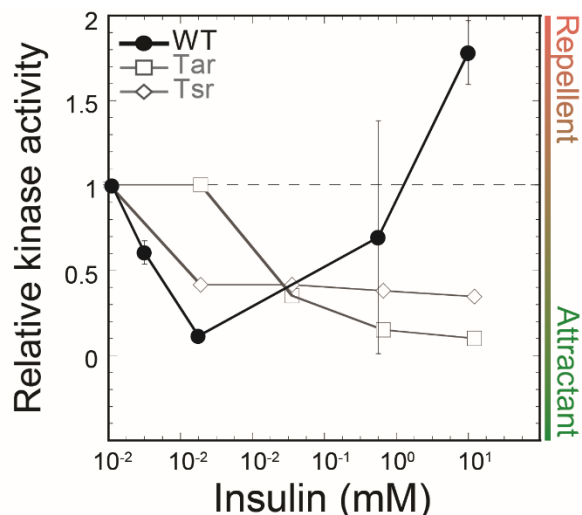


**Figure 22:** Dose responses of wild-type cells (black circles), Tar-only cells (white squares) or Tsr-only cells (white diamonds) to insulin, performed as in Figure 14. Error bars correspond to the standard error of the mean of three independent experiments.

As performed for the wild type results, the results obtained for the Tar and Tsr-only cells were confirmed with the chemotactic drift assay. The observed chemotactic behavior was consistent with the FRET responses for the single-receptor strains, as observed for the wild type, (Figure 23). The Tsr-only strain showed repellent responses to all tested hormones in the 0 to 1 mM gradient, similar to the dominant response observed in this concentration range by FRET. In contrast, Tar showed attractant responses to dopamine and NE, but a repellent response to DHMA, again consistent with the FRET data. For epinephrine, we observed an attractant response for all strains, consistent with a previous report (76). In addition, melatonin showed a repellent response in the two strains, consistent with the FRET data. Finally, Tar- and Tsr-only strains showed either attractant or no response to spermidine, respectively.

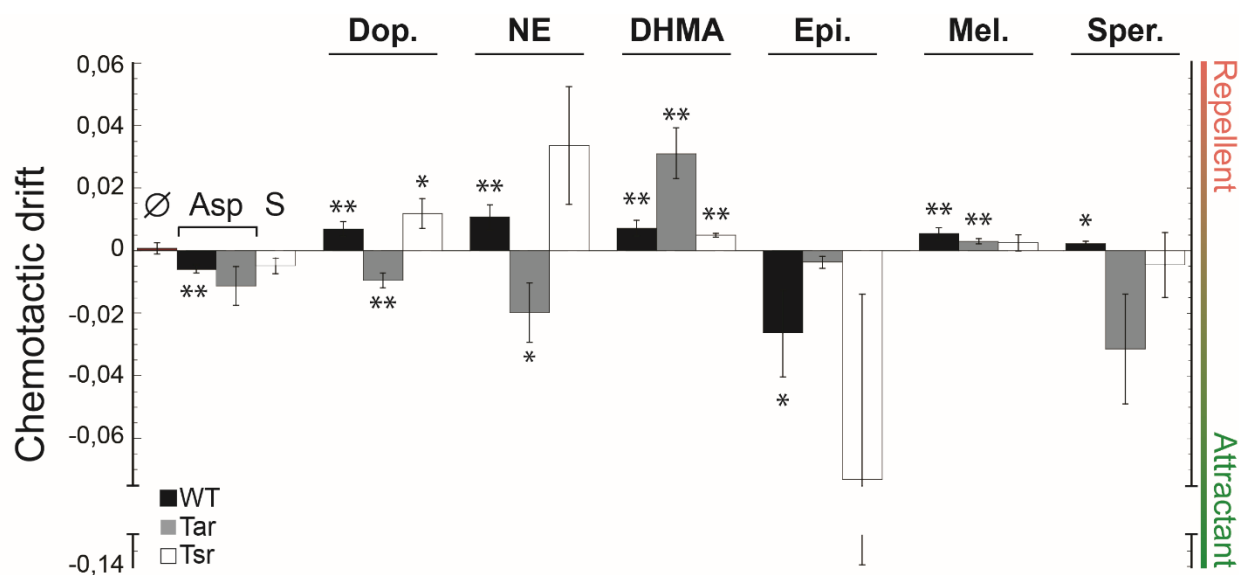


**Figure 23: Chemotactic response in gradients of gut compounds.** Chemotactic drift was measured in gradients of dopamine, NE, DHMA, Epinephrine (Epi.), Melatonin (Mel.), Spermidine (Sper.) or buffer ( $\emptyset$ ) established in a microfluidic device, performed as in Figure 20. For the positive control, the drift was measured in a gradient of 0 to 1 mM aspartate (Asp.) for the wild-type and Tar-only cells or in a gradient of 0 to 1 mM serine (S) for Tsr-only cells. One-tailed student *t*-test was performed to assess the significance of the response being different from 0 (\*\*:  $P \leq 0.05$ ; \*:  $P \leq 0.1$ ).

### 1.2.2. Response to hormones are mainly mediated by the signaling domain

As previously mentioned the conventional response to known ligands of the chemotaxis pathway is mediated by the ligand binding to the periplasmic sensory domain (25). To determine if the response to hormones is mediated by the periplasmic sensory domain of Tar and Tsr, we used “pinhead” Tar and Tsr constructs that lack the entire periplasmic domain, but are nevertheless able to activate the kinase (210).

Starting with dopamine, Tar-pinhead and Tsr-pinhead strains both mediated responses towards dopamine. While below 0.1 mM, the Tar-pinhead strain showed a repellent response similar to the Tar strain response, at higher concentrations, dopamine became an attractant for the full Tar while remaining repellent to Tar-pinhead. Interestingly the sudden shift to attractant observed in the Tsr-only cells could not be reproduced in the Tsr-pinhead strain (Figure 24A). These results suggest that the response to dopamine at high concentrations may be accounted by the sensory domain of the receptors.

The response of Tar and Tsr-pinhead strains followed the same trend as for the Tar and Tsr strains for the remaining hormones – NE, DHMA and melatonin. Though the amplitude of the response was generally weaker than for the full-length receptors (Figure 24B, C, D), this weaker response may be accounted by a different conformation of this strains. Interestingly, at 10 mM of NE the response for the pinhead constructs showed a stronger response than the full-length receptors (Figure 24B).

These results suggest that the sensing mechanism of these hormones probably originates in the signaling domain, since the responses had overall the same signal. However, for dopamine and NE the response at high concentrations may involve a different domain or mechanism. For example, at high concentrations the response is likely due to the sensory domain, which we did not observe at lower concentrations.

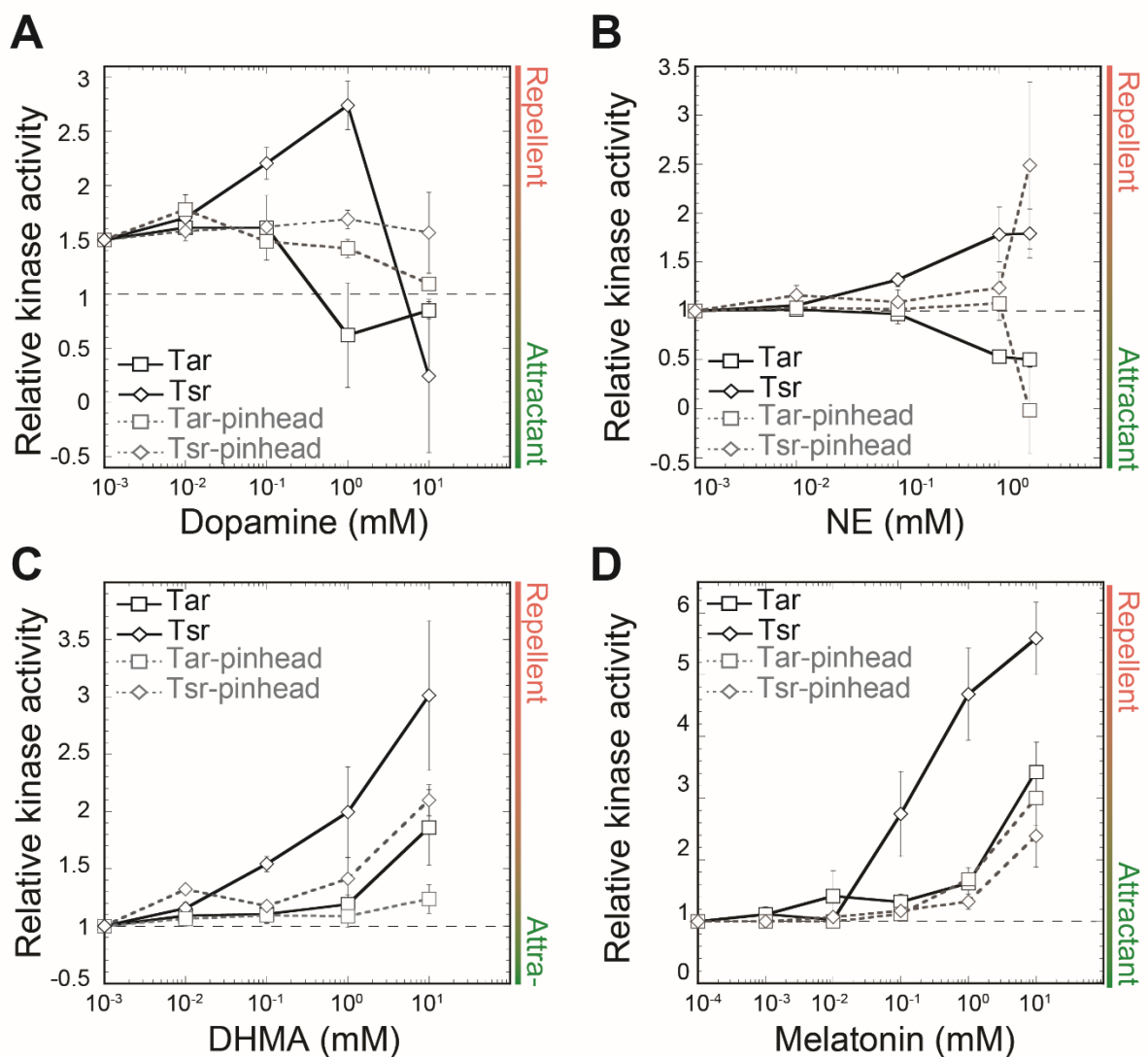


**Figure 24:** Dose responses of strains expressing only Tar (squares) or Tsr (diamonds) to dopamine (A), NE (B), DHMA (C), melatonin (D) and spermidine (E), as performed in Figure 14. Responses of strains harboring full-length receptors are represented with full lines, pinhead construct responses are shown with dashed lines. Error bars correspond to the standard error of the mean of three independent experiments.

In order to narrow down the hormones sensing mechanism we also investigated the response to catecholamines in hybrid receptors and Tar constructs.

We first investigated hybrids of Tar, with changes in the transmembrane region or in the HAMP domain, Tar<sup>TM</sup> and Tar<sup>HAMP</sup> strain respectively. In the Tar<sup>TM</sup> strain, two amino acids were added in the transmembrane region and in the Tar<sup>HAMP</sup> strain, a random linker was introduced after the HAMP domain (Figure 25). Both insertions invert the chemicals

response when the ligands are sensed upstream of the insertion. The Table 6 displays all strains used in this study, as well as the controls response to wild type, Tar- and Tsr-only. The studied hybrids combine the sensory domain of one receptor and the signaling domain of the other receptor (Figure 25) (28). Thus, the Tasr strain couples the sensory domain of Tar with the signaling domain of Tsr. Complementary, the Tsar strain combines the sensory domain of Tsr with the signaling domain of Tar. Surprisingly, an attractant response sensed by the Tar signaling domain elicits an increase in the kinase activity, which is translated into a typical repellent response in this strain. This inversion probably originates from a different conformation that appears to change the signal transduction through the receptor.

**Table 6: Chemotaxis responses to  $\alpha$ -methyl-DL-aspartate (MeAsp) and L-serine of all analyzed strains and constructs in this work.**

Strains	MeAsp response	Serine response	Refs
WT	+	+	(211)
Tar	+	+	(211)
Tsr	+	+	(211)
Pin-Head Tar	+	+	(28)
Tsar	-	+	(28)
Tasr	+	+	(28)
Tar <sup>HAMP</sup>	-	+	Shuangyu Bi, unpublished data
Tar <sup>TM</sup>	-	+	Shuangyu Bi, unpublished data

+: attractant response; -: repellent response; NA: no response or not determined

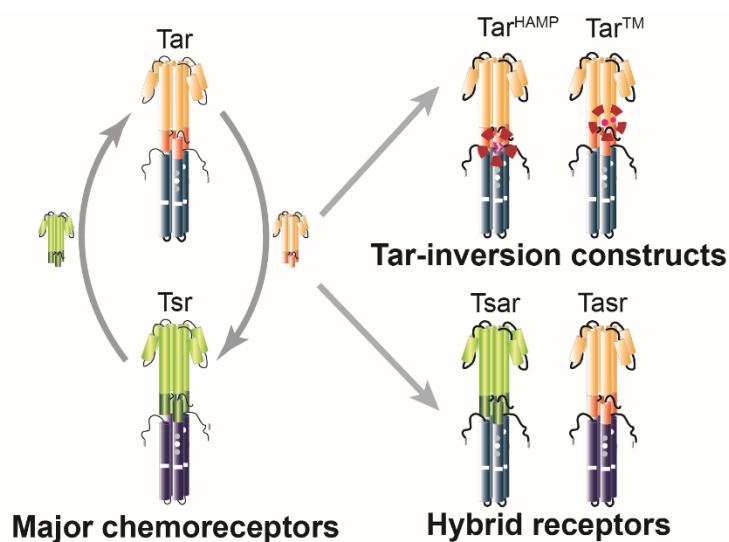


**Figure 25:** Cartoon illustrating Tar-Tsr hybrids (Tsar and Tasr) and Tar constructs (Tar<sup>HAMP</sup> and Tar<sup>TM</sup>). Domains of Tar are shown in orange and domains of Tsr in green. In the Tar<sup>TM</sup> strain two amino acids were added in the transmembrane region, marked with pink circles and in the Tar<sup>HAMP</sup> strain a random linker was introduced after the HAMP domain, marked as a pink string.

First, we identified which part of the Tar receptor is detecting dopamine. The response of the Tar<sup>HAMP</sup> construct to 1 mM dopamine was repellent (Figure 26B), which represents an inversion compared to Tar, suggesting that the sensing occurs upstream of HAMP. Additionally, the response to dopamine was abolished in the Tar<sup>TM</sup> strain. This strongly suggests that the sensory domain of Tar is responsible for sensing high concentrations of dopamine. This is in agreement with the results obtained for Tar-pinhead. To gain insights into the sensing mechanism of dopamine by Tsr, we also analyzed the Tasr strain. The Tasr strain showed a repellent response to 1 mM of dopamine (Figure 26G), as the Tsr-only strain and Tsr-pinhead did, suggesting that dopamine is sensed by the signaling domain of Tsr, and that the resulting receptor conformational change, and associated effect on kinase activity, is dominant over the one elicited by dopamine binding to the Tar sensory domain. Contrary to the wild type, Tar and Tsr responses at higher concentrations of dopamine (10 mM), we observed unspecific fluorescence changes for the mutant receptors, which prevented further analysis. Since we speculated that at high concentrations the dopamine sensing may have a different mechanism, this unspecific response may suggest that the response at high

concentrations may require both functional periplasmic and signaling domains. Overall, Tar senses dopamine via its sensory domain, while Tsr signaling domain is affected by the hormone. Although extrapolating the results obtained in the hybrid mutants should be done with caution, they suggest that the stimulation by dopamine of the signaling domain of Tsr elicits a stronger activity change than the stimulation of the sensory domain of Tar (Table 7). However, the explanation of the shift observed at 10 mM in the Tsr strains could not be explained by these experiments.

To study if a specific domain is responsible for sensing NE, we first analyzed the response in the Tar<sup>HAMP</sup> and Tar<sup>TM</sup> constructs. The response to NE of both strains was repellent from 1 mM of NE (Figure 26A, D), which is an inversion compared to the response of the full length Tar. This implies that NE sensing occurs again upstream of the TM region, contrary to the Tar-pinhead response. Nonetheless, the Tsr hybrid strain also elicited a repellent response, as the Tsr-only strain response, to NE (Figure 26F). As suggested for dopamine, these results imply that the stimulation by NE of the signaling domain of Tsr has a stronger activity than the sensory Tar domain (Table 7).

To identify the domain that elicits the chemotactic response to DHMA, we analyzed the response of Tar<sup>TM</sup> and Tar<sup>HAMP</sup>. The response of these constructs to DHMA was repellent (Figure 26C, D), as observed for the Tar strain. This suggests a strong role of Tar signaling domain in sensing DHMA, supported by the Tar-pinhead response. In order to understand the role of Tsr receptor the Tsr hybrid was analyzed. Here, we obtained an attractant response (Figure 26H), which represents an inversion compared to Tar and Tsr-only strains responses. As mentioned above the Tsr strain elicits an inversion of the signal when the origin of the signal is by the signaling domain, which further indicates a role of the Tar signaling domain in sensing DHMA (Table 7).

In conclusion, the signaling domains are dominant in the response to the catecholamines, suggesting that this taxis is mediated by effects on the cytosolic part of the receptors (Table 7). However, at high concentrations, specifically for dopamine, hormones sensing may involve the sensory domain in a yet unknown way.

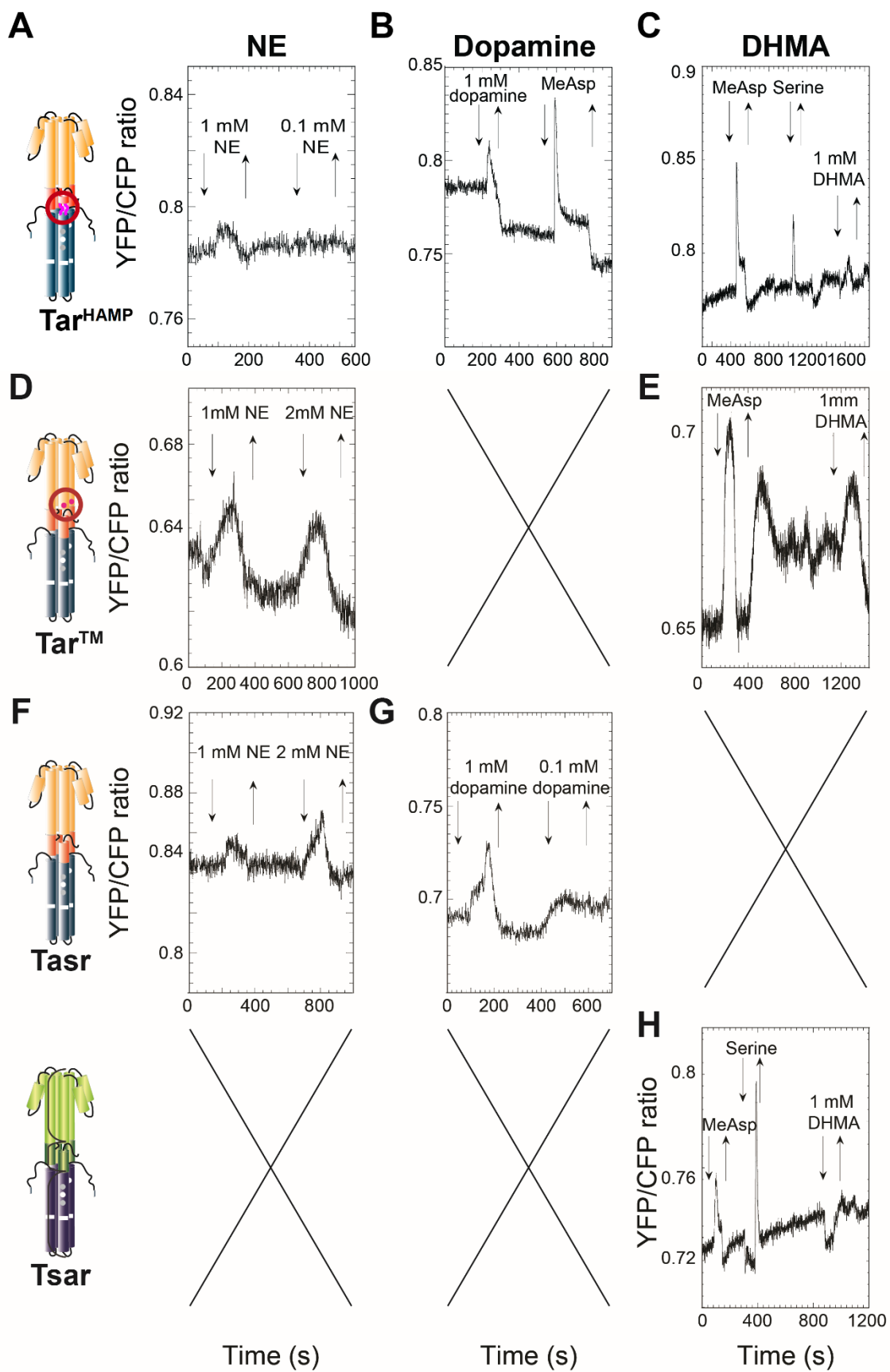


**Figure 26:** Typical chemotactic pathway responses for the hybrids Tar<sup>HAMP</sup> (A, B, C), Tar<sup>TM</sup> (D, E), Tsr (F, G) and Tsr (H) to NE, Dopamine and DHMA, performed as in Figure 14.  $\alpha$ -methyl-DL-aspartate (MeAsp) and L-serine were used as controls.

**Table 7:** Response to dopamine, NE and DHMA of strains harboring the listed receptor constructs, with domain dominating the response being indicated.

	WT	Tar	Tsr	Tsar	Tsar	Tar <sup>HAMP</sup>	Tar <sup>TM</sup>	Origin of the response
<b>DOPAMINE</b>	-	+	-	X	-	-	X	<b>Tsr signaling domain</b>
<b>NE</b>	-	+	-	X	-	-	-	<b>Tsr signaling domain</b>
<b>DHMA</b>	-	-	-	+	X	-	-	<b>Tar signaling domain</b>

Responses to 1mM of catecholamines. +: attractant response; -: repellent response; X: not determined

### 1.3. Mechanism of the spermidine response

In contrast to the hormone responses, the wild type response to spermidine could not be accounted by a combination of Tar- and Tsr-mediated responses. The single receptor strains (Tar and Tsr-only cells) were more sensitive to lower concentrations of spermidine ( $10^{-2}$  mM for Tar-only strain and  $10^{-1}$  for Tsr-only strain) than the wild type strain, although this response switched from repellent to attractant with the increase of the concentration (Figure 27A, Appendix-Figure 6I, J).

To determine the role of the periplasmic domain of Tar and Tsr in spermidine sensing, we used once more Tar- and Tsr-pinhead constructs that lack the entire periplasmic domain (210). The Tsr-pinhead construct had similar responses than the full-length receptor, but with a lower relative kinase activity (Figure 27B). On the other hand, the Tar-pinhead strain showed a delayed shift from repellent to attractant than the Tar-only strain. The different responses between strains harboring full-length receptors and pinhead constructs imply the dominant role of the signaling domain in spermidine sensing by Tar and Tsr. Furthermore, the single receptors Tar and Tsr showed weaker and biphasic responses, with attractant responses at high concentration where the wild type strain showed a clear repellent response. We thus hypothesized that the minor receptors probably mediate the response to spermidine in wild type *E. coli*.

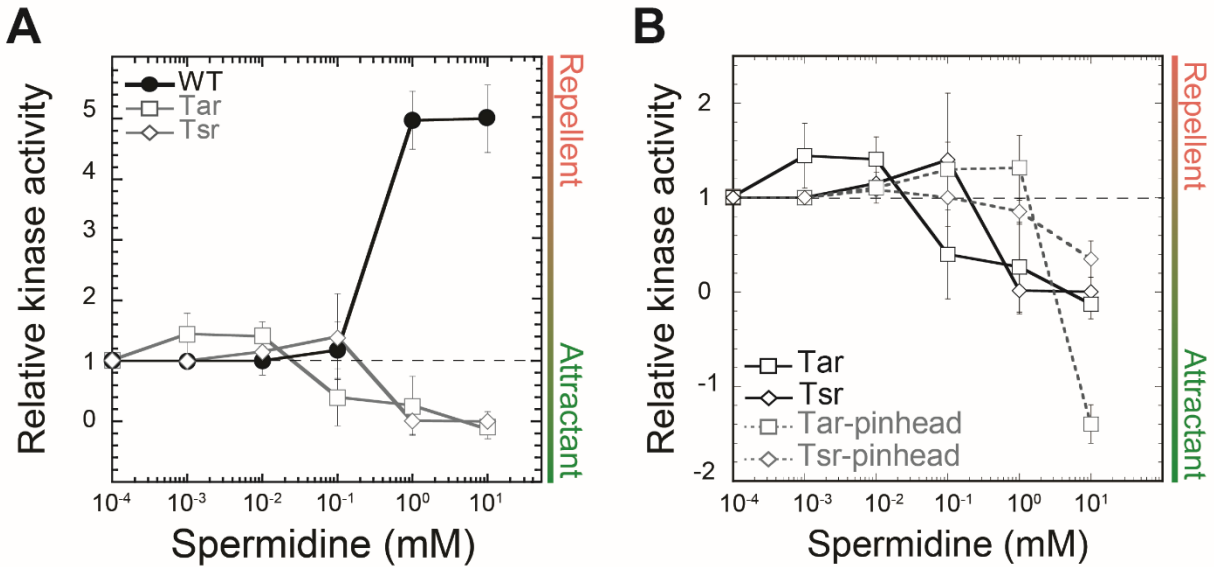


**Figure 27:** Dose responses of wild-type cells (black circles), Tar-only cells (white squares) or Tsr-only cells (white diamonds) to spermidine (A, B), as performed in Figure 14. Responses of strains harboring full-length receptors are represented with full lines, pinhead construct responses are shown with dashed lines. Error bars correspond to the standard error of the mean of three independent experiments.

### 1.3.1. *Trg* receptor mediates response to spermidine

As mentioned above, our data implied that the strong repellent response to spermidine, observed in wild type, appears to be mediated by one of the low-abundance receptors, Tap or Trg. Since neither Trg nor Tap can mediate chemotactic response as the sole receptor (29), we investigated the response of *trg* and *tap* deletions strains to determine the receptor specificity (Figure 28A).

Whereas  $\Delta tap$  strain responded to spermidine similarly to wild type, the response of  $\Delta trg$  strain was comparable to the one observed for Tar- and Tsr-only strains (Figure 28A, Appendix-Figure 8A). This clearly implies that Trg is mediating the wild type repellent response to spermidine. To further confirm the involvement of the Trg receptor in spermidine sensing, wild-type cells were adapted to a saturating concentration of ribose (Trg-specific attractant), before stimulation with spermidine (Appendix-Figure 8B). Adaptation to ribose indeed abolished the repellent response to spermidine, implying that the interaction of the periplasmic ribose-binding protein (RBP), with the sensory domain of Trg, which is known to mediate response to ribose (212, 213), interferes with the spermidine sensing.

### 1.3.2. Response to spermidine requires periplasmic BP PotD

Signaling via periplasmic binding proteins (BPs) is common not only to ribose but to all Trg- or Tap-specific chemoattractants for which the sensing mechanisms have been established. These periplasmic BPs are components of the ATP binding cassette (ABC) transporters, but they also interact with the low-abundance receptors and regulate their activity upon binding their ligands.

We thus hypothesized that the preferential *E. coli* ABC transporter for spermidine, PotABCD (162, 163), might be involved in Trg-mediated response.

The PotABCD transporter complex is composed of PotD, the periplasmic BP, PotA, the membrane-associated ATPase, and PotB and PotC, two membrane-spanning components of the transmembrane channel (162, 214). Notably, the crystal structure of the PotD protein complex with spermidine is very similar to *E. coli* D-Glucose/D-Galactose-binding protein (GBP) (215), another interaction partner of Trg.

We indeed observed that the deletion of *potD* abolished the specific repellent response to spermidine, thus having a similar effect as the *trg* deletion (Figure 28B, Appendix-Figure 8C). The attractant response was restored when *potD* was complemented by expression of plasmid-encoded PotD (Appendix-Figure 8D). On the other hand, the deletion of the membrane-associated ATPase *potA* showed a repellent response that was similar to that of the wild-type strain (Figure 28B). These data suggest that the interaction of the periplasmic BP PotD with Trg indeed mediates *E. coli* repellent response to spermidine.

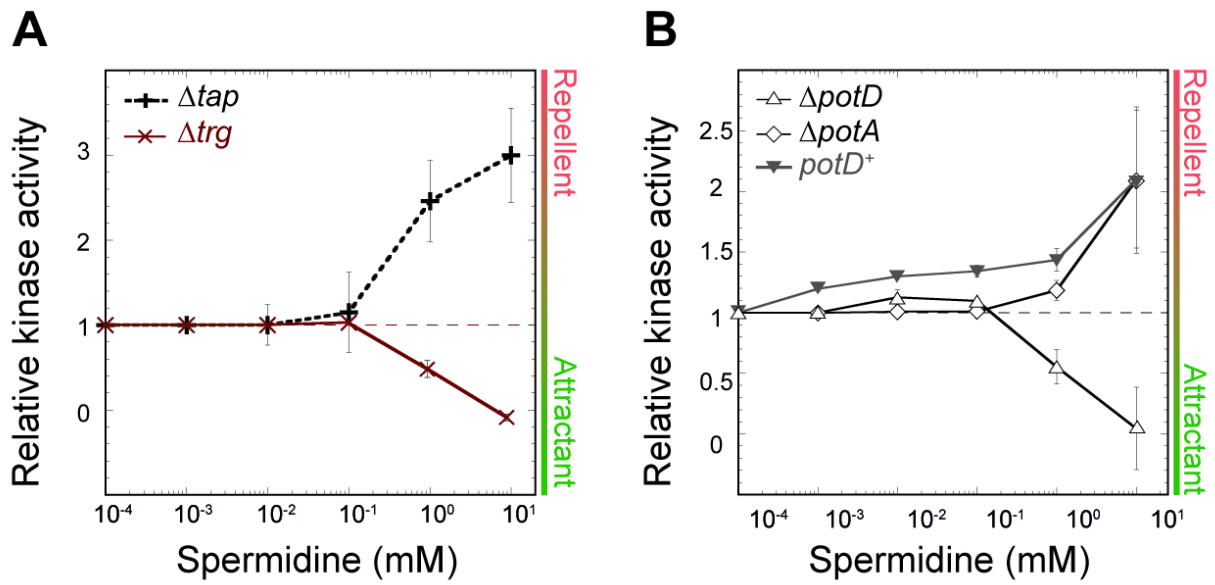


**Figure 28:** Dose responses to spermidine for (A)  $\Delta trg$  cells (red crosses) and  $\Delta tap$  cells (black crosses) and (B)  $\Delta potD$  (white triangles),  $\Delta potA$  (white diamonds), and  $\Delta potD/potD^+$  (grey triangles) cells (see Appendix-Figure 5). Differences between  $\Delta trg$  and  $\Delta tap$  responses in (A) and between  $\Delta potD$  and  $\Delta potA$  or  $\Delta potD/potD^+$  responses (B) are significant according to student  $t$ -test performed at 10 mM spermidine ( $P \leq 0.01$ ).

---

## 2. Physiological importance

### 2.1. Effects of the gut compounds on *E. coli* growth

To understand the physiological relevance of the observed chemotactic responses, we analyzed the effects of the compounds on growth of a planktonic *E. coli* MG1655 culture. Consistent with previous observations showing that some hormones influence bacterial growth (94, 132, 164), we detected effects of several compounds. In order to have comparable results and since the different tested compounds influence different stages of growth, we calculated the area below the curve of each experiment as a measure of time average OD (see Material and Methods, Appendix-Figure 9).

Among those, dopamine, L-DOPA and epinephrine enhanced *E. coli* growth, with the effect of dopamine being the most pronounced (Figure 29, Appendix-Figure 10), in agreement with previous reports (93, 164). As dopamine develops a black color during incubation, possibly due to its oxidation, we always subtracted a baseline calculated using growth medium with dopamine where no cells were inoculated. Additionally, we confirmed this result directly by performing colony-forming units counting assay were a higher number of viable cells in the cultures with dopamine was indeed determined (Figure 30). Although the exact mechanism of this growth stimulation remains to be investigated and will be discussed in a later chapter, it has been suggested that the effect may be due to the dopamine-mediated enhancement of iron uptake by *E. coli* (132, 164).

In contrast, DHMA and melatonin were growth-inhibitory, and even stronger growth inhibition was observed for spermidine. Interestingly, the effect of spermidine was only detected at 1 mM and above, whereas lower concentrations did not produce any significant effect (Figure 29). This decrease in the growth of *E. coli* with high concentrations of spermidine was previously observed and accounted by regulation of specific proteins, many of which are related to response to stress by basic pH (216). This range of concentration matches the range of chemorepellent response observed in this study.

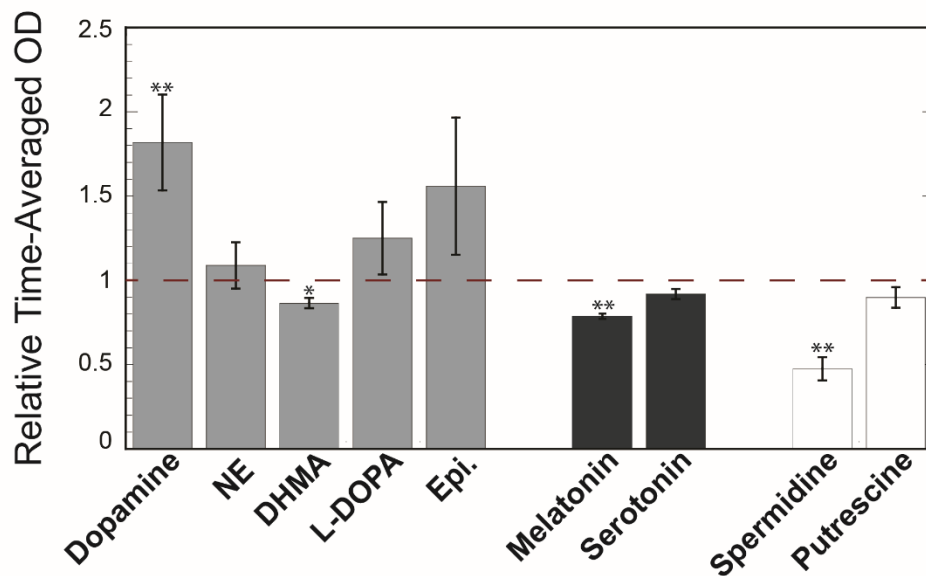


**Figure 29: Effect of the gut compounds on *E. coli* growth.** *E. coli* strain MG1655 was grown at 37°C in TB media containing the indicated compounds at a final concentration of 1 mM. Optical density of the culture was measured at 600 nm as described in Materials and Methods and the time-averaged OD was calculated as the area below the curve divided by the duration of the experiment. For each experiment, the time average OD was normalized to the time-average OD of the control culture in TB (red dashed line). Grey bars represent the catecholamine group; black bars the thyroid group; and white the polyamine group. One-tailed student *t*-test was performed against the control (\*\*:  $p \leq 0.01$ ; \*:  $p \leq 0.05$ ). Each bar represents the mean of at least three independent experiments, with error bars indicating standard deviation.

Addition of serotonin, putrescine and NE had no significant effect on growth at the tested concentration.

The same results for growth were obtained in the two tested minimal media (Appendix-Figure 11), M9 and SAPI, a minimal salts medium supplemented with 30% (v/v) adult bovine serum that exposes bacteria to conditions environmentally similar to most mammalian tissue, such as iron limitation, limited nutrient availability, and immune defense proteins such as antibodies (93).

Thus, except for NE and dopamine – which showed a biphasic response in FRET - the chemotactic response towards the tested compounds correlates with the observed growth effect, strongly suggesting that the observed chemotactic responses to gut compounds are indeed physiologically significant (Table 8).

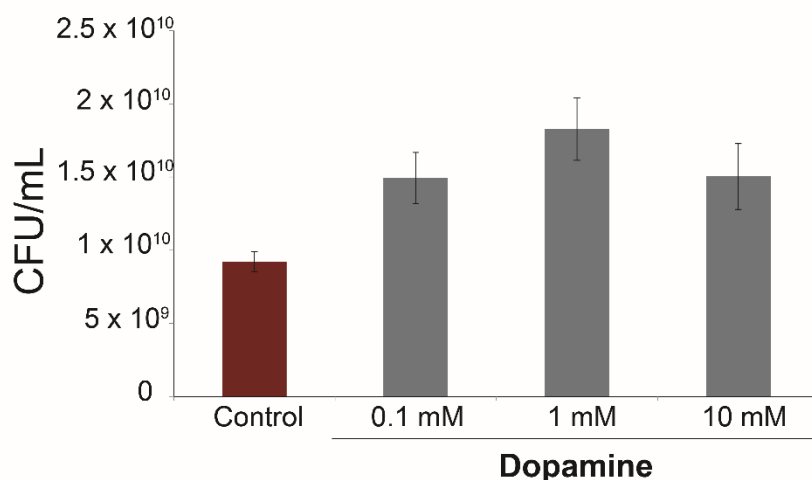


**Figure 30:** Effect of dopamine on the number of colony forming units (CFU) of *E. coli* cultures. CFU count was determined on LB plates for the culture grown at 37°C in TB with indicated dopamine concentrations as described in Material and Methods. Experiments were performed in triplicates. The CFU/ml is the number of colonies per volume of inoculation. Error bars indicate standard deviation.

**Table 8:** Effect of gut compounds on chemotaxis and growth in *E. coli*

Compounds	Chemotactic response <sup>a</sup>		Growth effect
	FRET	Chemotactic drift	
L-tyrosine	0	ND	0
L-DOPA	0	ND	0
Dopamine	-/+	-**	+***
Norepinephrine	+/-	-**	0
Epinephrine	ND	+*	+
DHMA	-	-**	-**
Serotonin	0	ND	0
Melatonin	-	-***	-***
Putrescine	0	ND	0
Spermidine	-	-*	-***

ND: not determined; 0: no response/effect; +: attractant/enhancement; -: repellent/inhibition

<sup>a</sup>Response of the wild-type cells.

\*, \*\*, \*\*\* One-tailed student t-test statistical significance to the control of  $P \leq 0.1$ ,  $P \leq 0.05$  and  $P \leq 0.01$ , respectively (based on Figure 20 and Figure 29)

## 2.2. Effects of the gut compounds on pathogenic bacteria

Recent work suggested that hormones trigger expression of virulence genes, therefore we analyzed the effect of hormones on pathogenic bacteria, which share the same natural environment as *E. coli* K-12 (217, 218). To this end, we evaluated the effect of hormones on the growth of *E. coli* EcoR64 and *Salmonella enterica* serovar *typhimurium* ATCC 14028.

All three strains *E. coli* MG1655, EcoR64 and *S. typhimurium* displayed a similar growth rate for all the tested compounds. However, in contrast to *E. coli* MG1655, where the addition of dopamine had approximately a 2-fold increase in the maximal OD, the growth in *S. typhimurium* was significantly reduced (Figure 31A, B). Interestingly, oxidation of dopamine, resulting in a darker color of the media, has not been observed. These results suggest that *Salmonella* may uptake and degrade dopamine. Still, the exact mechanism remains to be unraveled.

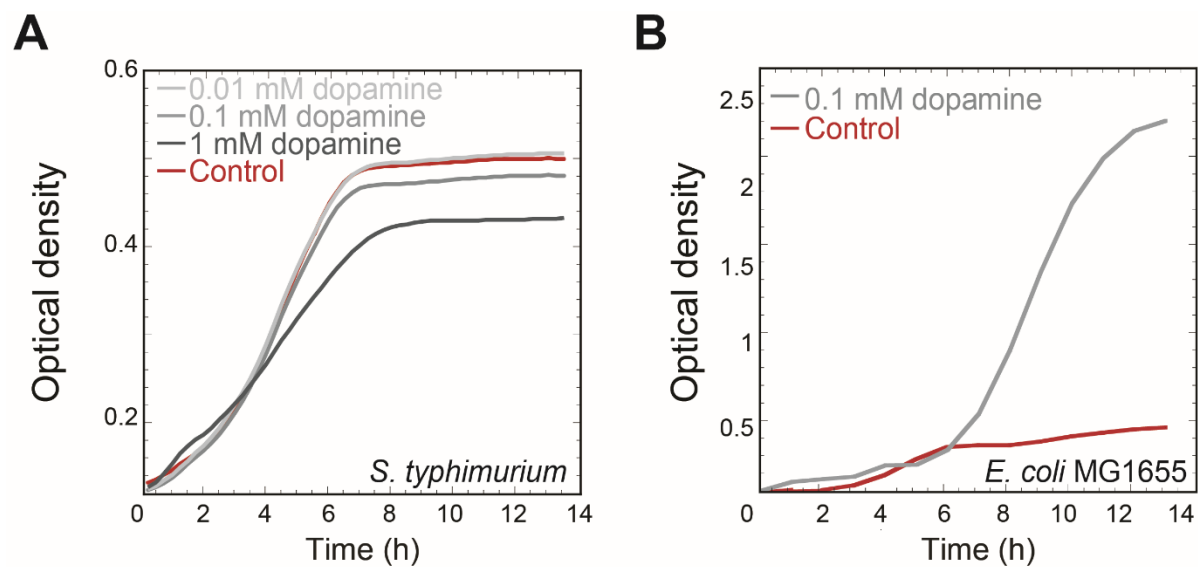


**Figure 31:** Effect of different concentrations of dopamine on *S. typhimurium* (A) and *E. coli* MG1655 (B). Cultures were grown at 37°C in TB media containing the indicated final concentrations of dopamine. Optical density of the culture was measured at 600 nm as described in Materials and Methods.

## 2.3. Hormones influence gene expression

In order to have a holistic picture and to understand how the addition of gut compounds can influence bacterial growth we performed RNA-sequencing (or RNA-seq). This technique

evaluates the changes in the cellular transcriptome and could help us understand the mechanism of hormone sensing, on a system level. We focused on the compounds that produced a stronger effect on *E. coli* growth, dopamine, melatonin and spermidine.

The Figure 32 scatter plots show the pattern of gene expression changes in the MG1655 strain upon addition of 1 mM of melatonin, dopamine and DHMA. Genes with more than 3-fold changes in the presence of the respective compounds are summarized in Table 9 (see complete table in Appendix-Table 1). These genes are good candidates to explore the influence of the compounds on growth.

In more detail, Figure 32A, B, C shows the gene expression pattern upon stimulation with dopamine, melatonin and DHMA, respectively. Interesting candidates are highlighted in the individual figures. The downregulated genes *fecB*, *fecA* and *tdcD* belong to two operons – *fec* and *tdc* (Figure 32A). *fecB* and *fecA* encode for a ferric citrate periplasmic binding protein and a ferric citrate extracellular receptor of the ABC ferric citrate transporter system, respectively (219). These genes belong to the class of iron transporters and together with the previous findings that the catechol ring in dopamine may behave as a siderophore ring, which improves the iron uptake in Gram-negative bacteria (164, 220), they may be relevant for the mechanism of catecholamines sensing and transport. The *tdc* operon encodes a pathway for the transport and anaerobic degradation of L-threonine to propionate (221). The *trpE* gene was upregulated with the dopamine stimuli, remarkably the *trp* operon encodes for the L-tryptophan pathway that is the precursor of the thyroid hormones (222). The correlation between the change in the gene expression of the last two genes and the effect of dopamine is difficult to grasp, however the *fec* operon suggests a connection between dopamine and iron uptake. We speculate that dopamine may reduce  $\text{Fe}^{3+}$  to  $\text{Fe}^{2+}$ , which then could be taken up by bacteria by either ferric (siderophore based) or ferrous iron uptake systems, since previous results propose that catecholamines can bind inorganic Fe(III) salts (223, 224).

For the two remaining experiments, finding candidates that might give us a clue on the effect of DHMA and melatonin in *E. coli*, was more complicated. Upon stimuli with DHMA the gene *ybiJ* was upregulated. YbiJ is a putative protein suggested to have a potential function

in iron acquisition (225), which may imply also a role in iron uptake, as for dopamine. The change in gene expression of *yhaK*, which encodes for a redox-sensitive bicupin (226), and *rrsH* and *rrsC* that encode for ribosomal RNA, along with *rrlD* with DHMA and melatonin stimuli remain to be elucidated and may just derive from noise inherent to the technique.

**Table 9: Genes with more than 3-fold changes between the control and incubation with DHMA, dopamine or melatonin**

	<i>Gene</i>	<i>Fold change</i>	<i>Gene description NCBI</i>
<b>DHMA</b>	<i>ybiJ</i>	4.978 up	DUF1471 family putative periplasmic protein
	<i>rrsH</i>	4.487 up	16S ribosomal RNA of <i>rrnH</i> operon
	<i>rrsC</i>	4.063 up	16S ribosomal RNA of <i>rrnH</i> operon
	<i>yhaK</i>	3.18 up	Redox-sensitive bicupin
<b>DOPAMINE</b>	<i>trpE</i>	7.084 up	Component I of anthranilate synthase
	<i>tdcD</i>	4.752 down	propionate kinase/acetate kinase C
	<i>fecB</i>	5.072 down	Ferric citrate ABC transporter periplasmic binding protein
	<i>fecA</i>	4.957 down	Ferric citrate extracellular receptor
	<i>fecE</i>	4.872 down	Ferric citrate ABC transporter permease
	<i>fecC</i>	4.628 down	Ferric citrate ABC transporter permease
	<i>fecD</i>	4.416 down	Ferric citrate ABC transporter permease
<b>MELATONIN</b>	<i>rrsH</i>	4.486 up	16S ribosomal RNA of <i>rrnH</i> operon
	<i>rrsC</i>	4.063 up	16S ribosomal RNA of <i>rrnH</i> operon
	<i>rrlH</i>	3.686 up	23S ribosomal RNA of <i>rrnH</i> operon
	<i>rrlA</i>	3.626 up	23S ribosomal RNA of <i>rrnH</i> operon
	<i>rrsD</i>	3.593 up	16S ribosomal RNA of <i>rrnD</i> operon
	<i>rrsA</i>	3.573 up	16S ribosomal RNA of <i>rrnD</i> operon
	<i>rrlC</i>	3.52 up	23S ribosomal RNA of <i>rrnC</i> operon
	<i>rrlD</i>	3.24 up	23S ribosomal RNA of <i>rrnD</i> operon

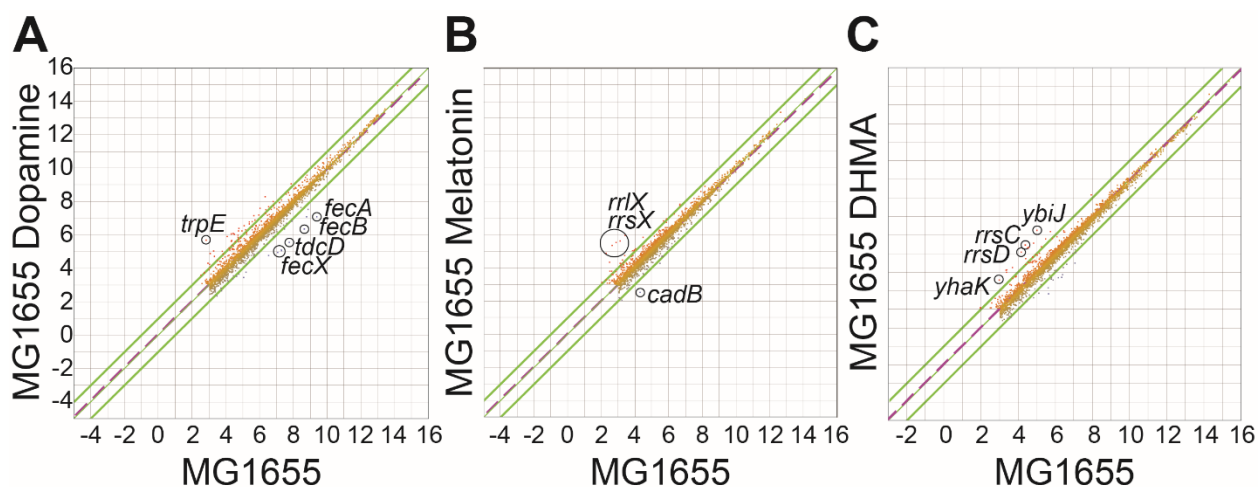


**Figure 32: Changes in gene expression in MG1655 after addition of dopamine (A), melatonin (B) and DHMA (C) stimuli.** Displayed are scatter plots where each dot is the expression level, in logarithmic scale, of a gene in media, comparing before and after the addition of dopamine, melatonin and DHMA. Genes falling on the dotted line have equal expression in both media. Genes falling above (respectively, below) the upper (lower) line experience a more than 3-fold up-(down-)regulation of the expression upon addition of the compound in the medium.

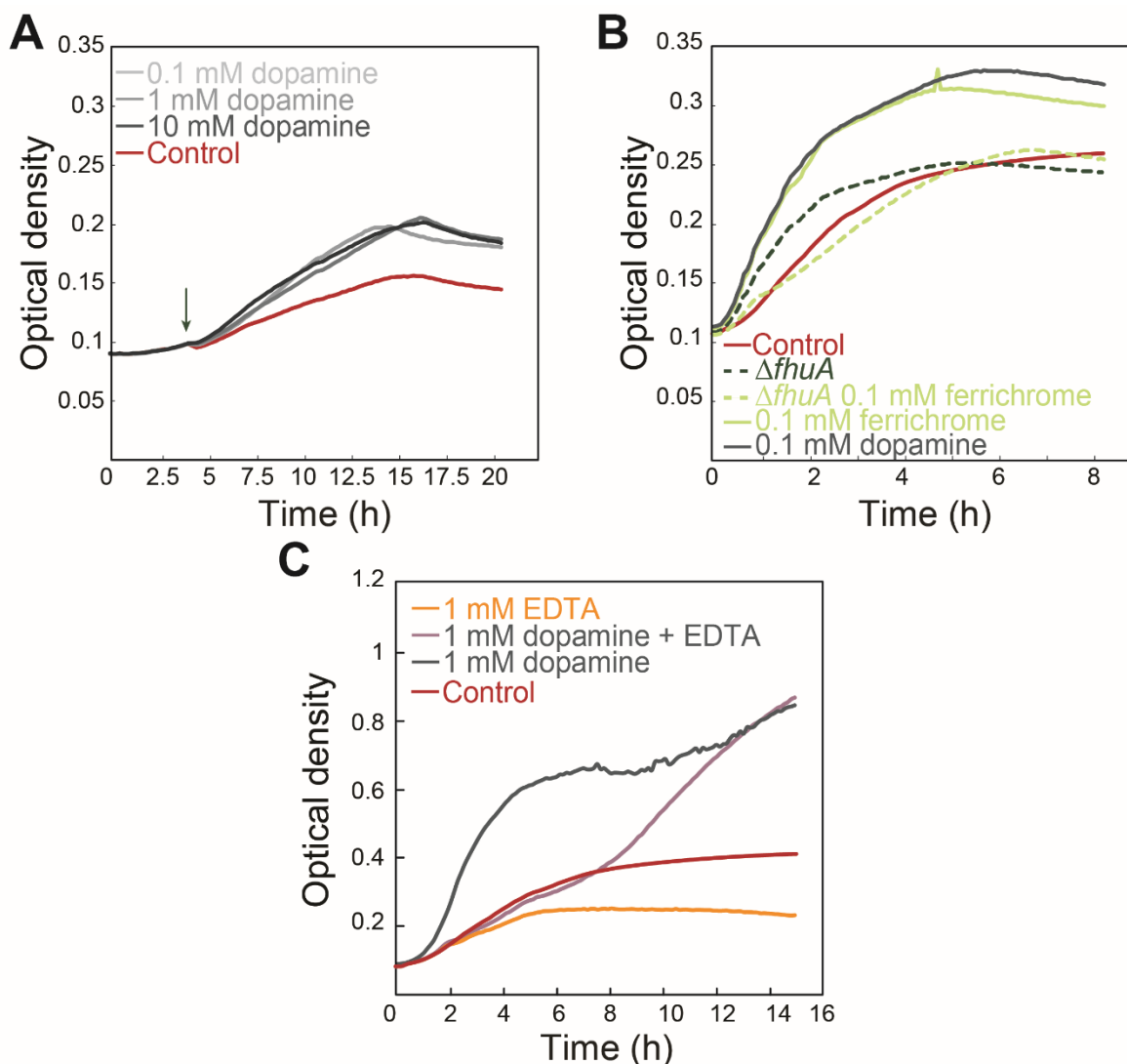
#### 2.4. Dopamine growth effect

Our data indicated that dopamine might function as a siderophore improving the iron uptake and, thus enhancing growth in *E. coli*, as previously suggested (132, 164). In order to exclude any influence of additional metals on growth we used glycerol-salts medium (227), which is depleted of trace metals. Under these conditions the enhancement of growth upon dopamine addition was less pronounced and observed already at lowest levels of dopamine (Figure 33A).

Furthermore, we compared the influence of dopamine to that of a known siderophore, ferrichrome. We compared the growth of cultures where dopamine or ferrichrome were added to TB medium at the same concentration. We found that dopamine and ferrichrome effects on *E. coli* cells growth were similar (Figure 33B), what may suggest that these compounds have a similar mode of action. As a control, a deletion strain in *fhuA* was used. FhuA is the transporter for ferrichrome and therefore no significant growth inhibition was observed.

We also decided to test a chelating agent to limit the free iron in the media, possibly preventing it from binding to dopamine. Therefore, to sequester the iron ions the chelating agent EDTA was also added to the cultures with dopamine (Figure 33C). The *E. coli* growth was delayed in the presence of EDTA, although the cells reached the same final OD after 14 h of incubation. Probably the concentration of EDTA has to be increased in order to completely block the dopamine effect. These results suggest that dopamine might have a siderophore-like effect, although if its exact role in promoting iron uptake and thereby cell growth remains to be elucidated.

Additionally, we performed liquid chromatography tandem-mass spectrometry (LC-MS/MS) assay, in order to determine if dopamine degrades after incubation, and no degradation was detected (data not shown).

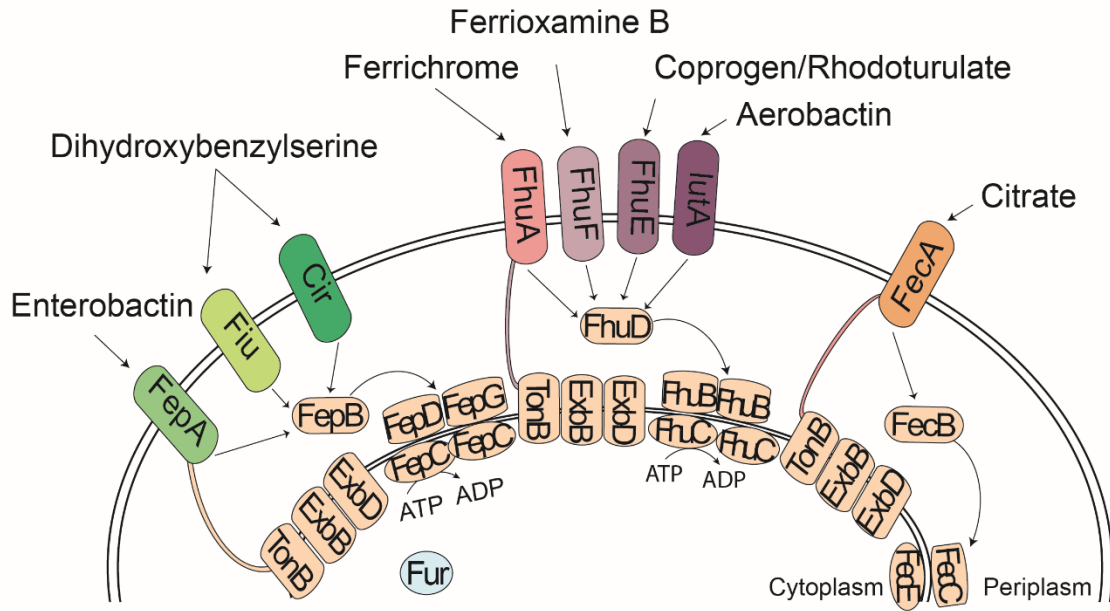
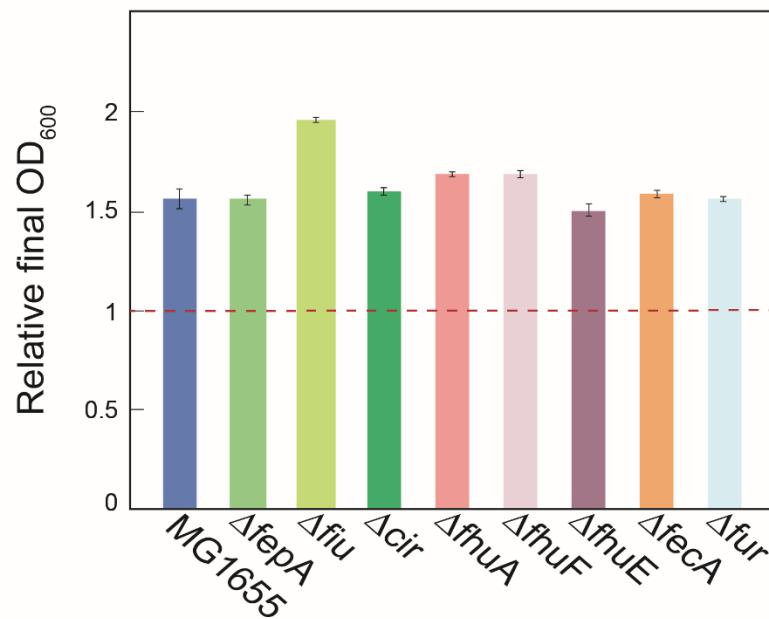


**Figure 33: Growth curves with *E. coli* MG1655 supplemented with different concentrations of dopamine (A), and ferrichrome (B) and EDTA (C).** As a negative control  $\Delta fhuA$  (B) strain was analyzed. Cultures were grown at 37°C in glycerol-salt medium (A) and TB media (B and C). Dopamine was added after 3 h of incubation indicated by the green arrow (A). Optical density of the culture was measured at 600 nm as described in Materials and Methods.

---

Additionally, we aimed to unravel the transport mechanism of dopamine, as implied by the RNA-seq data, where we observed a downregulation of the ferric citrate transporters. We speculated that some other receptors for iron uptake might also play a role for dopamine uptake. We performed growth experiments with deletion strains of the eight known iron transporters in *E. coli*: *fepA*, *fiu*, *cir*, *fhuA*, *fhuF*, *fhuE*, *lutA* and *fecA*, in the presence and absence of 1 mM dopamine. Furthermore, we also analyzed the growth of the deletion strain *fur*, the ferric uptake regulator of *E. coli* (Figure 34A). We expected that strains deleted for a putative dopamine transporter would not show any growth effect. The final OD was normalized to the OD in cultures where no dopamine was supplemented (Appendix-Figure 12). Interestingly, none of the strains showed a reduction in growth compared to the control strain, MG1655 (Figure 34B). The  $\Delta$ *fiu* strain even had an increase in the relative final OD. Thus, our results suggest demonstrate that dopamine is transported by a combination of transporters or via a different mechanism.

Additionally, it was also previously proposed that NE and epinephrine are sensed by QseBC, a two-component regulatory system, which is also involved in the regulation of flagella and motility by quorum sensing in *E. coli* (130, 133, 228). However, these data could not be corroborated by real-time qPCR, where no significant increase was observed in *qseC* or *qseB* gene expression level upon addition of either NE and dopamine (Appendix-Figure 13).

**A****B**

**Figure 34: Components of iron transport in *E. coli* growth (A; see Figure 9). Growth effect on transporter deletion strains upon addition of 1 mM of dopamine in *E. coli* MG1655 (B).** Cells were grown at 37°C in TB media with and without 1 mM of dopamine. Optical density of the culture was measured at 600 nm as described in Materials and Methods and the relative OD was calculated by normalization to the cultures with no dopamine supplemented. Values of relative final OD higher than 1 represent an enhancement in final OD when compared to no addition of dopamine, conversely values lower than 1 represent a comparative reduction in the final OD. Each bar represents the mean of at least three independent experiments, with error bars indicating standard deviation.

## DISCUSSION

Microbial endocrinology is an interdisciplinary research field that represents the intersection of microbiology, endocrinology and neurophysiology. Its main objective is to understand the ability of microorganisms to interact with a host under various physical and behavioral conditions, both in healthy hosts and during disease.

While most of the microbial endocrinology studies have focused on how different bacterial species change the concentrations of hormones in the GI tract, less attention has been paid to the reaction of the microbes themselves to these compounds (88, 94, 109). In this study, we used *Escherichia coli* as the model enteric bacterium to investigate chemotactic responses to a range of compounds that are present in the human gut. We focused our analysis on the following compounds: the catecholamines L-tyrosine, L-DOPA, dopamine, norepinephrine (NE), epinephrine and DHMA; the thyroid hormones serotonin and melatonin; the sex hormones estradiol and testosterone; insulin and the polyamines putrescine and spermidine (Table 10).

Compounds	Chemotactic responses in Wild Type <sup>a</sup>
-----------	---

**Table 10:** Summary of obtained chemotactic response to the tested gut compounds

<i>Catecholamines</i>	L-tyrosine	ND
	L-DOPA	ND
	Dopamine	<u>Biphasic</u> Repellent / Attractant
	Norepinephrine	<u>Biphasic</u> Attractant / Repellent
	Epinephrine	Attractant <sup>b</sup>
	DHMA	Repellent
<i>Thyroid hormones</i>	L-tryptophan	ND <sup>(190)</sup>
	Serotonin	ND
	Melatonin	Repellent
<i>Sex hormones</i>	Estradiol	ND
	Testosterone	Repellent
<i>Peptide</i>	Insulin	<u>Biphasic</u> Attractant / Repellent
<i>Polyamines</i>	Putrescine	ND
	Spermidine	Repellent

ND: Not detected; <sup>a</sup>: results of FRET experiments

### 1. Chemotactic responses correlate with the compound availability in the gut

Although measurements of the accurate concentration across the gut are complicated by the heterogeneity of the gut environment and strong dependence on food content and health state of the host (229-231), it is believed that the analyzed compounds accumulate in the GI tract at different rates. For instance, the catecholamines, L-tyrosine and L-DOPA are thought to not accumulate at high concentrations in the lumen of the gut. L-tyrosine has been shown to be taken up by the blood and concentrated within the brain and other catecholamine-synthesizing tissues (232-234), while L-DOPA is described to be rapidly converted to dopamine and the remaining absorbed mainly in the small intestine (128, 200, 235). Other compounds such as the polyamine putrescine are also believed to be rapidly converted into spermidine and spermine (205).

Remarkably, we observed chemotactic responses to the majority of the compounds that are known to accumulate in detectable concentrations in the gut, namely dopamine, NE, melatonin and spermidine (127, 141, 236-238). These compounds can reach micro- to millimolar levels across the gut lumen (127, 205, 239) and even higher concentrations are expected to be present in the vicinity of the mucous layer where these compounds are

---

secreted, consistent with the observed range of concentrations eliciting a chemotactic response. These responses seem to be physiologically relevant, considering that no response could be detected for their precursors with similar chemical structure (L-tyrosine, L-tryptophan, L-DOPA and putrescine). These compounds are primarily derived from food sources and are rapidly turned over in the GI tract (205, 240), and are therefore unlikely to form long-lived gradients that can be used for orientation in the intestine. Our results thus provide further evidence for the hypothesis that bacteria can specifically utilize host signals to detect their GI location, as previously suggested (75-78, 130, 241, 242).

In contrast, some exceptions were found in our results, namely for serotonin and epinephrine. Unexpectedly, we observed no significant chemotactic response for serotonin, although it has been estimated that approximately 95% of serotonin is found in the GI tract (202, 203), and it has been described to activate *Pseudomonas* virulence *in vivo*, within the intestines of mice (243). Since we did not observe any chemotactic response to serotonin, we speculate that this hormone may only affect pathogenic bacteria, or be a useful cue only for some bacteria. On the other hand, epinephrine elicited an attractant response in our experiments, consistent with a previous report (76). Nonetheless, this compound is believed to be present in the GI tract at lower concentrations than NE and dopamine, since the enzyme required for its synthesis from NE is not expressed in the intestinal mucosa (79). Interestingly, previous studies that correlate the effect of epinephrine with the regulation of virulence genes in bacteria have revealed a clear preference for NE and dopamine over epinephrine (76, 242). Therefore, despite epinephrine elicited a strong attractant response in *E. coli*, it is possible that in the gut natural environment NE and dopamine chemotactic responses would overcome the epinephrine response.

We also detected chemotactic responses to other hormones, insulin and testosterone, that have been described to accumulate in the gut, even if their role in microbial endocrinology has been less studied to date. Insulin has been described to influence significantly the microbiome composition in diabetic patients (151, 152). Despite the measurement being technically difficult, we observed a biphasic chemotactic response to insulin, changing from attractant to repellent when concentration increases. We conclude that the attractant

response is, however, not specific and comes possibly from insulin degradation to individual amino acids.

Examples of bacteria affected by sex hormones have been reported since the 1980s (147-149). In our study, a chemotactic repellent response was detected to testosterone and no response was elicited by estradiol. These hormones may elicit different responses in *E. coli*, since their range of concentration in the GI lumen is not the same. Bacteria may have adjusted to changes in concentration of testosterone, because this hormone was described to vary its concentration in the gut (244), while estradiol presents more stable concentrations. Sex hormones were also involved in the development of obesity and metabolic disorders, however the interrelationship between the balance of sex hormones and metabolism is complex, and the underlying mechanisms are still unclear.

In conclusion, our results provide evidence for the hypothesis that bacteria can utilize eukaryotic signals to detect their GI location (76, 130).

## **2. Hormone sensing mechanism - interplay between Tar and Tsr**

With the exception of epinephrine, all the analyzed hormones produced a repellent or biphasic response and the wild type chemotactic response appears to be the result of an interplay between the responses mediated by the two major *E. coli* chemoreceptors, Tar and Tsr. For almost all the hormones, the Tsr-mediated response seem to make a larger contribution to the behavior of the wild-type cells, consistent with Tsr being the most abundant receptor under our growth conditions (15, 209). Such interplay between Tar- and Tsr-mediated responses is similar to the previously characterized tactic behavior in gradients of pH and temperature (28, 61), but contrasts with the responses to conventional chemoattractants that specifically bind to the periplasmic sensory domains of the receptors. In those cases, ligands are sensed through the periplasmic sensory domains of receptors and typically possess high receptor specificity. The strongest effect of the Tsr chemoreceptor was especially prominent in the compounds sensed biphasically, dopamine and NE, where the Tsr response also inverted when concentration changed and determined the wild-type response.

---

Although the exact molecular mechanism(s) of the cytoplasmic sensing remains to be elucidated, it nevertheless appears to be specific, since chemically closely related precursor compounds elicited no response.

### 2.1. Repellent response to hormones

Typical repellents are potentially toxic chemicals that could harm the cells, such as high concentrations of heavy metal ions  $\text{Ni}^{2+}$  and  $\text{Cu}^{2+}$ , which form nonspecific complexes in the cell (53). Usually, attractant binds directly to the receptor's ligand-binding site or indirectly via the help of a periplasmic binding protein. It has been suggested that sensing of repellents by Tar is different from its sensing of attractants (59). Another possibility for sensing of repellent is through their effect on the properties of the membrane, as the membrane fluidity. However, it has been shown for most of the repellents that the sensing is not mediated by their general effect on the membrane fluidity (245). A non-classical sensing mechanism was recently proposed for phenol sensing by Tsr, in which phenol elicits a signaling response by diffusing into the cytoplasmic membrane and influencing the stability of the transmembrane helices thereby producing a conformational change in the HAMP domain that mimics the binding of ligand (246). Glycerol and ethylene were suggested to act through a similar mechanism as phenol (247). It was also demonstrated that repellent stimuli, as glycerol, indole, and L-leucine, are not sensed by the periplasmic domain (245).

In this study, we examined the chemotactic repellent response to DHMA. A chemotactic response towards DHMA had already been found in a previous study by Pasupuleti *et al.* (75). Since the response was only observed when the cells were incubated with NE, it was proposed that in *E. coli* the response to NE is due to its conversion to DHMA. A strong attractant response was observed to DHMA in that study, which decreased amplitude with the increase of concentration until 50  $\mu\text{M}$ , where the response ceased (75). As previously mentioned in our study, we detect a weak attractant response until 50  $\mu\text{M}$ , where the response shifts to repellent. Additionally, strains lacking the Tsr receptor did not elicit a response to DHMA in the referred study. Therefore, it was concluded that an intact serine-

binding site is required for sensing DHMA (75). Our analysis revealed an attractant response for NE in Tar-only strain, whereas Tsr sensed NE as a repellent over the entire concentration range. Additionally, for DHMA both Tar and Tsr mediated repellent responses. Our results suggest that the NE sensing at high concentrations could not be solely explained by its conversion into DHMA, since Tar responses to NE and DHMA were clearly different. The difference between results may be due to the different methods utilized. These experiments were done in a microfluidics assay, which requires an incubation period before the measurement (of at least 20 minutes) to acquire the concentration gradient (75). This incubation period may lead to a decrease in the response because the compounds may be taken up, similar to what we observed in our microfluidics experiments. Further investigations on the mechanism of the repellent response to DHMA were performed in the current report. The Tar constructs Tar<sup>TM</sup> and Tar<sup>HAMP</sup> with changes in the transmembrane region and the HAMP domain respectively, showed repellent responses to DHMA, as for the Tar strain. These responses suggest a dominant role of Tar signaling domain. Furthermore, the Tsr hybrid response to DHMA, that combines the Tsr sensory domain and the Tar signaling domain, was also mediated by the Tar signaling domain. In conclusion, it appears that the Tar signaling domain is dominant in the response to the DHMA. Repellent sensing by the cytoplasmic signaling domain of receptor has been previously shown for responses to the changes of cytoplasmic pH (248).

## 2.2. Biphasic response to hormones

Chemotactic signaling in *E. coli* involves transmission of both attractive and repulsive stimuli. Biphasic chemotaxis to some compounds – where the responses are repellent or attractant depending on the concentration range - have been described before, for example for L-leucine (249), or pH (60). For example, wild-type *E. coli* bacteria were described to be attracted to leucine at concentration between 5 to 120  $\mu$ M, but repelled from concentrations over 0.5 mM. While NE elicited such an attractant-to-repellent biphasic chemotactic response, we observed for the chemotactic response of *E. coli* to dopamine an inversion for a repellent response to an attractant when the concentration increased.

---

Biphasic taxis towards chemicals were so far observed to rely on the counteraction of two receptors with opposite responses to the compound, the strengths of which are modulated when concentration changes. For example, protons are sensed by Tar as attractant and by Tsr as repellent (60), similarly to the mechanism of L-leucine sensing (249). While NE was also an attractant for Tar and a repellent for Tsr, the situation was extremely unconventional in the case of dopamine, since both Tsr and Tar switched from sensing it as repellent to attractant as concentration increased. For both compounds, Tsr response had the highest weight in the global response of the wild-type cells, in line with its higher abundance in our growth conditions.

To rationalize our results at the level of single receptors, we examined the mechanism of chemotactic sensing of dopamine and NE by the receptors. The repellent response of the Tar<sup>HAMP</sup> construct to 1 mM dopamine, means an inversion compared to Tar, suggesting that the attractant sensing at high concentration occurs upstream of HAMP. Additionally, the response to dopamine was abolished in the Tar<sup>TM</sup> strain. This strongly suggests that the sensory domain of Tar is responsible for attractant sensing of high concentrations of dopamine. Tar-pinhead sensed dopamine at all concentrations, suggesting that the cytoplasmic part of the receptor is responsible for the low concentration repellent response of Tar, which then is overcome by the sensory domain response at high concentration. On the other hand, the Tasr strain that combines the Tar sensory domain with the Tsr signaling domain, showed a repellent response to 1 mM of dopamine, as the Tsr-only strain. This suggests that dopamine is sensed as a repellent by the signaling domain of Tsr up to a concentration of 1 mM – as also supported by the repellent response of Tsr-pinhead, and that the resulting receptor conformational change, and associated effect on kinase activity, is dominant over the one elicited by dopamine binding to the Tar sensory domain. Overall, Tar senses dopamine via its sensory domain, while Tsr signaling domain is affected by the hormone (Figure 35). Although extrapolating the results obtained in the hybrid mutants should be done with caution, it seems that the stimulation by dopamine of the signaling domain of Tsr elicits a stronger activity change than the stimulation of the sensory domain of Tar.

The response to NE of Tar<sup>HAMP</sup> and Tar<sup>TM</sup> was repellent, which implies that NE sensing appears to be upstream of the TM domain of Tar. These results support the role of the sensory domain of Tar in sensing NE. Additionally, the Tsr hybrid elicited a repellent response to NE, as did Tsr. Combined with the repellent response of Tsr-pinhead, these results imply that NE is sensed by Tsr, primarily via its signaling domain, and that the stimulation by NE of the signaling domain of Tsr induces a stronger activity change than that of the sensory Tar domain (Figure 35).

In conclusion, the biphasic sensing mechanism to NE seems to be a typical interplay between the Tar and Tsr receptor, where the Tsr signaling domain plays a stronger role.

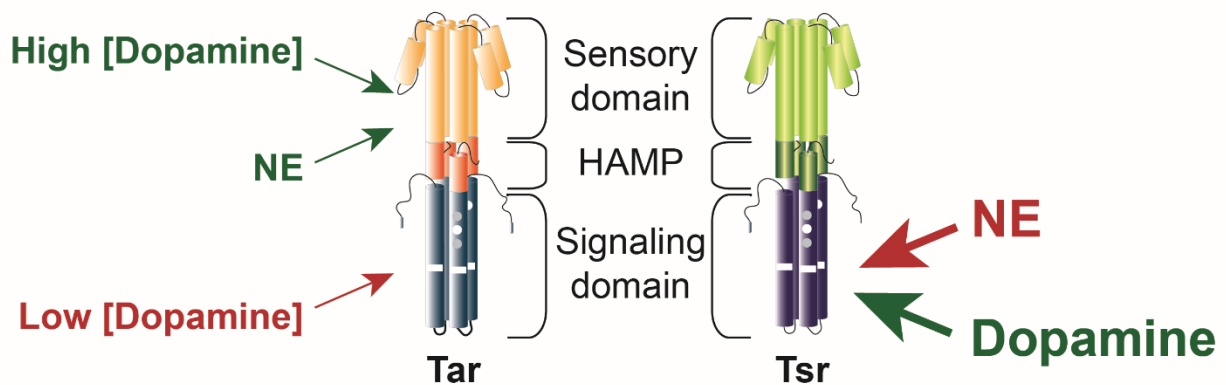


**Figure 35: Schematic drawing of the biphasic sensing mechanism to NE and dopamine of Tar and Tsr.** High and low concentrations of dopamine ([dopamine]) are sensed by different parts of the Tar receptor. Bigger arrows highlight stronger role of the Tsr signaling domain. Green labelling represents an attractant response, while red labelling represents a repellent response.

### 3. Repellent response to spermidine mediated by Trg/PotD

Although the mechanism of hormone sensing by *E. coli* chemoreceptors remains to be investigated, we could show that spermidine is specifically sensed as a repellent by the minor receptor Trg. So far, Trg has been only implicated in attractant responses to ribose, glucose and galactose, mediated by the interactions of its sensory domain with a periplasmic binding proteins, RBP (for ribose) and GBP (for glucose and galactose). Our results suggest that the response to spermidine similarly involves the periplasmic binding protein PotD, which is part of the spermidine uptake system PotABCD. To our knowledge, this is the first example of a repellent response mediated by a minor chemoreceptor. It is

also the first example of a repellent response involving a periplasmic binding protein – although nickel binding protein has been initially implicated in the repellent response mediated by Tar (250), this finding was subsequently disproved (251).

#### 4. Correlation between chemotactic response and growth effects

*E. coli* chemotaxis towards amino acids has been shown to correlate with their order of utilization and effect during growth (190). In the gut, *E. coli* is exposed to amino acid gradients of varying composition and it benefits from being able to follow gradients with the highest metabolic value (190).

The effects of hormones on bacterial growth have been previously described extensively (132, 147, 164, 218, 220, 223, 242, 252). Here we analyzed the chemotactic preferences of the studied gut compounds in relation to their growth effects. In summary, chemotactic responses correlated with the growth effects of individual compounds. Although this relation was less clear for hormones that elicited biphasic responses, such as dopamine and NE, high concentrations of dopamine led to a strong attractant response that was consistent with the growth-promoting effect of dopamine. In contrast, for NE both the

effect on growth and chemotactic responses were very weak. Low concentrations of dopamine and high concentrations of NE, however elicited responses unrelated or opposite to growth effects.

For the compounds that elicited a repellent response, namely DHMA, melatonin and spermidine, there was a pronounced correlation with growth inhibition. Although low concentrations of DHMA were previously shown to elicit a highly sensitive attractant response (75, 77, 78), at high concentrations of DHMA, which affected growth, the behavior of *E. coli* in gradients was apparently dominated by the repellent response. The repellent response to melatonin and the observed growth inhibition are consistent with recently proposed effects of this hormone on the microbiome, as discussed later (144, 253). As previously discussed, serotonin affected neither growth nor chemotaxis of *E. coli*.

The only compound that elicited a straight attractant response in the wild-type cells was epinephrine, consistent with a previous study (76) and correlating again with its growth-promoting effect for *E. coli*.

#### **4.1. NE might behave as a signaling compound**

During homeostasis NE is probably the predominant signal in the intestine (134). It is known that this hormone acts in the GI tract and has receptors in the epithelium walls and that its activity change with their concentration (237). In stress situations, for example, the concentration of NE in the lumen gut increases and NE binds to the  $\beta$  adrenoceptors and A2 adenosine receptors. This leads to an increase in the cAMP levels and an increase of the permeability of the intestinal epithelium, which allows antigens to penetrate through the epithelium and thus activating the immune response (237, 254).

One theory proposes that NE works as signaling molecule for bacterial pathogens to aid towards their successful adaptation and survival within the host (93, 94, 134), since its concentration in the gut increases in stress situations, leading to the activation of the immune response (237, 254). We hypothesize that the biphasic chemotactic response observed may have evolved to sense the different concentrations of NE, in order to detect the host physiology. In this way, *E. coli* senses NE when its concentration reaches a certain threshold switching the chemotactic response to repellent, in order to predict and escape

the subsequent immune response. This may be the reason why at higher concentrations NE is repellent, since *E. coli* may have evolved to “run away” from the epithelium when there is an immune response and towards the epithelium when the concentration of NE is lower (Figure 36). It is therefore not surprising that mammals appear to have evolved protective mechanisms to tightly regulate levels of gut catecholamines and that catecholamine-degrading enzymes are present throughout the entire length of the human gastrointestinal tract (255).

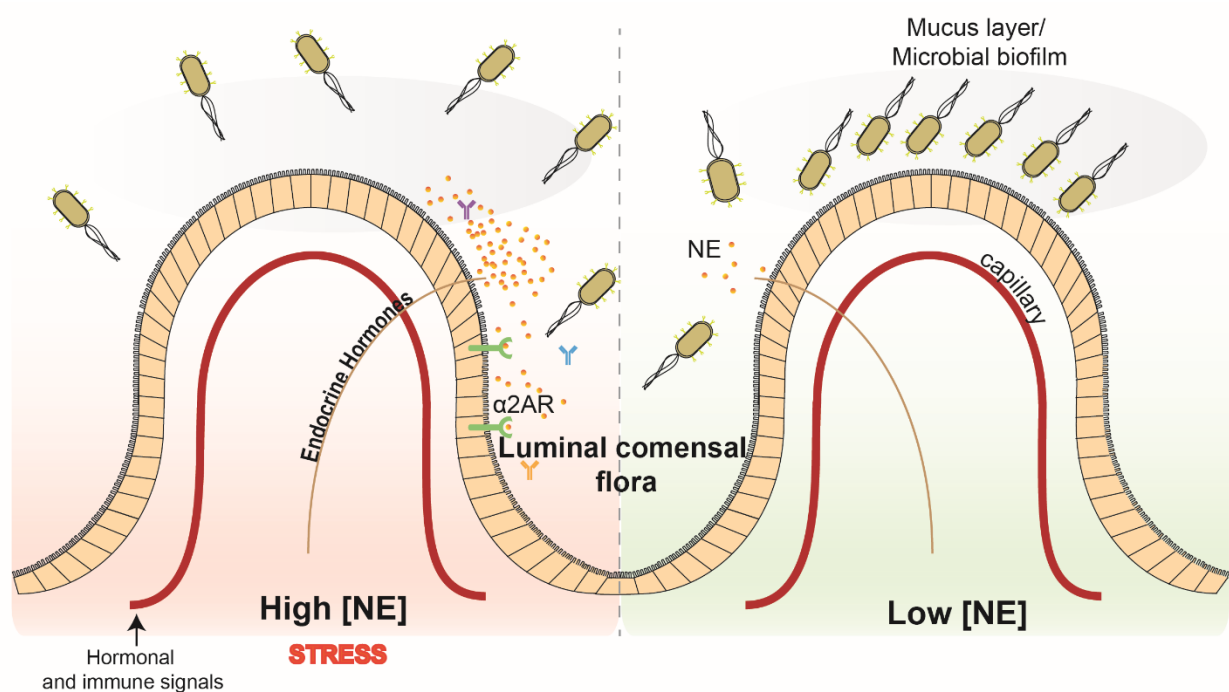


**Figure 36: Model of the NE signaling between host and microbiota.** NE is released into the gut lumen and sensed by bacterial receptors and by the host adrenoceptors. Activation of  $\alpha 2AR$  increases the cAMP levels that leads to increase of the permeability of the intestinal epithelium, which allows antigens to penetrate through the epithelium and thus activate the immune response.  $\alpha 2AR$ -  $\alpha 2$  adrenergic receptor

#### 4.2. Melatonin modulates the microbiome

Melatonin is a critical player of the host circadian mechanism and in the homeostasis maintenance of the GI tract (142, 143). The emerging role of the gut microbiome as an important modulator of gastrointestinal function has recently included the role of circadian rhythms. Several studies support the idea of an interaction between melatonin and the

microbiome (144, 145, 253) and suggest that microbial signaling plays a critical role in homeostatic maintenance of intestinal function along with the host circadian mechanism (142, 143). Further studies have expanded this view and have shown that disruption of the circadian clock, either via dietary restriction or time shifting affects temporal distribution of the gut microbiome constituents (144, 256). While it is clear from some studies that commensal bacteria and gut tissues do communicate, it is not clear which signal or signals the microbiome exploits to sustain its own homeostasis.

We suggest that melatonin can be disadvantageous to commensal bacteria, as supported by our results where we obtained a repellent chemotactic response and inhibition in growth, but simultaneously beneficial for pathogenic bacteria, as suggested for *Enterobacter aerogenes* (145), and hence modulating the microbiome composition.

#### **4.3. Dopamine growth effect**

Until now, the only explanation for the strong effect of the catecholamines (in our case dopamine) on the growth of bacteria relates to the iron restriction imposed by a majority of host tissues for the growth of most microbial pathogens. A strategy that bacteria often employ to scavenge nutritionally essential iron is the production and utilization of siderophores, which are secreted low molecular weight catecholate or hydroxamate molecules that possess high affinity for ferric iron (257). It has been described that the same catechol ring found in many siderophores is also present in the catecholamines (220). Freestone *et al.* shown that NE, epinephrine and dopamine, various inotropes (isoprenaline, dobutamine), and a few metabolites (DHMA and dihydroxyphenylglycol) all share the ability to facilitate bacterial acquisition of normally inaccessible transferrin and lactoferrin bound iron (95, 132, 164, 223, 242). Mechanistically, the catechol ring has been shown to form a complex with the ferric iron when it is bound with transferrin or lactoferrin, reducing the iron binding affinity of these proteins (132, 164, 223, 242). This releases the iron from transferrin or lactoferrin, the free iron can then bind to bacterial ferric iron binding siderophores, such as enterobactin (223). The precise molecular details of how catecholamines release transferrin and lactoferrin complexed iron remains to be elucidated,

for bacteria such as *E. coli* (223, 258) or *Salmonella* (259). However, this does not explain the results observed in the present study where dopamine produced a strong enhancement of growth in a rich medium, where neither transferrin nor lactoferrin were added. Additionally, as mentioned above, the enhancement effect on bacterial growth was also described for DHMA and NE, which was not reproduced in our experiments. Nonetheless, the differences between studies may be explained by differences in media and concentrations of catecholamines, as previously suggested (94). Since catecholamines were described to bind to inorganic iron ( $\text{Fe}^{3+}$ ), we speculate that dopamine may be able to reduce free iron to  $\text{Fe}^{2+}$  by itself, which then could be taken up by bacteria.

## 5. Concluding remarks

Approaching the microbial endocrinology field from the microbiome perspective may provide a better understanding of the specific mechanisms by which microorganisms can influence the host and vice versa. Specifically, considering chemotaxis in the context of the host-microbe interactions may provide a deeper understanding of the behavior of enteric bacteria within the host. Although the mechanism of hormone sensing by *E. coli* chemoreceptors remains to be further elucidated, we could show that spermidine is specifically sensed as a repellent by the low abundance receptor Trg and that this response is mediated by the periplasmic binding protein PotD.

Since bacterial chemotaxis is primarily a single-cell behavior, it may be highly important for the survival and proliferation of enterobacteria in the GI tract (74). The apparent correlation found between chemotactic preferences, growth effects and the nature of the tested gut compounds (i.e., food-derived or secreted) suggest that bacteria are exposed to gradients of hormones and other host-derived compounds in the mammalian gut. Consequently, *E. coli*, and most likely other motile enteric bacteria, seem to have evolved specific tactic responses as a way not only to avoid harmful (or locate beneficial) levels of these compounds, but also to orient themselves in the gut. In this context, repellent responses observed at high concentrations of compounds that are secreted from the gut epithelium may enable bacteria to limit immediate contact with the mucus layer of the GI tract, which is known to contain high levels of antimicrobial proteins and immunoglobulin A (IgA) (260, 261). Furthermore, the interplay between these repellent responses and attractant responses mediated by low concentrations of NE and DMHA, as observed previously (75-78, 130) and in our work, could explain chemotactic accumulation of *E. coli* at a certain distance from the mucosal surface (262). This area might represent a specific growth niche in the intestine (263), where bacteria can benefit from rapidly diffusing nutrients released by the

epithelium without being harmed by the mucosal antimicrobials. Intestinal inflammation has been previously shown to lead to an enhance release of nutrients (74) and electron acceptors (72, 264) along with a reduced hormone secretion (265-267). This might shift the accumulation pattern of EHEC or *Salmonella*, which possess chemotaxis systems that are nearly identical to that of the commensal *E. coli*, towards the mucosal surface, possibly promoting proliferation of *Proteobacteria* and infection (268).

## REFERENCES

1. Miller LD, Russell MH, Alexandre G. 2009. Diversity in bacterial chemotactic responses and niche adaptation. *Adv Appl Microbiol* 66:53-75.
2. Harshey RM. 2003. Bacterial motility on a surface: many ways to a common goal. *Annu Rev Microbiol* 57:249-73.
3. Manson MD, Tedesco P, Berg HC, Harold FM, Van der Drift C. 1977. A protonmotive force drives bacterial flagella. *Proc Natl Acad Sci U S A* 74:3060-4.
4. Kojima S, Yamamoto K, Kawagishi I, Homma M. 1999. The polar flagellar motor of *Vibrio cholerae* is driven by an Na<sup>+</sup> motive force. *J Bacteriol* 181:1927-30.
5. Berg HC, Brown DA. 1972. Chemotaxis in *Escherichia coli* analysed by three-dimensional tracking. *Nature* 239:500-4.
6. Wadhams GH, Armitage JP. 2004. Making sense of it all: bacterial chemotaxis. *Nat Rev Mol Cell Biol* 5:1024-37.
7. Darnton NC, Turner L, Rojevsky S, Berg HC. 2007. On torque and tumbling in swimming *Escherichia coli*. *J Bacteriol* 189:1756-64.
8. Sourjik V, Berg HC. 2004. Functional interactions between receptors in bacterial chemotaxis. *Nature* 428:437-41.
9. Vladimirov N, Sourjik V. 2009. Chemotaxis: how bacteria use memory. *Biol Chem* 390:1097-104.
10. Tindall MJ, Gaffney EA, Maini PK, Armitage JP. 2012. Theoretical insights into bacterial chemotaxis. *Wiley Interdiscip Rev Syst Biol Med* 4:247-59.
11. Macnab RM, Koshland DE, Jr. 1972. The gradient-sensing mechanism in bacterial chemotaxis. *Proc Natl Acad Sci U S A* 69:2509-12.
12. Segall JE, Block SM, Berg HC. 1986. Temporal comparisons in bacterial chemotaxis. *Proc Natl Acad Sci U S A* 83:8987-91.
13. Berg HC, Purcell EM. 1977. Physics of chemoreception. *Biophys J* 20:193-219.
14. Adler J, Hazelbauer GL, Dahl MM. 1973. Chemotaxis toward sugars in *Escherichia coli*. *J Bacteriol* 115:824-47.
15. Kalinin Y, Neumann S, Sourjik V, Wu M. 2010. Responses of *Escherichia coli* bacteria to two opposing chemoattractant gradients depend on the chemoreceptor ratio. *J Bacteriol* 192:1796-800.
16. Barkai N, Leibler S. 1997. Robustness in simple biochemical networks. *Nature* 387:913-7.
17. Kollmann M, Lovdok L, Bartholome K, Timmer J, Sourjik V. 2005. Design principles of a bacterial signalling network. *Nature* 438:504-7.
18. Studdert CA, Parkinson JS. 2005. Insights into the organization and dynamics of bacterial chemoreceptor clusters through *in vivo* crosslinking studies. *Proc Natl Acad Sci U S A* 102:15623-8.
19. Bibikov SI, Biran R, Rudd KE, Parkinson JS. 1997. A signal transducer for aerotaxis in *Escherichia coli*. *J Bacteriol* 179:4075-9.
20. Taylor BL, Zhulin IB, Johnson MS. 1999. Aerotaxis and other energy-sensing behavior in bacteria. *Annu Rev Microbiol* 53:103-28.
21. Mesibov R, Adler J. 1972. Chemotaxis toward amino acids in *Escherichia coli*. *J Bacteriol* 112:315-26.

22. Mesibov R, Ordal GW, Adler J. 1973. The range of attractant concentrations for bacterial chemotaxis and the threshold and size of response over this range. Weber law and related phenomena. *J Gen Physiol* 62:203-23.
23. Li M, Hazelbauer GL. 2004. Cellular stoichiometry of the components of the chemotaxis signaling complex. *J Bacteriol* 186:3687-94.
24. Li M, Hazelbauer GL. 2005. Adaptational assistance in clusters of bacterial chemoreceptors. *Mol Microbiol* 56:1617-26.
25. Neumann S, Hansen CH, Wingreen NS, Sourjik V. 2010. Differences in signalling by directly and indirectly binding ligands in bacterial chemotaxis. *EMBO J* 29:3484-95.
26. Sourjik V, Berg HC. 2002. Receptor sensitivity in bacterial chemotaxis. *Proc Natl Acad Sci U S A* 99:123-7.
27. Yi TM, Huang Y, Simon MI, Doyle J. 2000. Robust perfect adaptation in bacterial chemotaxis through integral feedback control. *Proc Natl Acad Sci U S A* 97:4649-53.
28. Yang Y, Sourjik V. 2012. Opposite responses by different chemoreceptors set a tunable preference point in *Escherichia coli* pH taxis. *Mol Microbiol* 86:1482-9.
29. Feng X, Baumgartner JW, Hazelbauer GL. 1997. High- and low-abundance chemoreceptors in *Escherichia coli*: differential activities associated with closely related cytoplasmic domains. *J Bacteriol* 179:6714-20.
30. Weerasuriya S, Schneider BM, Manson MD. 1998. Chimeric chemoreceptors in *Escherichia coli*: signaling properties of Tar-Tap and Tap-Tar hybrids. *J Bacteriol* 180:914-20.
31. Kristich CJ, Glekas GD, Ordal GW. 2003. The conserved cytoplasmic module of the transmembrane chemoreceptor McpC mediates carbohydrate chemotaxis in *Bacillus subtilis*. *Mol Microbiol* 47:1353-66.
32. Reyes-Darias JA, Yang Y, Sourjik V, Krell T. 2015. Correlation between signal input and output in PctA and PctB amino acid chemoreceptor of *Pseudomonas aeruginosa*. *Mol Microbiol* 96:513-25.
33. Reyes-Darias JA, Garcia V, Rico-Jimenez M, Corral-Lugo A, Lesouhaitier O, Juarez-Hernandez D, Yang Y, Bi S, Feuilloley M, Munoz-Rojas J, Sourjik V, Krell T. 2015. Specific gamma-aminobutyrate chemotaxis in *Pseudomonas* with different lifestyle. *Mol Microbiol* 97:488-501.
34. Salis H, Tamsir A, Voigt C. 2009. Engineering bacterial signals and sensors. *Contrib Microbiol* 16:194-225.
35. Bi S, Pollard AM, Yang Y, Jin F, Sourjik V. 2016. Engineering Hybrid Chemotaxis Receptors in Bacteria. *ACS Synth Biol* 5:989-1001.
36. DePamphilis ML, Adler J. 1971. Fine structure and isolation of the hook-basal body complex of flagella from *Escherichia coli* and *Bacillus subtilis*. *J Bacteriol* 105:384-95.
37. Dimmitt K, Simon M. 1971. Purification and thermal stability of intact *Bacillus subtilis* flagella. *J Bacteriol* 105:369-75.
38. Aizawa SI, Dean GE, Jones CJ, Macnab RM, Yamaguchi S. 1985. Purification and characterization of the flagellar hook-basal body complex of *Salmonella typhimurium*. *J Bacteriol* 161:836-49.
39. Macnab RM. 2003. How bacteria assemble flagella. *Annu Rev Microbiol* 57:77-100.
40. Berg HC. 2003. The rotary motor of bacterial flagella. *Annu Rev Biochem* 72:19-54.

41. Paul K, Brunstetter D, Titen S, Blair DF. 2011. A molecular mechanism of direction switching in the flagellar motor of *Escherichia coli*. *Proc Natl Acad Sci U S A* 108:17171-6.
42. Hazelbauer GL, Falke JJ, Parkinson JS. 2008. Bacterial chemoreceptors: high-performance signaling in networked arrays. *Trends Biochem Sci* 33:9-19.
43. Hazelbauer GL, Lai WC. 2010. Bacterial chemoreceptors: providing enhanced features to two-component signaling. *Curr Opin Microbiol* 13:124-32.
44. Segall JE, Manson MD, Berg HC. 1982. Signal processing times in bacterial chemotaxis. *Nature* 296:855-7.
45. Alon U, Surette MG, Barkai N, Leibler S. 1999. Robustness in bacterial chemotaxis. *Nature* 397:168-71.
46. Amin DN, Hazelbauer GL. 2010. The chemoreceptor dimer is the unit of conformational coupling and transmembrane signaling. *J Bacteriol* 192:1193-200.
47. Berg HC, Tedesco PM. 1975. Transient response to chemotactic stimuli in *Escherichia coli*. *Proc Natl Acad Sci U S A* 72:3235-9.
48. Neumann S, Vladimirov N, Krembel AK, Wingreen NS, Sourjik V. 2014. Imprecision of adaptation in *Escherichia coli* chemotaxis. *PLoS One* 9:e84904.
49. Goy MF, Springer MS, Adler J. 1977. Sensory transduction in *Escherichia coli*: role of a protein methylation reaction in sensory adaptation. *Proc Natl Acad Sci U S A* 74:4964-8.
50. Brown DA, Berg HC. 1974. Temporal stimulation of chemotaxis in *Escherichia coli*. *Proc Natl Acad Sci U S A* 71:1388-92.
51. Hedblom ML, Adler J. 1983. Chemotactic response of *Escherichia coli* to chemically synthesized amino acids. *J Bacteriol* 155:1463-6.
52. Manson MD, Blank V, Brade G, Higgins CF. 1986. Peptide chemotaxis in *E. coli* involves the Tap signal transducer and the dipeptide permease. *Nature* 321:253-6.
53. Tso WW, Adler J. 1974. Negative chemotaxis in *Escherichia coli*. *J Bacteriol* 118:560-76.
54. Maeda K, Imae Y, Shioi JI, Oosawa F. 1976. Effect of temperature on motility and chemotaxis of *Escherichia coli*. *J Bacteriol* 127:1039-46.
55. Adler J, Li C, Boileau AJ, Qi Y, Kung C. 1988. Osmotaxis in *Escherichia coli*. *Cold Spring Harb Symp Quant Biol* 53 Pt 1:19-22.
56. Qi YL, Adler J. 1989. Salt taxis in *Escherichia coli* bacteria and its lack in mutants. *Proc Natl Acad Sci U S A* 86:8358-62.
57. Li C, Adler J. 1993. *Escherichia coli* shows two types of behavioral responses to osmotic upshift. *J Bacteriol* 175:2564-7.
58. Slonczewski JL, Macnab RM, Alger JR, Castle AM. 1982. Effects of pH and repellent tactic stimuli on protein methylation levels in *Escherichia coli*. *J Bacteriol* 152:384-99.
59. Krikos A, Conley MP, Boyd A, Berg HC, Simon MI. 1985. Chimeric chemosensory transducers of *Escherichia coli*. *Proc Natl Acad Sci U S A* 82:1326-30.
60. Khan S, Spudich JL, McCray JA, Trentham DR. 1995. Chemotactic signal integration in bacteria. *Proc Natl Acad Sci U S A* 92:9757-61.
61. Paulick A, Jakovljevic V, Zhang S, Erickstad M, Groisman A, Meir Y, Ryu WS, Wingreen NS, Sourjik V. 2017. Mechanism of bidirectional thermotaxis in *Escherichia coli*. *Elife* 6.

62. Maeda K, Imae Y. 1979. Thermosensory transduction in *Escherichia coli*: inhibition of the thermoresponse by L-serine. *Proc Natl Acad Sci U S A* 76:91-5.
63. Imae Y, Mizuno T, Maeda K. 1984. Chemosensory and thermosensory excitation in adaptation-deficient mutants of *Escherichia coli*. *J Bacteriol* 159:368-74.
64. Lee L, Mizuno T, Imae Y. 1988. Thermosensing properties of *Escherichia coli* *tsr* mutants defective in serine chemoreception. *J Bacteriol* 170:4769-74.
65. Laganenka L, Colin R, Sourjik V. 2016. Chemotaxis towards autoinducer 2 mediates autoaggregation in *Escherichia coli*. *Nat Commun* 7:12984.
66. Jani S, Seely AL, Peabody VG, Jayaraman A, Manson MD. 2017. Chemotaxis to self-generated AI-2 promotes biofilm formation in *Escherichia coli*. *Microbiology* doi:10.1099/mic.0.000567.
67. Keilberg D, Ottemann KM. 2016. How *Helicobacter pylori* senses, targets and interacts with the gastric epithelium. *Environ Microbiol* 18:791-806.
68. Huang JY, Sweeney EG, Sigal M, Zhang HC, Remington SJ, Cantrell MA, Kuo CJ, Guillemin K, Amieva MR. 2015. Chemodetection and Destruction of Host Urea Allows *Helicobacter pylori* to Locate the Epithelium. *Cell Host Microbe* 18:147-56.
69. Chandrashekhar K, Gangaiah D, Pina-Mimbela R, Kassem, II, Jeon BH, Rajashekara G. 2015. Transducer like proteins of *Campylobacter jejuni* 81-176: role in chemotaxis and colonization of the chicken gastrointestinal tract. *Front Cell Infect Microbiol* 5:46.
70. Day CJ, King RM, Shewell LK, Tram G, Najnin T, Hartley-Tassell LE, Wilson JC, Fleetwood AD, Zhulin IB, Korolik V. 2016. A direct-sensing galactose chemoreceptor recently evolved in invasive strains of *Campylobacter jejuni*. *Nat Commun* 7:13206.
71. Rahman H, King RM, Shewell LK, Semchenko EA, Hartley-Tassell LE, Wilson JC, Day CJ, Korolik V. 2014. Characterisation of a multi-ligand binding chemoreceptor CcmL (Tlp3) of *Campylobacter jejuni*. *PLoS Pathog* 10:e1003822.
72. Rivera-Chavez F, Lopez CA, Zhang LF, Garcia-Pastor L, Chavez-Arroyo A, Lokken KL, Tsolis RM, Winter SE, Baumler AJ. 2016. Energy Taxis toward Host-Derived Nitrate Supports a *Salmonella* Pathogenicity Island 1-Independent Mechanism of Invasion. *MBio* 7.
73. Stecher B, Hapfelmeier S, Muller C, Kremer M, Stallmach T, Hardt WD. 2004. Flagella and chemotaxis are required for efficient induction of *Salmonella enterica* serovar *Typhimurium* colitis in streptomycin-pretreated mice. *Infect Immun* 72:4138-50.
74. Stecher B, Barthel M, Schlumberger MC, Haberli L, Rabsch W, Kremer M, Hardt WD. 2008. Motility allows *S. Typhimurium* to benefit from the mucosal defence. *Cell Microbiol* 10:1166-80.
75. Pasupuleti S, Sule N, Cohn WB, MacKenzie DS, Jayaraman A, Manson MD. 2014. Chemotaxis of *Escherichia coli* to norepinephrine (NE) requires conversion of NE to 3,4-dihydroxymandelic acid. *J Bacteriol* 196:3992-4000.
76. Bansal T, Englert D, Lee J, Hegde M, Wood TK, Jayaraman A. 2007. Differential effects of epinephrine, norepinephrine, and indole on *Escherichia coli* O157:H7 chemotaxis, colonization, and gene expression. *Infect Immun* 75:4597-607.
77. Sule N, Pasupuleti S, Kohli N, Menon R, Dangott LJ, Manson MD, Jayaraman A. 2017. The Norepinephrine Metabolite 3,4-Dihydroxymandelic Acid Is Produced by the

- Commensal Microbiota and Promotes Chemotaxis and Virulence Gene Expression in Enterohemorrhagic *Escherichia coli*. *Infect Immun* 85.
78. Pasupuleti S, Sule N, Manson MD, Jayaraman A. 2018. Conversion of Norepinephrine to 3,4-Dihydroxymandelic Acid in *Escherichia coli* Requires the QseBC Quorum-Sensing System and the FeaR Transcription Factor. *J Bacteriol* 200.
  79. Furness JB. 2012. The enteric nervous system and neurogastroenterology. *Nat Rev Gastroenterol Hepatol* 9:286-94.
  80. Johnson LR. 1988. Regulation of gastrointestinal mucosal growth. *Physiol Rev* 68:456-502.
  81. Johnson LR. 1977. Gastrointestinal hormones and their functions. *Annu Rev Physiol* 39:135-58.
  82. Ley RE, Peterson DA, Gordon JI. 2006. Ecological and evolutionary forces shaping microbial diversity in the human intestine. *Cell* 124:837-48.
  83. Flint HJ, Scott KP, Louis P, Duncan SH. 2012. The role of the gut microbiota in nutrition and health. *Nat Rev Gastroenterol Hepatol* 9:577-89.
  84. Maurice CF, Haiser HJ, Turnbaugh PJ. 2013. Xenobiotics shape the physiology and gene expression of the active human gut microbiome. *Cell* 152:39-50.
  85. Cryan JF, Dinan TG. 2012. Mind-altering microorganisms: the impact of the gut microbiota on brain and behaviour. *Nat Rev Neurosci* 13:701-12.
  86. Hsiao EY. 2013. Immune dysregulation in autism spectrum disorder. *Int Rev Neurobiol* 113:269-302.
  87. Sandler RH, Finegold SM, Bolte ER, Buchanan CP, Maxwell AP, Vaisanen ML, Nelson MN, Wexler HM. 2000. Short-term benefit from oral vancomycin treatment of regressive-onset autism. *J Child Neurol* 15:429-35.
  88. Evans JM, Morris LS, Marchesi JR. 2013. The gut microbiome: the role of a virtual organ in the endocrinology of the host. *J Endocrinol* 218:R37-47.
  89. Rhee SH, Pothoulakis C, Mayer EA. 2009. Principles and clinical implications of the brain-gut-enteric microbiota axis. *Nat Rev Gastroenterol Hepatol* 6:306-14.
  90. Lenard J. 1992. Mammalian hormones in microbial cells. *Trends Biochem Sci* 17:147-50.
  91. Traub WH, Bauer D, Wolf U. 1991. Virulence of clinical and fecal isolates of *Clostridium perfringens* type A for outbred NMRI mice. *Chemotherapy* 37:426-35.
  92. LeRoith D, Shiloach J, Roth J, Lesniak MA. 1981. Insulin or a closely related molecule is native to *Escherichia coli*. *J Biol Chem* 256:6533-6.
  93. Lyte M, Ernst S. 1992. Catecholamine induced growth of gram negative bacteria. *Life Sci* 50:203-12.
  94. Lyte M. 2004. Microbial endocrinology and infectious disease in the 21st century. *Trends Microbiol* 12:14-20.
  95. Freestone PP, Haigh RD, Lyte M. 2008. Catecholamine inotrope resuscitation of antibiotic-damaged staphylococci and its blockade by specific receptor antagonists. *J Infect Dis* 197:1044-52.
  96. Freestone PP, Sandrini SM, Haigh RD, Lyte M. 2008. Microbial endocrinology: how stress influences susceptibility to infection. *Trends Microbiol* 16:55-64.

97. Le Roith D, Shiloach J, Roth J, Lesniak MA. 1980. Evolutionary origins of vertebrate hormones: substances similar to mammalian insulins are native to unicellular eukaryotes. *Proc Natl Acad Sci U S A* 77:6184-8.
98. Tsavkelova EA, Botvinko IV, Kudrin VS, Oleskin AV. 2000. Detection of neurotransmitter amines in microorganisms with the use of high-performance liquid chromatography. *Dokl Biochem* 372:115-7.
99. Iyer LM, Aravind L, Coon SL, Klein DC, Koonin EV. 2004. Evolution of cell-cell signaling in animals: did late horizontal gene transfer from bacteria have a role? *Trends Genet* 20:292-9.
100. Stephenson M, Rowatt E. 1947. The production of acetylcholine by a strain of *Lactobacillus plantarum*. *J Gen Microbiol* 1:279-98.
101. Hsu SC, Johansson KR, Donahue MJ. 1986. The bacterial flora of the intestine of *Ascaris suum* and 5-hydroxytryptamine production. *J Parasitol* 72:545-9.
102. Devalia JL, Grady D, Harmanyeri Y, Tabaqchali S, Davies RJ. 1989. Histamine synthesis by respiratory tract micro-organisms: possible role in pathogenicity. *J Clin Pathol* 42:516-22.
103. Liss JL, Alpers D, Woodruff RA, Jr. 1973. The irritable colon syndrome and psychiatric illness. *Dis Nerv Syst* 34:151-7.
104. Manichanh C, Rigottier-Gois L, Bonnaud E, Gloux K, Pelletier E, Frangeul L, Nalin R, Jarrin C, Chardon P, Marteau P, Roca J, Dore J. 2006. Reduced diversity of faecal microbiota in Crohn's disease revealed by a metagenomic approach. *Gut* 55:205-11.
105. Ott SJ, Musfeldt M, Wenderoth DF, Hampe J, Brant O, Folsch UR, Timmis KN, Schreiber S. 2004. Reduction in diversity of the colonic mucosa associated bacterial microflora in patients with active inflammatory bowel disease. *Gut* 53:685-93.
106. Frank DN, St Amand AL, Feldman RA, Boedeker EC, Harpaz N, Pace NR. 2007. Molecular-phylogenetic characterization of microbial community imbalances in human inflammatory bowel diseases. *Proc Natl Acad Sci U S A* 104:13780-5.
107. Kleessen B, Kroesen AJ, Buhr HJ, Blaut M. 2002. Mucosal and invading bacteria in patients with inflammatory bowel disease compared with controls. *Scand J Gastroenterol* 37:1034-41.
108. Dinan TG, Stanton C, Cryan JF. 2013. Psychobiotics: a novel class of psychotropic. *Biol Psychiatry* 74:720-6.
109. Dinan TG, Cryan JF. 2012. Regulation of the stress response by the gut microbiota: implications for psychoneuroendocrinology. *Psychoneuroendocrinology* 37:1369-78.
110. Reiche EM, Nunes SO, Morimoto HK. 2004. Stress, depression, the immune system, and cancer. *Lancet Oncol* 5:617-25.
111. Winek K, Dirnagl U, Meisel A. 2016. The Gut Microbiome as Therapeutic Target in Central Nervous System Diseases: Implications for Stroke. *Neurotherapeutics* 13:762-774.
112. Dinan TG, Cryan JF. 2017. Gut-brain axis in 2016: Brain-gut-microbiota axis - mood, metabolism and behaviour. *Nat Rev Gastroenterol Hepatol* 14:69-70.
113. Finegold SM. 1986. Normal human intestinal flora. *Ann Ist Super Sanita* 22:731-7.
114. Moller AK, Leatham MP, Conway T, Nuijten PJ, de Haan LA, Krogfelt KA, Cohen PS. 2003. An *Escherichia coli* MG1655 lipopolysaccharide deep-rough core mutant grows

- and survives in mouse cecal mucus but fails to colonize the mouse large intestine. *Infect Immun* 71:2142-52.
115. Maroncle N, Balestrino D, Rich C, Forestier C. 2002. Identification of *Klebsiella pneumoniae* genes involved in intestinal colonization and adhesion using signature-tagged mutagenesis. *Infect Immun* 70:4729-34.
  116. Favre-Bonte S, Licht TR, Forestier C, Krogfelt KA. 1999. *Klebsiella pneumoniae* capsule expression is necessary for colonization of large intestines of streptomycin-treated mice. *Infect Immun* 67:6152-6.
  117. Marteau P, Pochart P, Dore J, Bera-Maillet C, Bernalier A, Corthier G. 2001. Comparative study of bacterial groups within the human cecal and fecal microbiota. *Appl Environ Microbiol* 67:4939-42.
  118. Potten CS, Allen TD. 1977. Ultrastructure of cell loss in intestinal mucosa. *J Ultrastruct Res* 60:272-7.
  119. Miranda RL, Conway T, Leatham MP, Chang DE, Norris WE, Allen JH, Stevenson SJ, Laux DC, Cohen PS. 2004. Glycolytic and gluconeogenic growth of *Escherichia coli* O157:H7 (EDL933) and *E. coli* K-12 (MG1655) in the mouse intestine. *Infect Immun* 72:1666-76.
  120. Licht TR, Krogfelt KA, Cohen PS, Poulsen LK, Urbance J, Molin S. 1996. Role of lipopolysaccharide in colonization of the mouse intestine by *Salmonella typhimurium* studied by *in situ* hybridization. *Infect Immun* 64:3811-7.
  121. McCormick BA, Laux DC, Cohen PS. 1990. Neither motility nor chemotaxis plays a role in the ability of *Escherichia coli* F-18 to colonize the streptomycin-treated mouse large intestine. *Infect Immun* 58:2957-61.
  122. Conway T, Krogfelt KA, Cohen PS. 2004. The Life of Commensal *Escherichia coli* in the Mammalian Intestine. *EcoSal Plus* 1.
  123. Fahlbusch R, Barocka A. 1995. Hormones and behaviour. *Acta Neurochir (Wien)* 132:169-77.
  124. Lodish H BA, Zipursky SL, et al. 2000. Neurotransmitters, Synapses, and Impulse Transmission. In Freeman WH (ed), *Molecular Cell Biology*, vol 4th edition, New York.
  125. Costa M, Brookes SJ, Hennig GW. 2000. Anatomy and physiology of the enteric nervous system. *Gut* 47 Suppl 4:iv15-9; discussion iv26.
  126. Goldstein DS, Eisenhofer G, Kopin IJ. 2003. Sources and significance of plasma levels of catechols and their metabolites in humans. *J Pharmacol Exp Ther* 305:800-11.
  127. Eisenhofer G, Aneman A, Friberg P, Hooper D, Fandriks L, Lonroth H, Hunyady B, Mezey E. 1997. Substantial production of dopamine in the human gastrointestinal tract. *J Clin Endocrinol Metab* 82:3864-71.
  128. Vieira-Coelho MA, Soares-da-Silva P. 1993. Dopamine formation, from its immediate precursor 3,4-dihydroxyphenylalanine, along the rat digestive tract. *Fundam Clin Pharmacol* 7:235-43.
  129. Glaser R, Kiecolt-Glaser JK. 2005. Stress-induced immune dysfunction: implications for health. *Nat Rev Immunol* 5:243-51.
  130. Sperandio V, Torres AG, Jarvis B, Nataro JP, Kaper JB. 2003. Bacteria-host communication: the language of hormones. *Proc Natl Acad Sci U S A* 100:8951-6.
  131. Pierantozzi M, Pietroiusti A, Brusa L, Galati S, Stefani A, Lunardi G, Fedele E, Sancesario G, Bernardi G, Bergamaschi A, Magrini A, Stanzione P, Galante A. 2006.

- Helicobacter pylori* eradication and l-dopa absorption in patients with PD and motor fluctuations. *Neurology* 66:1824-9.
132. Freestone PP, Lyte M, Neal CP, Maggs AF, Haigh RD, Williams PH. 2000. The mammalian neuroendocrine hormone norepinephrine supplies iron for bacterial growth in the presence of transferrin or lactoferrin. *J Bacteriol* 182:6091-8.
  133. Clarke MB, Hughes DT, Zhu C, Boedeker EC, Sperandio V. 2006. The QseC sensor kinase: a bacterial adrenergic receptor. *Proc Natl Acad Sci U S A* 103:10420-5.
  134. Pacheco AR, Sperandio V. 2009. Inter-kingdom signaling: chemical language between bacteria and host. *Curr Opin Microbiol* 12:192-8.
  135. Pullinger GD, Carnell SC, Sharaff FF, van Diemen PM, Dziva F, Morgan E, Lyte M, Freestone PP, Stevens MP. 2010. Norepinephrine augments *Salmonella enterica*-induced enteritis in a manner associated with increased net replication but independent of the putative adrenergic sensor kinases QseC and QseE. *Infect Immun* 78:372-80.
  136. Pullinger GD, van Diemen PM, Carnell SC, Davies H, Lyte M, Stevens MP. 2010. 6-hydroxydopamine-mediated release of norepinephrine increases faecal excretion of *Salmonella enterica* serovar *Typhimurium* in pigs. *Vet Res* 41:68.
  137. Gershon MD, Tack J. 2007. The serotonin signaling system: from basic understanding to drug development for functional GI disorders. *Gastroenterology* 132:397-414.
  138. Manocha M, Khan WI. 2012. Serotonin and GI Disorders: An Update on Clinical and Experimental Studies. *Clin Transl Gastroenterol* 3:e13.
  139. Wikoff WR, Anfora AT, Liu J, Schultz PG, Lesley SA, Peters EC, Siuzdak G. 2009. Metabolomics analysis reveals large effects of gut microflora on mammalian blood metabolites. *Proc Natl Acad Sci U S A* 106:3698-703.
  140. Matsumoto M, Kakizoe K, Benno Y. 2007. Comparison of fecal microbiota and polyamine concentration in adult patients with intractable atopic dermatitis and healthy adults. *Microbiol Immunol* 51:37-46.
  141. Bubenik GA. 2002. Gastrointestinal melatonin: localization, function, and clinical relevance. *Dig Dis Sci* 47:2336-48.
  142. Mukherji A, Kobiita A, Ye T, Chambon P. 2013. Homeostasis in intestinal epithelium is orchestrated by the circadian clock and microbiota cues transduced by TLRs. *Cell* 153:812-27.
  143. de Kivit S, Tobin MC, Forsyth CB, Keshavarzian A, Landay AL. 2014. Regulation of Intestinal Immune Responses through TLR Activation: Implications for Pro- and Prebiotics. *Front Immunol* 5:60.
  144. Voigt RM, Forsyth CB, Green SJ, Mutlu E, Engen P, Vitaterna MH, Turek FW, Keshavarzian A. 2014. Circadian disorganization alters intestinal microbiota. *PLoS One* 9:e97500.
  145. Paulose JK, Cassone VM. 2016. The melatonin-sensitive circadian clock of the enteric bacterium *Enterobacter aerogenes*. *Gut Microbes* doi:10.1080/19490976.2016.1208892:1-4.
  146. Ogino Y, Sato T, Iguchi T. 2016. Gonadal Steroids, p Pages 504–506. *In* Takei Y, Ando H, Tsutsui K (ed), *Handbook of Hormones*. Academic Press, The Boulevard, Langford Lane, Kidlington, Oxford OX5 1GB.

147. Kornman KS, Loesche WJ. 1982. Effects of estradiol and progesterone on *Bacteroides melaninogenicus* and *Bacteroides gingivalis*. *Infect Immun* 35:256-63.
148. Ridlon JM, Ikegawa S, Alves JM, Zhou B, Kobayashi A, Iida T, Mitamura K, Tanabe G, Serrano M, De Guzman A, Cooper P, Buck GA, Hylemon PB. 2013. *Clostridium scindens*: a human gut microbe with a high potential to convert glucocorticoids into androgens. *J Lipid Res* 54:2437-49.
149. Haro C, Rangel-Zuniga OA, Alcalá-Díaz JF, Gomez-Delgado F, Perez-Martinez P, Delgado-Lista J, Quintana-Navarro GM, Landa BB, Navas-Cortes JA, Tena-Sempere M, Clemente JC, Lopez-Miranda J, Perez-Jimenez F, Camargo A. 2016. Intestinal Microbiota Is Influenced by Gender and Body Mass Index. *PLoS One* 11:e0154090.
150. Woods DE, Jones AL, Hill PJ. 1993. Interaction of insulin with *Pseudomonas pseudomallei*. *Infect Immun* 61:4045-50.
151. Khan MT, Nieuwdorp M, Backhed F. 2014. Microbial modulation of insulin sensitivity. *Cell Metab* 20:753-60.
152. Qin J, Li Y, Cai Z, Li S, Zhu J, Zhang F, Liang S, Zhang W, Guan Y, Shen D, Peng Y, Zhang D, Jie Z, Wu W, Qin Y, Xue W, Li J, Han L, Lu D, Wu P, Dai Y, Sun X, Li Z, Tang A, Zhong S, Li X, Chen W, Xu R, Wang M, Feng Q, Gong M, Yu J, Zhang Y, Zhang M, Hansen T, Sanchez G, Raes J, Falony G, Okuda S, Almeida M, LeChatelier E, Renault P, Pons N, Batto JM, Zhang Z, Chen H, Yang R, Zheng W, Li S, Yang H, et al. 2012. A metagenome-wide association study of gut microbiota in type 2 diabetes. *Nature* 490:55-60.
153. Tabor CW, Tabor H. 1984. Polyamines. *Annu Rev Biochem* 53:749-90.
154. Pegg AE. 1986. Recent advances in the biochemistry of polyamines in eukaryotes. *Biochem J* 234:249-62.
155. Gerner EW, Meyskens FL, Jr. 2004. Polyamines and cancer: old molecules, new understanding. *Nat Rev Cancer* 4:781-92.
156. Sawada Y, Pereira SP, Murphy GM, Dowling RH. 1994. Polyamines in the intestinal lumen of patients with small bowel bacterial overgrowth. *Biochem Soc Trans* 22:392S.
157. van Dam L, Korolev N, Nordenskiöld L. 2002. Polyamine-nucleic acid interactions and the effects on structure in oriented DNA fibers. *Nucleic Acids Res* 30:419-28.
158. Igarashi K, Kashiwagi K. 2006. Polyamine Modulon in *Escherichia coli*: genes involved in the stimulation of cell growth by polyamines. *J Biochem* 139:11-6.
159. Chattopadhyay MK, Tabor CW, Tabor H. 2003. Polyamines protect *Escherichia coli* cells from the toxic effect of oxygen. *Proc Natl Acad Sci U S A* 100:2261-5.
160. Patel CN, Wortham BW, Lines JL, Fetherston JD, Perry RD, Oliveira MA. 2006. Polyamines are essential for the formation of plague biofilm. *J Bacteriol* 188:2355-63.
161. Kashiwagi K, Kobayashi H, Igarashi K. 1986. Apparently unidirectional polyamine transport by proton motive force in polyamine-deficient *Escherichia coli*. *J Bacteriol* 165:972-7.
162. Pistocchi R, Kashiwagi K, Miyamoto S, Nukui E, Sadakata Y, Kobayashi H, Igarashi K. 1993. Characteristics of the operon for a putrescine transport system that maps at 19 minutes on the *Escherichia coli* chromosome. *J Biol Chem* 268:146-52.

163. Furuchi T, Kashiwagi K, Kobayashi H, Igarashi K. 1991. Characteristics of the gene for a spermidine and putrescine transport system that maps at 15 min on the *Escherichia coli* chromosome. *J Biol Chem* 266:20928-33.
164. Freestone PP, Haigh RD, Lyte M. 2007. Blockade of catecholamine-induced growth by adrenergic and dopaminergic receptor antagonists in *Escherichia coli* O157:H7, *Salmonella enterica* and *Yersinia enterocolitica*. *BMC Microbiol* 7:8.
165. Coulanges V, Andre P, Ziegler O, Buchheit L, Vidon DJ. 1997. Utilization of iron-catecholamine complexes involving ferric reductase activity in *Listeria monocytogenes*. *Infect Immun* 65:2778-85.
166. Albrecht-Gary AM, Crumbliss AL. 1998. Coordination chemistry of siderophores: thermodynamics and kinetics of iron chelation and release. *Met Ions Biol Syst* 35:239-327.
167. Larsen RA, Thomas MG, Postle K. 1999. Protonmotive force, ExbB and ligand-bound FepA drive conformational changes in TonB. *Mol Microbiol* 31:1809-24.
168. Hantke K. 1997. Ferrous iron uptake by a magnesium transport system is toxic for *Escherichia coli* and *Salmonella typhimurium*. *J Bacteriol* 179:6201-4.
169. Hantke K. 1987. Selection procedure for deregulated iron transport mutants (*fur*) in *Escherichia coli* K 12: *fur* not only affects iron metabolism. *Mol Gen Genet* 210:135-9.
170. Braun V. 1997. Surface signaling: novel transcription initiation mechanism starting from the cell surface. *Arch Microbiol* 167:325-31.
171. Ferguson AD, Hofmann E, Coulton JW, Diederichs K, Welte W. 1998. Siderophore-mediated iron transport: crystal structure of FhuA with bound lipopolysaccharide. *Science* 282:2215-20.
172. Crosa JH. 1984. The relationship of plasmid-mediated iron transport and bacterial virulence. *Annu Rev Microbiol* 38:69-89.
173. Braun V, Gross R, Koster W, Zimmermann L. 1983. Plasmid and chromosomal mutants in the iron(III)-aerobactin transport system of *Escherichia coli*. Use of streptonigrin for selection. *Mol Gen Genet* 192:131-9.
174. Sauer M, Hantke K, Braun V. 1987. Ferric-coprogen receptor FhuE of *Escherichia coli*: processing and sequence common to all TonB-dependent outer membrane receptor proteins. *J Bacteriol* 169:2044-9.
175. Matzanke BF, Anemuller S, Schunemann V, Trautwein AX, Hantke K. 2004. FhuF, part of a siderophore-reductase system. *Biochemistry* 43:1386-92.
176. Nau CD, Konisky J. 1989. Evolutionary relationship between the TonB-dependent outer membrane transport proteins: nucleotide and amino acid sequences of the *Escherichia coli* colicin I receptor gene. *J Bacteriol* 171:1041-7.
177. Hantke K. 1990. Dihydroxybenzoylserine--a siderophore for *E. coli*. *FEMS Microbiol Lett* 55:5-8.
178. Kammler M, Schon C, Hantke K. 1993. Characterization of the ferrous iron uptake system of *Escherichia coli*. *J Bacteriol* 175:6212-9.
179. Patzer SI, Hantke K. 2001. Dual repression by Fe<sup>(2+)</sup>-Fur and Mn<sup>(2+)</sup>-MntR of the *mntH* gene, encoding an NRAMP-like Mn<sup>(2+)</sup> transporter in *Escherichia coli*. *J Bacteriol* 183:4806-13.

180. Blattner FR, Plunkett G, 3rd, Bloch CA, Perna NT, Burland V, Riley M, Collado-Vides J, Glasner JD, Rode CK, Mayhew GF, Gregor J, Davis NW, Kirkpatrick HA, Goeden MA, Rose DJ, Mau B, Shao Y. 1997. The complete genome sequence of *Escherichia coli* K-12. *Science* 277:1453-62.
181. Parkinson JS, Houts SE. 1982. Isolation and behavior of *Escherichia coli* deletion mutants lacking chemotaxis functions. *J Bacteriol* 151:106-13.
182. Endres RG, Oleksiuk O, Hansen CH, Meir Y, Sourjik V, Wingreen NS. 2008. Variable sizes of *Escherichia coli* chemoreceptor signaling teams. *Mol Syst Biol* 4:211.
183. Ames P, Studdert CA, Reiser RH, Parkinson JS. 2002. Collaborative signaling by mixed chemoreceptor teams in *Escherichia coli*. *Proc Natl Acad Sci U S A* 99:7060-5.
184. Baba T, Ara T, Hasegawa M, Takai Y, Okumura Y, Baba M, Datsenko KA, Tomita M, Wanner BL, Mori H. 2006. Construction of *Escherichia coli* K-12 in-frame, single-gene knockout mutants: the Keio collection. *Mol Syst Biol* 2:2006 0008.
185. Judicial Commission of the International Committee on Systematics of P. 2005. The type species of the genus *Salmonella Lignieres* 1900 is *Salmonella enterica* (ex Kauffmann and Edwards 1952) Le Minor and Popoff 1987, with the type strain LT2T, and conservation of the epithet *enterica* in *Salmonella enterica* over all earlier epithets that may be applied to this species. Opinion 80. *Int J Syst Evol Microbiol* 55:519-20.
186. Ochman H, Selander RK. 1984. Standard reference strains of *Escherichia coli* from natural populations. *J Bacteriol* 157:690-3.
187. Guzman LM, Belin D, Carson MJ, Beckwith J. 1995. Tight regulation, modulation, and high-level expression by vectors containing the arabinose PBAD promoter. *J Bacteriol* 177:4121-30.
188. Buron-Barral MC, Gosink KK, Parkinson JS. 2006. Loss- and gain-of-function mutations in the F1-HAMP region of the *Escherichia coli* aerotaxis transducer Aer. *J Bacteriol* 188:3477-86.
189. Cherepanov PP, Wackernagel W. 1995. Gene disruption in *Escherichia coli*: TcR and KmR cassettes with the option of Flp-catalyzed excision of the antibiotic-resistance determinant. *Gene* 158:9-14.
190. Yang Y, A MP, Hofler C, Poschet G, Wirtz M, Hell R, Sourjik V. 2015. Relation between chemotaxis and consumption of amino acids in bacteria. *Mol Microbiol* 96:1272-82.
191. Sommer E. 2012. *In vivo* study of the two-component signaling network in *Escherichia coli*. Doctor of Natural Sciences. University of Heidelberg, Heidelberg, Germany.
192. Chung CT, Niemela SL, Miller RH. 1989. One-step preparation of competent *Escherichia coli*: transformation and storage of bacterial cells in the same solution. *Proc Natl Acad Sci U S A* 86:2172-5.
193. Thomason LC, Costantino N, Court DL. 2007. *E. coli* genome manipulation by P1 transduction. *Curr Protoc Mol Biol* Chapter 1:Unit 1 17.
194. Datsenko KA, Wanner BL. 2000. One-step inactivation of chromosomal genes in *Escherichia coli* K-12 using PCR products. *Proc Natl Acad Sci U S A* 97:6640-5.
195. Peng S, Stephan R, Hummerjohann J, Tasara T. 2014. Evaluation of three reference genes of *Escherichia coli* for mRNA expression level normalization in view of salt and organic acid stress exposure in food. *FEMS Microbiol Lett* 355:78-82.

196. Kentner D, Sourjik V. 2009. Dynamic map of protein interactions in the *Escherichia coli* chemotaxis pathway. *Mol Syst Biol* 5:238.
197. Si G, Yang W, Bi S, Luo C, Ouyang Q. 2012. A parallel diffusion-based microfluidic device for bacterial chemotaxis analysis. *Lab Chip* 12:1389-94.
198. Colin R, Zhang R, Wilson LG. 2014. Fast, high-throughput measurement of collective behaviour in a bacterial population. *J R Soc Interface* 11:20140486.
199. Joseph R. Bianchine Ph.D. MD, Leonor R. Calimlim M.D., John P. Morgan M.D., Carlos A. Dujuvne M.D., Louis Lasagna M.D. 1971. Metabolism and absorption of L-3,4 dihydroxyphenylalanine in patients with parkinson's disease. *Annals of the New York Academy of Sciences* 179:126–139.
200. Vieira-Coelho MA, Soares-Da-Silva P. 1998. Uptake and intracellular fate of L-DOPA in a human intestinal epithelial cell line: Caco-2. *Am J Physiol* 275:C104-12.
201. Reigstad CS, Salmonson CE, Rainey JF, 3rd, Szurszewski JH, Linden DR, Sonnenburg JL, Farrugia G, Kashyap PC. 2015. Gut microbes promote colonic serotonin production through an effect of short-chain fatty acids on enterochromaffin cells. *FASEB J* 29:1395-403.
202. O'Mahony SM, Clarke G, Borre YE, Dinan TG, Cryan JF. 2015. Serotonin, tryptophan metabolism and the brain-gut-microbiome axis. *Behav Brain Res* 277:32-48.
203. Kim DY, Camilleri M. 2000. Serotonin: a mediator of the brain-gut connection. *Am J Gastroenterol* 95:2698-709.
204. Camilleri M. 2009. Serotonin in the gastrointestinal tract. *Curr Opin Endocrinol Diabetes Obes* 16:53-9.
205. Milovic V. 2001. Polyamines in the gut lumen: bioavailability and biodistribution. *Eur J Gastroenterol Hepatol* 13:1021-5.
206. Los DA, Murata N. 2004. Membrane fluidity and its roles in the perception of environmental signals. *Biochim Biophys Acta* 1666:142-57.
207. Olivia A, Fariña JB, Lladrés M. 1996. Influence of temperature and shaking on stability of insulin preparations: Degradation kinetics. *Int J Pharm* Volume 143:Pages 163-170.
208. Wilson LG, Martinez VA, Schwarz-Linek J, Tailleur J, Bryant G, Pusey PN, Poon WC. 2011. Differential dynamic microscopy of bacterial motility. *Phys Rev Lett* 106:018101.
209. Salman H, Libchaber A. 2007. A concentration-dependent switch in the bacterial response to temperature. *Nat Cell Biol* 9:1098-100.
210. Gosink KK, Buron-Barral MC, Parkinson JS. 2006. Signaling interactions between the aerotaxis transducer Aer and heterologous chemoreceptors in *Escherichia coli*. *J Bacteriol* 188:3487-93.
211. Clausznitzer D, Oleksiuk O, Lovdok L, Sourjik V, Endres RG. 2010. Chemotactic response and adaptation dynamics in *Escherichia coli*. *PLoS Comput Biol* 6:e1000784.
212. Binnie RA, Zhang H, Mowbray S, Hermodson MA. 1992. Functional mapping of the surface of *Escherichia coli* ribose-binding protein: mutations that affect chemotaxis and transport. *Protein Sci* 1:1642-51.
213. Ames GF. 1986. Bacterial periplasmic transport systems: structure, mechanism, and evolution. *Annu Rev Biochem* 55:397-425.

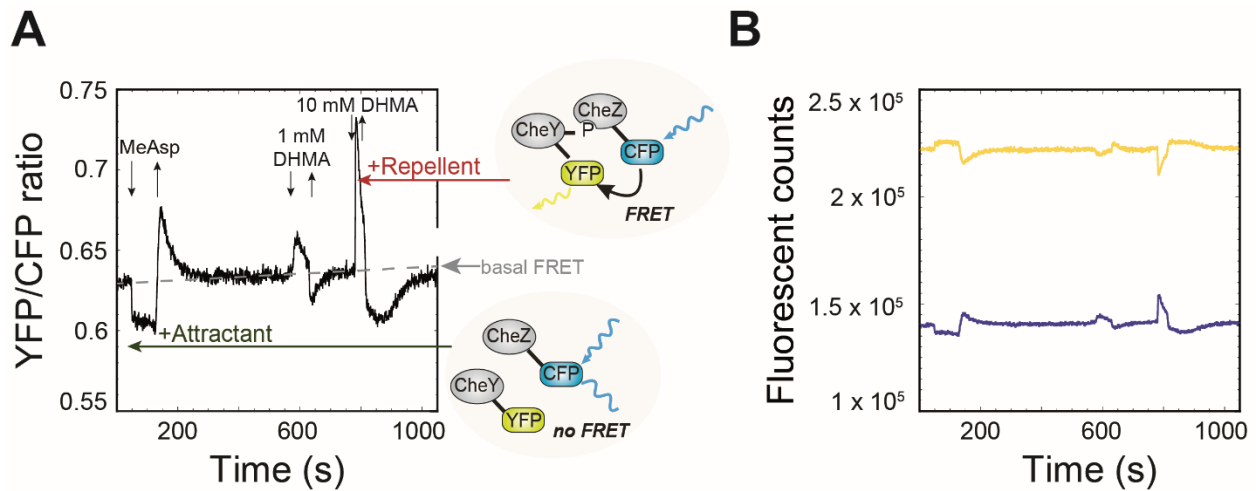
214. Kashiwagi K, Hosokawa N, Furuchi T, Kobayashi H, Sasakawa C, Yoshikawa M, Igarashi K. 1990. Isolation of polyamine transport-deficient mutants of *Escherichia coli* and cloning of the genes for polyamine transport proteins. *J Biol Chem* 265:20893-7.
215. Sugiyama S, Matsuo Y, Maenaka K, Vassilyev DG, Matsushima M, Kashiwagi K, Igarashi K, Morikawa K. 1996. The 1.8-Å X-ray structure of the *Escherichia coli* PotD protein complexed with spermidine and the mechanism of polyamine binding. *Protein Sci* 5:1984-90.
216. Yohannes E, Thurber AE, Wilks JC, Tate DP, Slonczewski JL. 2005. Polyamine stress at high pH in *Escherichia coli* K-12. *BMC Microbiol* 5:59.
217. Lyte M, Frank CD, Green BT. 1996. Production of an autoinducer of growth by norepinephrine cultured *Escherichia coli* O157:H7. *FEMS Microbiol Lett* 139:155-9.
218. Lyte M, Arulanandam B, Nguyen K, Frank C, Erickson A, Francis D. 1997. Norepinephrine induced growth and expression of virulence associated factors in enterotoxigenic and enterohemorrhagic strains of *Escherichia coli*. *Adv Exp Med Biol* 412:331-9.
219. Wagegg W, Braun V. 1981. Ferric citrate transport in *Escherichia coli* requires outer membrane receptor protein fecA. *J Bacteriol* 145:156-63.
220. Kinney KS, Austin CE, Morton DS, Sonnenfeld G. 2000. Norepinephrine as a growth stimulating factor in bacteria--mechanistic studies. *Life Sci* 67:3075-85.
221. Hesslinger C, Fairhurst SA, Sawers G. 1998. Novel keto acid formate-lyase and propionate kinase enzymes are components of an anaerobic pathway in *Escherichia coli* that degrades L-threonine to propionate. *Mol Microbiol* 27:477-92.
222. Yanofsky C, Platt T, Crawford IP, Nichols BP, Christie GE, Horowitz H, VanCleemput M, Wu AM. 1981. The complete nucleotide sequence of the tryptophan operon of *Escherichia coli*. *Nucleic Acids Res* 9:6647-68.
223. Freestone PP, Haigh RD, Williams PH, Lyte M. 2003. Involvement of enterobactin in norepinephrine-mediated iron supply from transferrin to enterohaemorrhagic *Escherichia coli*. *FEMS Microbiol Lett* 222:39-43.
224. Sandrini SM, Shergill R, Woodward J, Muralikuttan R, Haigh RD, Lyte M, Freestone PP. 2010. Elucidation of the mechanism by which catecholamine stress hormones liberate iron from the innate immune defense proteins transferrin and lactoferrin. *J Bacteriol* 192:587-94.
225. McHugh JP, Rodriguez-Quinones F, Abdul-Tehrani H, Svistunenko DA, Poole RK, Cooper CE, Andrews SC. 2003. Global iron-dependent gene regulation in *Escherichia coli*. A new mechanism for iron homeostasis. *J Biol Chem* 278:29478-86.
226. Gurmu D, Lu J, Johnson KA, Nordlund P, Holmgren A, Erlandsen H. 2009. The crystal structure of the protein YhaK from *Escherichia coli* reveals a new subclass of redox sensitive enterobacterial bicupins. *Proteins* 74:18-31.
227. Ratledge C, Winder FG. 1964. Effect of Iron and Zinc on Growth Patterns of *Escherichia coli* in Iron-Deficient Medium. *J Bacteriol* 87:823-7.
228. Sperandio V, Torres AG, Kaper JB. 2002. Quorum sensing *Escherichia coli* regulators B and C (QseBC): a novel two-component regulatory system involved in the regulation of flagella and motility by quorum sensing in *E. coli*. *Mol Microbiol* 43:809-21.

229. Sandrini S, Aldriwesh M, Alruways M, Freestone P. 2015. Microbial endocrinology: host-bacteria communication within the gut microbiome. *J Endocrinol* 225:R21-34.
230. Magro F, Vieira-Coelho MA, Fraga S, Serrao MP, Veloso FT, Ribeiro T, Soares-da-Silva P. 2002. Impaired synthesis or cellular storage of norepinephrine, dopamine, and 5-hydroxytryptamine in human inflammatory bowel disease. *Dig Dis Sci* 47:216-24.
231. Magro F, Fraga S, Ribeiro T, Soares-da-Silva P. 2004. Decreased availability of intestinal dopamine in transmural colitis may relate to inhibitory effects of interferon-gamma upon L-DOPA uptake. *Acta Physiol Scand* 180:379-86.
232. Neame KD. 1962. Uptake of L-histidine, L-proline, L-tyrosine and L-ornithine by brain, intestinal mucosa, testis, kidney, spleen, liver, heart muscle, skeletal muscle and erythrocytes of the rat *in vitro*. *J Physiol* 162:1-12.
233. Huang KC. 1965. Uptake of L-tyrosine and 3-O-methylglucose by isolated intestinal epithelial cells. *Life Sci* 4:1201-6.
234. Schulz C, Eisenhofer G, Lehnert H. 2004. Principles of catecholamine biosynthesis, metabolism and release. *Front Horm Res* 31:1-25.
235. Gundert-Remy U, Hildebrandt R, Stiehl A, Weber E, Zurcher G, Da Prada M. 1983. Intestinal absorption of *levodopa* in man. *Eur J Clin Pharmacol* 25:69-72.
236. Pizzi C, Pignata S, Calderopoli R, D'Agostino L, Tritto G, D'Adamo G, Esposito G, Daniele B, Mazzacca G, Bianco AR, et al. 1994. Cell kinetics and polyamine enzymes in the intestinal mucosa of rats with azoxymethane induced tumours. *Int J Exp Pathol* 75:305-11.
237. Straub RH, Wiest R, Strauch UG, Harle P, Scholmerich J. 2006. The role of the sympathetic nervous system in intestinal inflammation. *Gut* 55:1640-9.
238. Haskel Y, Hanani M. 1994. Inhibition of gastrointestinal motility by MPTP via adrenergic and dopaminergic mechanisms. *Dig Dis Sci* 39:2364-7.
239. Huether G. 1993. The contribution of extrapineal sites of melatonin synthesis to circulating melatonin levels in higher vertebrates. *Experientia* 49:665-70.
240. Bianchine JR, Calimlim LR, Morgan JP, Dujuvne CA, Lasagna L. 1971. Metabolism and absorption of L-3,4 dihydroxyphenylalanine in patients with Parkinson's disease. *Ann N Y Acad Sci* 179:126-40.
241. Walters M, Sperandio V. 2006. Autoinducer 3 and epinephrine signaling in the kinetics of locus of enterocyte effacement gene expression in enterohemorrhagic *Escherichia coli*. *Infect Immun* 74:5445-55.
242. Freestone PP, Haigh RD, Lyte M. 2007. Specificity of catecholamine-induced growth in *Escherichia coli* O157:H7, *Salmonella enterica* and *Yersinia enterocolitica*. *FEMS Microbiol Lett* 269:221-8.
243. Knecht LD, O'Connor G, Mittal R, Liu XZ, Daftarian P, Deo SK, Daunert S. 2016. Serotonin Activates Bacterial Quorum Sensing and Enhances the Virulence of *Pseudomonas aeruginosa* in the Host. *EBioMedicine* 9:161-9.
244. Yurkovetskiy L, Burrows M, Khan AA, Graham L, Volchkov P, Becker L, Antonopoulos D, Umesaki Y, Chervonsky AV. 2013. Gender bias in autoimmunity is influenced by microbiota. *Immunity* 39:400-12.

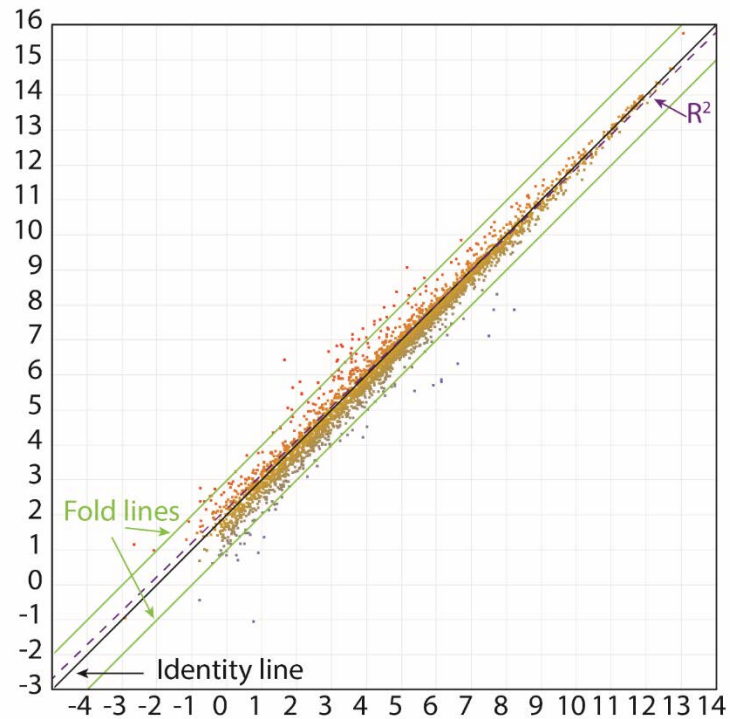
245. Eisenbach M, Constantinou C, Aloni H, Shinitzky M. 1990. Repellents for *Escherichia coli* operate neither by changing membrane fluidity nor by being sensed by periplasmic receptors during chemotaxis. *J Bacteriol* 172:5218-24.
246. Pham HT, Parkinson JS. 2011. Phenol sensing by *Escherichia coli* chemoreceptors: a nonclassical mechanism. *J Bacteriol* 193:6597-604.
247. Oosawa K, Imae Y. 1983. Glycerol and ethylene glycol: members of a new class of repellents of *Escherichia coli* chemotaxis. *J Bacteriol* 154:104-12.
248. Umemura T, Matsumoto Y, Ohnishi K, Homma M, Kawagishi I. 2002. Sensing of cytoplasmic pH by bacterial chemoreceptors involves the linker region that connects the membrane-spanning and the signal-modulating helices. *J Biol Chem* 277:1593-8.
249. Khan S, Trentham DR. 2004. Biphasic excitation by leucine in *Escherichia coli* chemotaxis. *J Bacteriol* 186:588-92.
250. de Pina K, Navarro C, McWalter L, Boxer DH, Price NC, Kelly SM, Mandrand-Berthelot MA, Wu LF. 1995. Purification and characterization of the periplasmic nickel-binding protein NikA of *Escherichia coli* K12. *Eur J Biochem* 227:857-65.
251. Englert DL, Adase CA, Jayaraman A, Manson MD. 2010. Repellent taxis in response to nickel ion requires neither Ni<sup>2+</sup> transport nor the periplasmic NikA binding protein. *J Bacteriol* 192:2633-7.
252. Schultz CL, Edrington TS, Callaway TR, Schroeder SB, Hallford DM, Genovese KJ, Anderson RC, Nisbet DJ. 2006. The influence of melatonin on growth of *E. coli* O157:H7 in pure culture and exogenous melatonin on faecal shedding of *E. coli* O157:H7 in experimentally infected wethers. *Lett Appl Microbiol* 43:105-10.
253. Paulose JK, Wright JM, Patel AG, Cassone VM. 2016. Human Gut Bacteria Are Sensitive to Melatonin and Express Endogenous Circadian Rhythmicity. *PLoS One* 11:e0146643.
254. Straub RH, Schaller T, Miller LE, von Horsten S, Jessop DS, Falk W, Scholmerich J. 2000. Neuropeptide Y cotransmission with norepinephrine in the sympathetic nerve-macrophage interplay. *J Neurochem* 75:2464-71.
255. Harris RM, Picton R, Singh S, Waring RH. 2000. Activity of phenolsulfotransferases in the human gastrointestinal tract. *Life Sci* 67:2051-7.
256. Zarrinpar A, Chaix A, Yooseph S, Panda S. 2014. Diet and feeding pattern affect the diurnal dynamics of the gut microbiome. *Cell Metab* 20:1006-17.
257. Ratledge C, Dover LG. 2000. Iron metabolism in pathogenic bacteria. *Annu Rev Microbiol* 54:881-941.
258. Burton CL, Chhabra SR, Swift S, Baldwin TJ, Withers H, Hill SJ, Williams P. 2002. The growth response of *Escherichia coli* to neurotransmitters and related catecholamine drugs requires a functional enterobactin biosynthesis and uptake system. *Infect Immun* 70:5913-23.
259. Williams PH, Rabsch W, Methner U, Voigt W, Tschape H, Reissbrodt R. 2006. Catecholate receptor proteins in *Salmonella enterica*: role in virulence and implications for vaccine development. *Vaccine* 24:3840-4.
260. McGuckin MA, Linden SK, Sutton P, Florin TH. 2011. Mucin dynamics and enteric pathogens. *Nat Rev Microbiol* 9:265-78.
261. Hooper LV, Macpherson AJ. 2010. Immune adaptations that maintain homeostasis with the intestinal microbiota. *Nat Rev Immunol* 10:159-69.

- 
262. Allweiss B, Dostal J, Carey KE, Edwards TF, Freter R. 1977. The role of chemotaxis in the ecology of bacterial pathogens of mucosal surfaces. *Nature* 266:448-50.
  263. Li H, Limenitakis JP, Fuhrer T, Geuking MB, Lawson MA, Wyss M, Brugiroux S, Keller I, Macpherson JA, Rupp S, Stolp B, Stein JV, Stecher B, Sauer U, McCoy KD, Macpherson AJ. 2015. The outer mucus layer hosts a distinct intestinal microbial niche. *Nat Commun* 6:8292.
  264. Rivera-Chavez F, Winter SE, Lopez CA, Xavier MN, Winter MG, Nuccio SP, Russell JM, Laughlin RC, Lawhon SD, Sterzenbach T, Bevins CL, Tsolis RM, Harshey R, Adams LG, Baumler AJ. 2013. *Salmonella* uses energy taxis to benefit from intestinal inflammation. *PLoS Pathog* 9:e1003267.
  265. Mittal R, Debs LH, Patel AP, Nguyen D, Patel K, O'Connor G, Grati M, Mittal J, Yan D, Eshraghi AA, Deo SK, Daunert S, Liu XZ. 2017. Neurotransmitters: The Critical Modulators Regulating Gut-Brain Axis. *J Cell Physiol* 232:2359-2372.
  266. Khan WI, Ghia JE. 2010. Gut hormones: emerging role in immune activation and inflammation. *Clin Exp Immunol* 161:19-27.
  267. De Palma G, Collins SM, Bercik P, Verdu EF. 2014. The microbiota-gut-brain axis in gastrointestinal disorders: stressed bugs, stressed brain or both? *J Physiol* 592:2989-97.
  268. Litvak Y, Byndloss MX, Tsolis RM, Baumler AJ. 2017. Dysbiotic Proteobacteria expansion: a microbial signature of epithelial dysfunction. *Curr Opin Microbiol* 39:1-6.

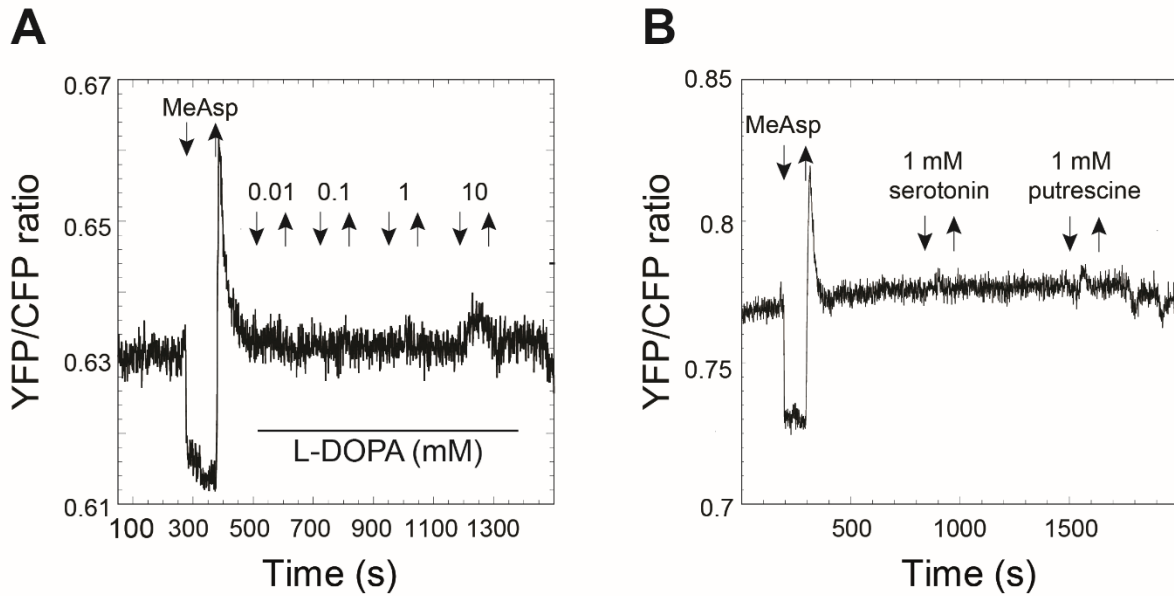
## APPENDIX



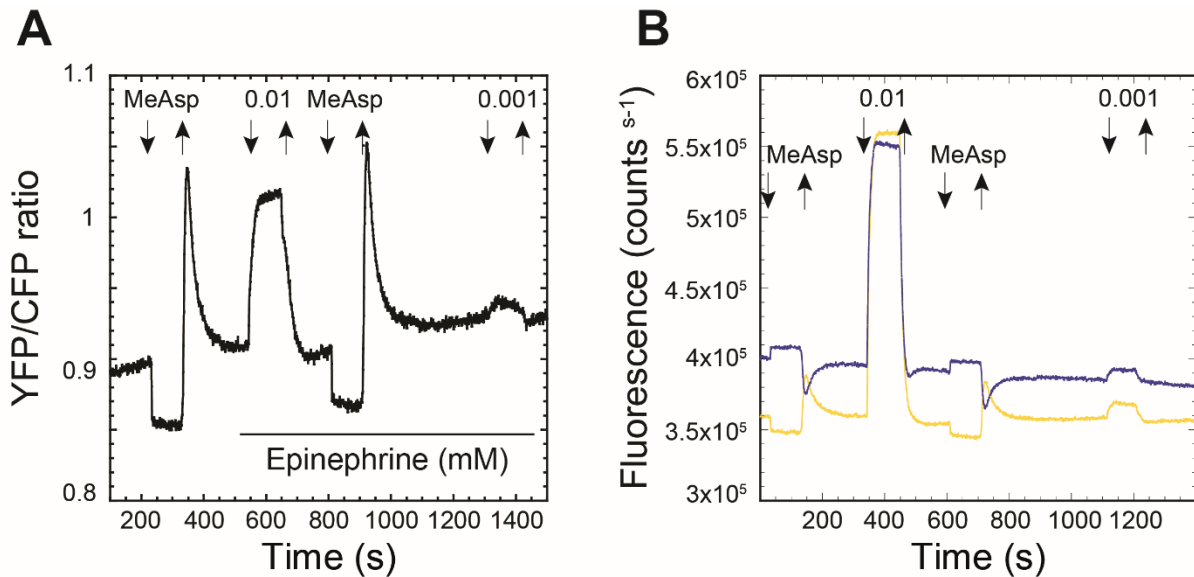
**Appendix-Figure 1: FRET-based analysis of *E. coli* chemotaxis pathway responses.** **(A)** Wild-type cells expressing CheY-YFP and CheZ-CFP were stimulated by addition and subsequent removal of attractant, 1 mM  $\alpha$ -methyl-DL-aspartate (MeAsp) and addition and subsequent removal of repellent, 1 mM and 10 mM 3,4-dihydroxymandelic acid (DHMA), at the time points indicated by arrows. Attractants inhibit the kinase activity of CheA, leading to a decrease in FRET, which is observed as a decrease in the YFP/CFP ratio due to the reduced numbers of CheY-P-CheZ complexes. Conversely, removal of attractants or stimulation by repellents leads to an increase in the YFP/CFP ratio. **(B)** Time traces of fluorescence intensity in the YFP (yellow) and CFP (cyan) channels for the FRET response observed in (A). Opposite changes in the two channels, characterize specific FRET response.



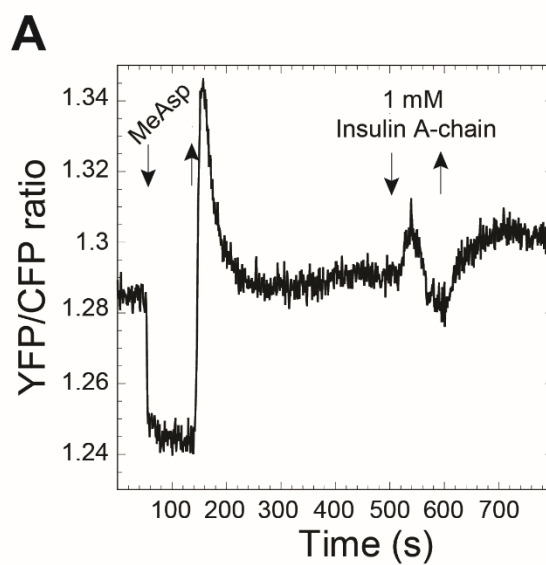
**Appendix-Figure 2: Example of a scatter plot of RNA-seq data.** As a means to study variations in the expression levels of genes between different experiments, we use the fold change between one experiment serving as a control and a second experiment. In the scatter plots, a fold change of 0 represents no changes in the gene expression between the two experiments and appears on the identity line in the middle of the plot. A fold change more than 2 can be found outside the fold lines parallel to the identity line of the scatter plot. Genes upregulated in comparison with the control experiment have a positive value in tables and can be found in the experiment's half of the scatter plot. Consequently, genes on the other half of the plot are downregulated in comparison with the control experiment and have a negative value in tables.



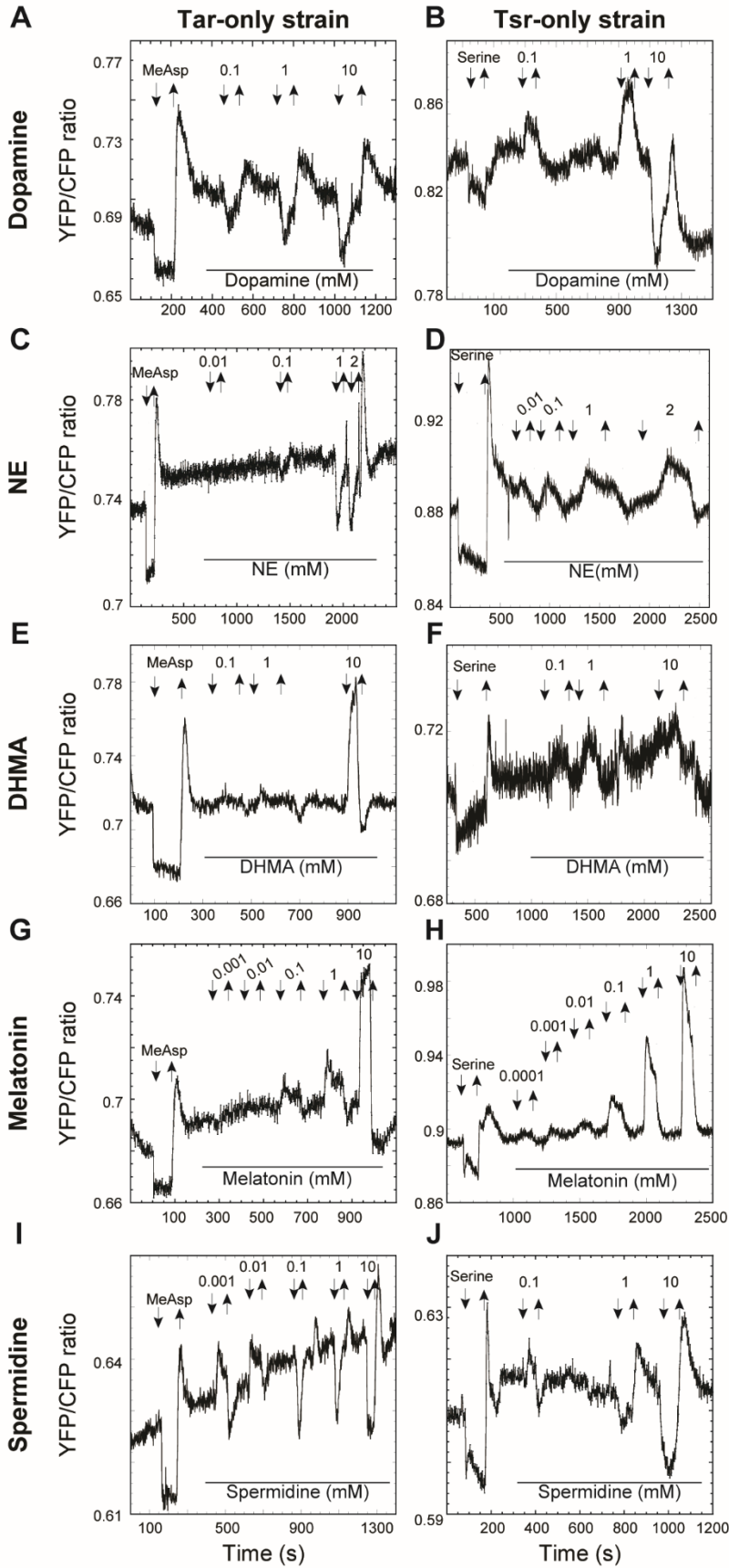
**Appendix-Figure 3:** Typical FRET measurements of the wild-type cells to L-3,4-dihydroxyphenylalanine (L-DOPA) (A) and serotonin and putrescine (B). Measurements were performed and plotted as in Figure 14.



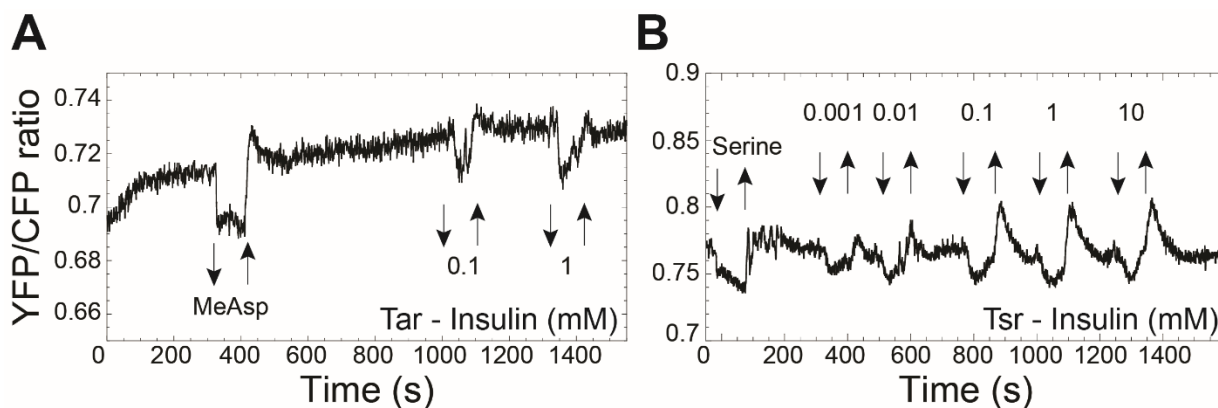
**Appendix-Figure 4:** Typical FRET measurements responses of wild-type cells to epinephrine (A, B). B shows the individual fluorescence channels changes with epinephrine. Measurements were performed and plotted as in Figure 14.



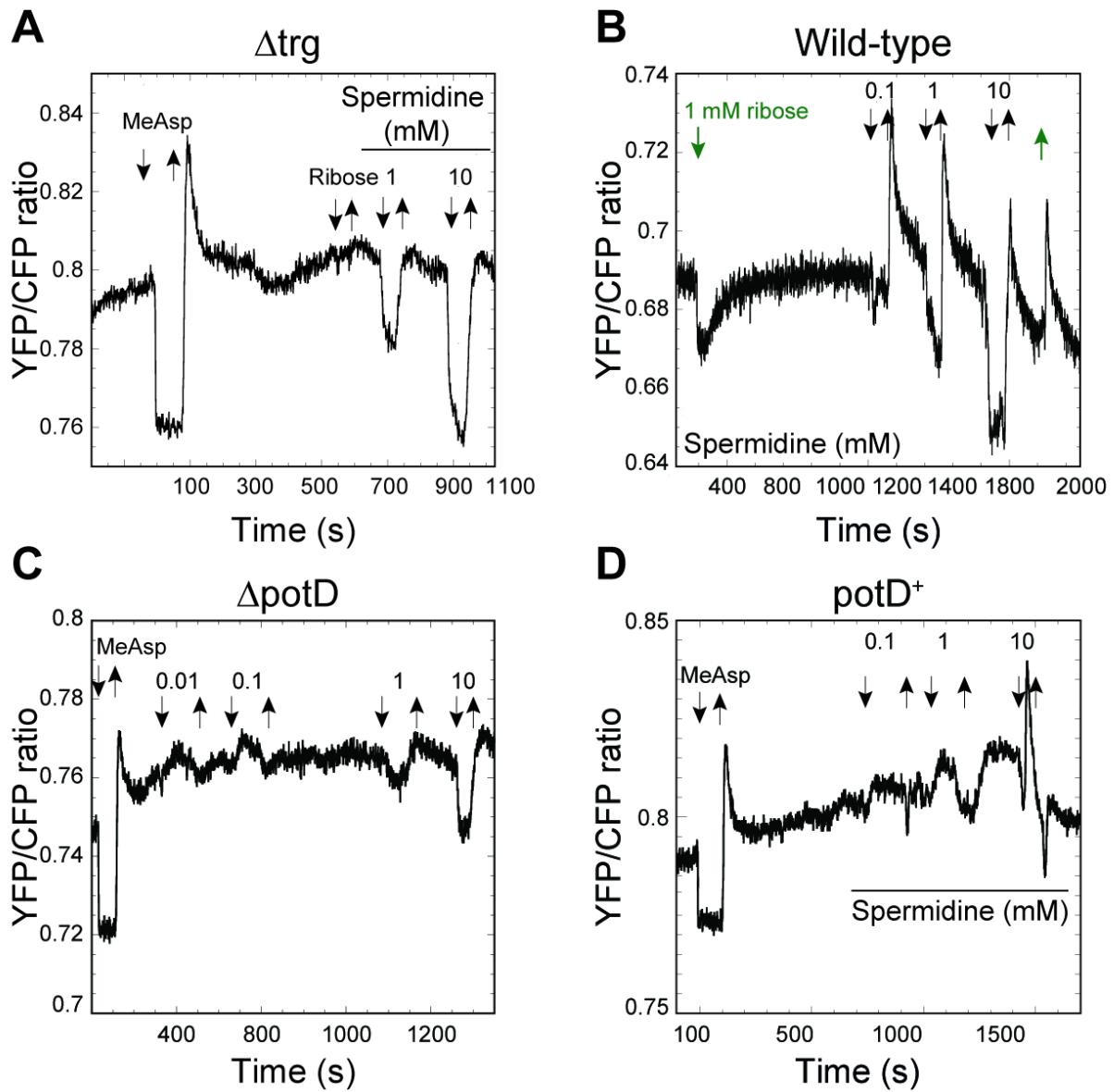
**Appendix-Figure 5:** Typical FRET measurements responses of wild-type cells to 1 mM of A-chain of insulin. Measurements were performed and plotted as in Figure 14.



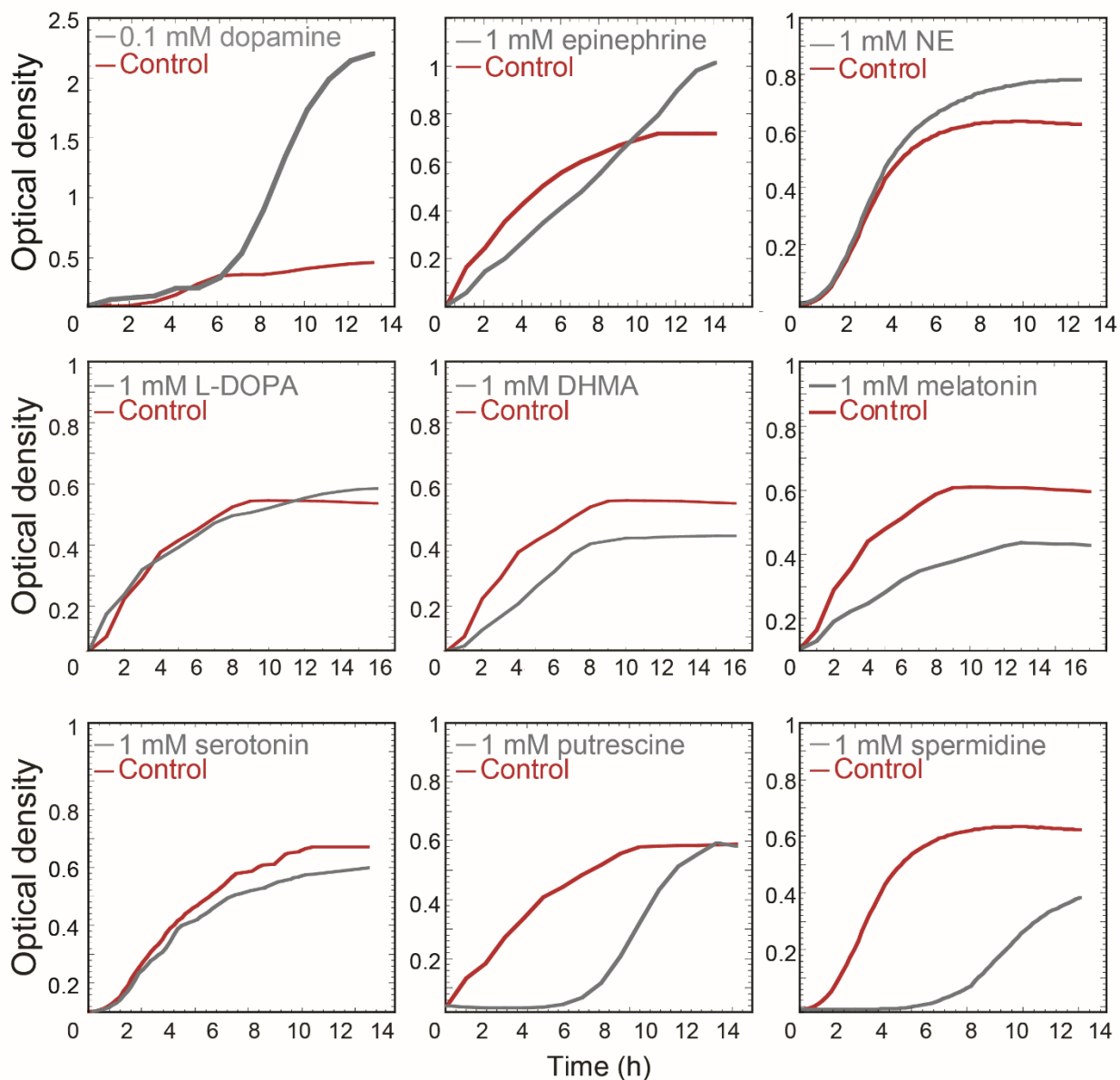
**Appendix-Figure 6:** Typical Examples of FRET measurements for Tar-only cells (left side) and Tsr-only cells (right side). Responses to dopamine (A, B), NE (C, D), DHMA (E, F), melatonin (G, H) and spermidine (I, J) are shown. Measurements were performed and plotted as in Figure 14.



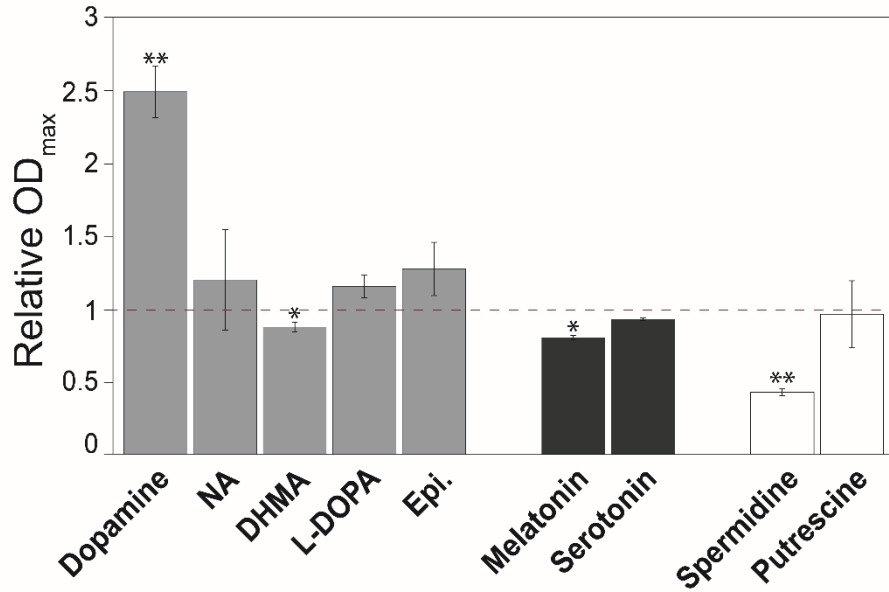
**Appendix-Figure 7:** Typical Examples of FRET measurements for Tar-only cells (A) and Tsr-only cells (B) to insulin. Measurements were performed and plotted as in Figure 14.



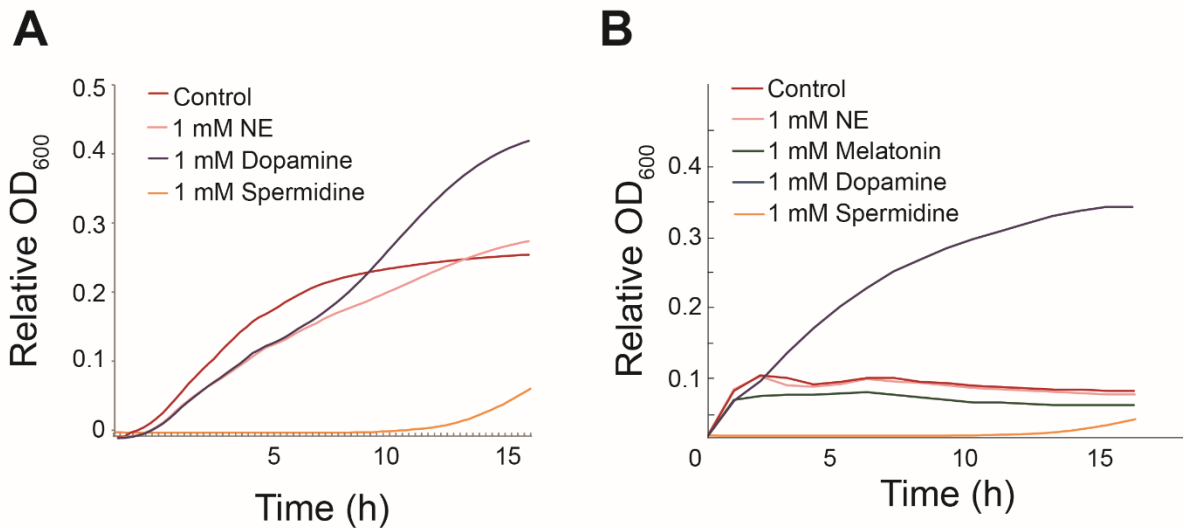
**Appendix-Figure 8: Typical FRET measurements of responses to spermidine. Measurement examples for  $\Delta$ trg strain (A), wild-type cells (B),  $\Delta$ potD strain (C) and  $\Delta$ potD complemented with the plasmid pJL02 ( $potD^+$ ) (D). The absence of response to 1 mM of ribose was used as negative control demonstrating Trg receptor deletion (A). Cells adapted to 1 mM of ribose (indicated by the green arrows), stimulated with increasing concentrations of spermidine (B). Measurements were performed and plotted as in Figure 14.**



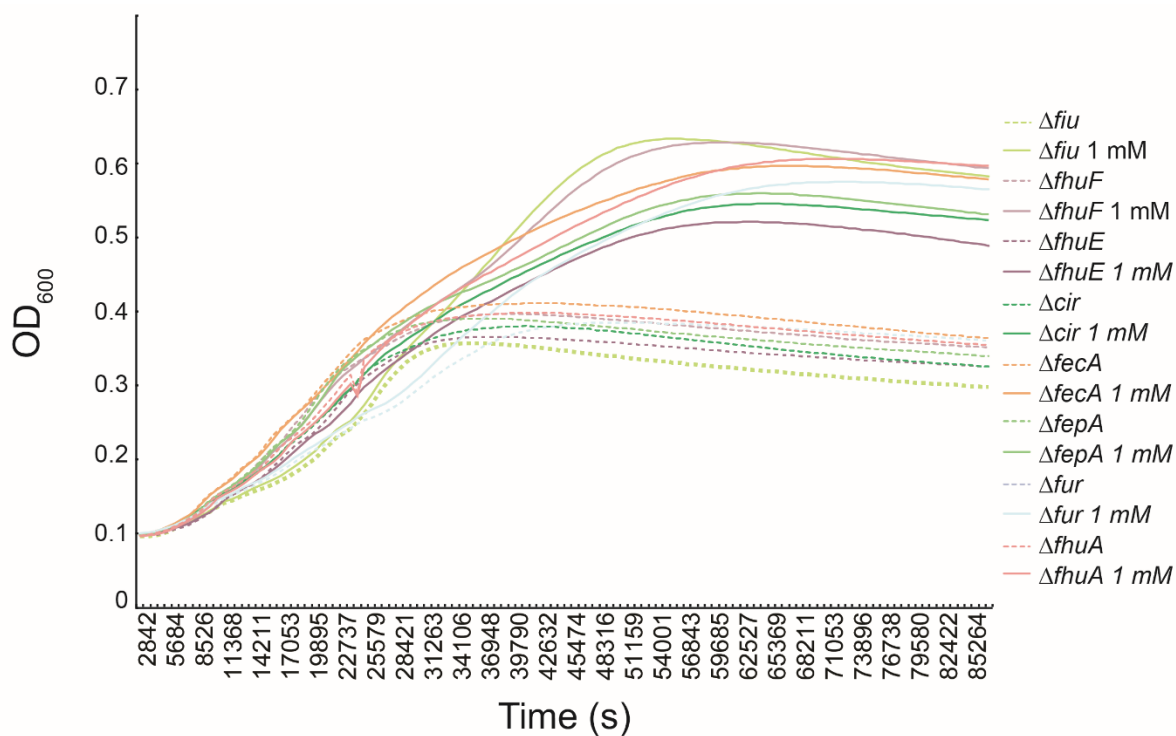
**Appendix-Figure 9: Typical examples of growth curves in presence of gut compounds.** MG1655 cells were grown as in Figure 29, at 37°C in TB (control – red curve) and supplemented with 1 mM of dopamine, epinephrine, NE, L-DOPA, DHMA, melatonin, serotonin, putrescine or spermidine as indicated (grey curves). The optical density (OD<sub>600</sub>) was measured every hour.



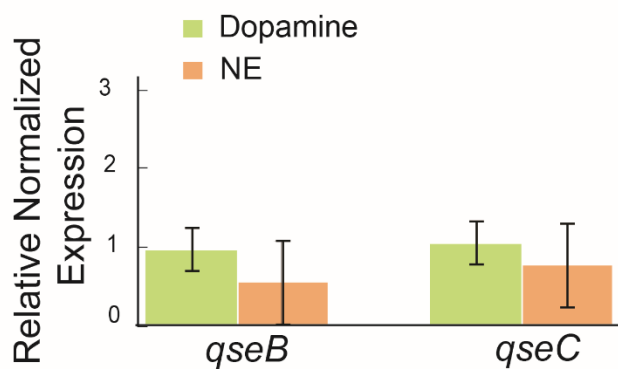
**Appendix-Figure 10: Effects of the gut compounds on maximal OD of *E. coli* culture.** Cells were grown as in Figure 29. Culture density was determined after 14 h OD<sub>600</sub> values were plotted normalized to the control culture with untreated cells (red line). Error bars indicates the standard deviation.



**Appendix-Figure 11: Example of growth curves in presence of gut compounds in M9 medium (A) and SAPI medium (B).** MG1655 cells were grown as in Figure 29 at 37°C in the respective media (control – red curve) and supplemented with the indicated compounds. The optical density (OD<sub>600</sub>) was measured every hour.



**Appendix-Figure 12:** Example of growth curves of deletion strains of iron transporters in *E. coli* in the presence (filled line) and absence (dashed line) of 1 mM of dopamine. MG1655 cells were grown as in Figure 29, at 37°C in TB media.



**Appendix-Figure 13:** Analysis of *qseB* and *qseC* genes transcript abundance when dopamine and NE were added. qRT-PCR analysis was performed to compare the *qseB* and *qseC* gene transcript abundance between the control (no supplement) and 1 mM of dopamine and NE in MG1655 strain.

**Appendix-Table 1: Genes with more than 1-fold changes between the control and the correspondent experiments: Melatonin, Dopamine and DHMA**

	<i>Gene</i>	<i>Control expression level</i>	<i>Experiment expression level</i>	<i>Fold change</i>
<b>DHMA</b>	<i>ybjJ</i>	4.99791	7.3135	4.978 up
	<i>rrsH</i>	4.37075	6.53634	4.487 up
	<i>rrsC</i>	4.13163	6.15435	4.063 up
	<i>yhak</i>	5.61523	3.90685	3.18 up
	<i>ydfB</i>	2.12861	-1.18107	9.915 down
	<i>leuP</i>	2.5857	-0.63449	9.319 down
	<i>rhaM</i>	2.5857	0.30173	4.072 down
	<i>citD</i>	2.32763	-0.40587	4.035 down
	<i>tauB</i>	1.60681	-0.82306	3.609 down

	<i>ylcI</i>	1.02864	0.36209	3.376 down	
	<i>yahM</i>	2.11747	0.86594	3.268 down	
<b>DOPAMINE</b>	<i>tdcD</i>	7.8243	7.65679	7.084 up	
	<i>fecB</i>	8.71909	8.35577	4.752 down	
	<i>fecA</i>	9.44297	9.06653	5.072 down	
	<i>fecC</i>	7.35204	6.92396	4.957 down	
	<i>fecD</i>	7.11429	6.64099	4.872 down	
	<i>fecE</i>	7.35982	6.84933	4.628 down	
	<i>trpE</i>	2.87698	3.47354	4.416 down	
	<i>tyrU</i>	1.98774	2.19154	1.151 up	
	<i>yncl</i>	-2.32697	1.22349	11.716 up	
	<b>MELATONIN</b>	<i>rrsH</i>	4.37075	6.53634	4.486 up
		<i>rrsC</i>	4.13163	6.15435	4.063 up
<i>rrlH</i>		4.47799	6.36015	3.686 up	
<i>rrlA</i>		4.54066	6.39942	3.626 up	
<i>rrsD</i>		3.32387	5.16936	3.593 up	
<i>rrsA</i>		3.36313	5.20056	3.573 up	
<i>rrlC</i>		4.81539	6.63114	3.52 up	
<i>rrlD</i>		3.35774	5.05405	3.24 up	
<i>cadB</i>		5.10414	5.76898	1.585 up	
<i>dcuC</i>		7.37603	6.80627	1.484 down	
<i>fdnG</i>		5.58797	6.10085	1.426 up	
<i>narH</i>		8.51779	8.9337	1.334 down	
<i>tdcB</i>		8.93905	8.53902	1.319 down	
<i>fdnH</i>		4.39913	4.77402	1.296 up	
<i>narJ</i>		6.94695	7.29189	1.27 up	
<i>narK</i>		9.0451	9.3864	1.266 up	
<i>tdcC</i>		8.8498	8.56456	1.218 down	
<i>nikB</i>		5.85117	6.13592	1.218 up	
<i>narI</i>		6.87043	7.14733	1.211 up	
<i>nikA</i>		5.79321	6.05035	1.195 up	
<i>nirD</i>		9.61348	9.3569	1.194 down	
<i>ansB</i>		8.57096	8.3151	1.194 down	
<i>nirB</i>		9.5536	9.29802	1.193 down	
<i>narG</i>		10.13059	10.38224	1.19 up	
<i>dmsA</i>		7.89024	7.64589	1.184 down	
<i>nikC</i>		5.77265	6.01113	1.179 up	
<i>yjjW</i>		6.49289	6.25604	1.178 down	
<i>dmsB</i>		7.65029	7.41899	1.173 down	
<i>tdcD</i>		7.8243	7.65679	1.123 down	
<i>dmsC</i>		7.47147	7.30872	1.119 down	
<i>yech</i>		4.81791	4.70869	1.078 down	

<i>nirC</i>	7.9817	7.9121	1.049 down
<i>nikD</i>	5.70084	5.76043	1.042 up
<i>adiY</i>	4.99123	5.0478	1.039 up
<i>napA</i>	7.48937	7.5244	1.024 up
<i>yhbV</i>	5.62688	5.64595	1.013 up

---

## Erklärung

Hiermit versichere ich, dass ich die vorliegende Dissertation mit dem Titel

**“Chemotaxis of *Escherichia coli* to compounds present in human gut”**

selbstständig verfasst, keine anderen als die im Text angegebenen Hilfsmittel verwendet und sämtliche Stellen, die dem Wortlaut oder dem Sinn nach aus anderen Werken entnommen sind, mit Quellenangabe kenntlich gemacht habe. Die Dissertation wurde in der jetzigen oder einer ähnlichen Form noch bei keiner anderen Hochschule eingereicht und hat noch keinem anderen Prüfungszweck gedient.

Marburg, den \_\_\_\_ . \_\_\_\_ . \_\_\_\_

---

Joana Lopes